GEOCHEMICAL AND GEOTECHNICAL CHARACTERIZATION OF BARYTE MINERALISATION IN LESSEL AND IHUGH AREAS, LOWER BENUE TROUGH, NIGERIA

BY

NGUKPOSU AHEN LABE

DEPARTMENT OF GEOLOGY
FACULTY OF SCIENCE
AHMADU BELLO UNIVERSITY,
ZARIA, NIGERIA

NOVEMBER, 2015

GEOCHEMICAL AND GEOTECHNICAL CHARACTERIZATION OF BARYTE MINERALISATION IN LESSEL AND IHUGH AREAS, LOWER BENUE TROUGH, NIGERIA

BY

Ngukposu Ahen LABE
B.Sc. (A.B.U) 2008
M.Sc./Sci/6433/10-11

A THESIS SUBMITTED TO THE SCHOOL OF POSTGRADUATE STUDIES, AHMADU BELLO UNIVERSITY, ZARIA, IN PARTIAL FULFILLMENT OF THE REQUIREMENTS FOR THE AWARD OF MASTER OF SCIENCE DEGREE IN GEOLOGY

DEPARTMENT OF GEOLOGY
FACULTY OF SCIENCE
AHMADU BELLO UNIVERSITY,
ZARIA, NIGERIA

NOVEMBER, 2015

DECLARATION

I declare that the work in this thesis entitled "GEOCHEMICAL AND GEOTECHNICAL CHARACTERIZATION OF BARYTE MINERALIZATION IN LESSEL AND IHUGH AREAS, LOWER BENUE TROUGH, NIGERIA" has been carried out by me in the Department of Geology, Ahmadu Bello University, Zaria. The information derived from the literature has been duly acknowledged in the text and a list of references provided. No part if this thesis has been presented for another degree or diploma at any institution.

Ngukposu Ahen LABE	_____	_____
Name of Student	**Signature**	**Date**

CERTIFICATION

This thesis entitled "GEOCHEMICAL AND GEOTECHNICAL CHARACTERIZATION OF BARYTE MINERALIZATION IN LESSEL AND IHUGH AREAS, LOWER BENUE TROUGH, NIGERIA" by Ngukposu Ahen LABE meets the regulations governing the award of the degree of Master of Science of the Ahmadu Bello University, and is approved for its contribution to knowledge and literary presentation.

_____ _____

Prof. P.O. Ogunleye **Date**
Chairman, Supervisory Committee

_____ _____

Dr. A.A. Ibrahim **Date**
Member, Supervisory Committee

_____ _____

Dr. H. Hamza **Date**
Head of Department

_____ _____

Prof. K. Bala **Date**
Dean, School of Postgraduate Studies

DEDICATION

This project is dedicated to God Almighty and to my parents Dr. Daniel Ahen Labe and Mrs. Esther Mbanengen Labe for ensuring that I have a good education.

ACKNOWLEDGEMENT

My profound gratitude goes to God Almighty 'The Solid Rock'; all that I am in life is because of His faithfulness.

I say a big thank you to my supervisors Prof. P.O. Ogunleye and Dr. A.A. Ibrahim; it has been a privilege working with you. I appreciate the time you have put in to make sure that this work is what it is today. Your advices and criticisms drove me to work harder and think better.

My gratitude also goes to Dr. T. Najime for igniting the 'love for baryte' in me, your advice and assistance throughout my entire study is appreciated. Mr. S.S. Magaji for pushing me especially when I had writer's block and being ready to help whenever I came to him with a problem. I also appreciate the staff of the Department of Geology for your help in one way or another; Prof. I. Garba, Prof. P.M. Zaborski, Prof. U.A. Danbatta, Prof. K. Schoneich, Prof. S.A. Alagbe, Dr. H. Hamza, Dr. A.E. Ikpokonte, Dr. E.O. Obiosio, Dr. I. Hamidu, Dr. I.Y. Abubakar, Dr. M.L. Garba, Mr. I.I. Ahmed, Mr. A.L. Yola, Mr. A.K. Amuda, Mr. S.M. Elatikpo, Mr. E.B. Animashawun, Mr. C.U. Onyeamachi, Mr. P.J. Gbaje, Mr. G. Amedu, Mr. J.O. Eka, Mr. U. Mohammed, Mr. N.I. Dayyib, Late Mrs. H.O. Iguisi, Mr. F.C. Echendu, Mr. J.H. Yashe and Mr. S.P.M. Gadzama.

I also thank Engr. J. Ochepo, Engr. A. Shauibu, Engr. W.C. Ejembi, Engr. Rotimi, Mr. Abel, staff of the Department of Civil Engineering, Mr. B. Jimoh of Physics Department and Mr. I. Akaahar, Mr. S. Abubakar of the Nigerian Geological Survey Agency for helping out with the geotechnical analyses.

I would like to thank most profoundly, the Chairman of Ushongo Local Government Area, Mr. T. Orduen and the head of baryte miners Mr. Asongo Avertse who made sure that my field work went on unhindered. The baryte miners at Lessel, Mr. Cosmos, Late Mr. P. Momoh, Mr. M. Jibunoh, the Ihugh district head, Mr. A. Adem and the Tarzoho family for giving me the opportunity to study the baryte pits in their compound. The assistance of Mr. Patrick Kogi from Ikyobo baryte mining area is also appreciated. My guide Papa, Ayangebee Labe and Hembadoon Labe, I could not have done it on my own. I thank you for your patience and help in the field.

My colleagues Edward Clement Edache, Aminu Gidado, Benedicta Ojisua, Abubakar Ibrahim, Thaddeus Akuh, Fabian Adukwu, Ma'aji Usman (Nassarawa), Innocent Duru, Anthony Nwanya, Folake Aponbiede (Mrs), Christiana Ohwoafasa (Mrs). The 'Pre-Cambrian geologists'; Rebecca Mathew (Mrs), Ebenezer, Abdullahi Kana, Rose Solomon, Victor Gana, Adoze Usman (Kogi), Juliet Akoh, Tende Andongma, Helen Onaji, Fred Ochella. The 'Cretaceous geologists' Vanessa Aber, Musa Bala, Abubakar Usman (Gombe), Segun Micheals, Allen Daniel, Ephraim Ishaya, Hussaina Olaifa (Mrs), Mustapha Osman and Abubakar Tahir. The 'Paleogene geologists'; Aliyu Umar, Aliyu Abubakar, Nana Abdulmalik, Celestine Joro, Femi Adeyeye, Tunji Fajulugbe and the 'Recent geologists", you are all amazing bunch even with our busy schedules you still took out time to help; it was nice studying with you all.

Prof. and Mrs. D.J.M. Yakubu, Dr. T. Dzenda thank you so much for your support morally, spiritually and financially. Engr. A.A. Agba and Judith Damsue, thank you also for contributing to the success of this work

I am also grateful to my friends who have encouraged me Emmanuel Atama, Mam Tawey, Joel Iroegbu, Dayspring Adenusi, Emmanuel (NAPE) Abah, Peter Williams, Regina Agbo Agunpopo, Agaba Ujah, Akumir Hinjari, Patience Zaki, Shade Bonire Ojeleye, Magaret Ewule, Omowumi Owoshagba, Sunday Eke, Terver Enger, Akor Agada, Tony Ukah, Adobe Kwanashie, Taiye Lasisi, Habibat Lawal, Susan Odumu; and also my dear friend Elizabeth Hauwa Angulu, I thank God for making our friendship a unique one right from undergraduate days; we have been through many ups and downs but you never cease to encourage and stand by me. The one that makes me skip a beat whenever I lay eyes on him, my dear friend Onoruoyiza (Oyisi) Asuku Ibrahim, thank you for being with me through it all, for listening to me even when you had no 'geological idea' about what I was saying.

I truly appreciate my parents Dr. and Mrs. D.A. Labe for the educational foundation they have laid for me. Without you I would not have made it to this point. Thank you for praying for me, for supporting me financially, morally and in every way a parent supports a child. Your labour will not be in vain. My siblings Yuana, Fanyam, Azua, Atema, Iorhuan and Kpilaior I thank you for standing by me all the way and also

assisting in every way possible. I say a big thank you to my brother-in-law Tyozungwe Awua and the little Awuas – Dooyum, Verem and Zahemen who always made sure they left series of drawing on the draft of this thesis or sometimes even tear off a portion of it whenever they laid hands on it. Thank God for the joy of having a family, I Love You all.

Mr. and Mrs. T. Ityovenda and Mrs. T. Atoato thank you so much for your encouragement, for accommodating and taking good care of me throughout my fieldwork (lest I forget thank you aunty Nguveren Ityovenda for trying so hard to fatten me during the fieldwork). Uncle Hange thank you for your encouragement. Uncle Iorember thank you for taking me around during my fieldwork. I thank my cousins Weghgba Ityovenda for helping me out; Iorker Ityovenda who located some ‘stones’ while taking his animals to graze, those ‘stones’ actually turned out to be outcrop of granite.

ABSTRACT

The Lessel-Ihugh area lies within the Lower Benue Trough, southeastern Nigeria. The area, which was mapped on the scale of 1:10,000 is underlain by Precambrian rocks comprising of gneiss, medium-grained muscovite granite, coarse-grained biotite muscovite granite, and Turonian arenaceous Lessel Sandstone. Baryte mineralization occurs generally as vein and cavity type deposits in Lessel Sandstone at Lessel-Mbagwa and Mbaakase (southwest of Ihugh) and also in banded gneiss at Bunde (northeast of Lessel Town). Baryte veins mapped in the area trending mainly in the NE-SW direction with minor NW-SE trends. The veins at Lessel area contain minor amounts of quartz, galena and sphalerite as associated minerals. Petrographic studies on the granitic and vein rocks collected from the area were carried out using transmitted light microscope. Whole rock geochemical analysis of granitic rocks, sandstones and baryte veins were carried out using ICP-AES and ICP-MS to chemically characterize baryte mineralization in the Lessel-Ihugh area. In addition, baryte minerals were subjected to density, moisture content and uniaxial compressive strength tests to establish their geotechnical attributes, variety and quality. Cross-cutting relationship of baryte veins suggests that opaque minerals (galena, sphalerite, iron-oxides), quartz was first deposited followed by early baryte, late baryte and lastly again by the opaque minerals. Geochemical data indicate that the granitic rocks are generally peraluminous calc-alkaline granites believed to have been emplaced during the compressional tectonism resulting from the Pan-African orogeny. Geochemical classification constrained the Lessel Sandstones as wacke, litharenite, sub-litharenite and quartz-arenite sandstones derived from granite and gneiss terrane. Barytes from the Lessel-

Ihugh area is characterized by enrichment in Ba, Sr, depletion in major oxides and trace elements, low ΣREE (7.2 – 39.4 ppm), negative Eu anomalies (0.02 – 0.05), positive Ce and negative Ce anomalies (0.06 – 1.3) in addition to positive Gd anomalies (17.1 – 21.4). Trace element data indicates Ba was leached from Ba-rich magmatic rocks. Ce_N/Sm_N versus Ce_N/Yb_N plot suggests that the mineralizing fluid was derived from seawater dominated hydrothermal fluid. The interaction of Ba-rich fluid with sulphate-rich fluid led to precipitation of baryte under oxic and anoxic conditions in fractures during the Santonian to Campanian. Geotechnical investigations reveal that the Lessel-Ihugh barytes have low uniaxial compressive strength (2.02 – 5.36 N/mm^2), moderate moisture content (0.42 – 1.18%) and specific gravity (3.65 – 4.01). Based on the geochemical and geotechnical characteristics of barytes in this study, the Lessel-Ihugh baryte fall below international standard specifications, and are therefore of relatively moderate quality or Grade II barytes.

TABLE OF CONTENTS

Cover Page……. i

Title Page……. ii

Declaration…….. iii

Certification…… iv

Dedication…….. v

Acknowledgement……. vi

Abstract…….. ix

Table of Contents…… xi

List of Figures……. xiv

List of Tables…….. xvii

List of Plates…… xix

List of Appendices…….. xxi

CHAPTER ONE: INTRODUCTION

1.1 General Introduction…… 1

1.1.1 Types of baryte deposit……..…..…….. 3

1.1.2 Uses of baryte…….. 6

1.2 Location and Accessibility…… 6

1.3 Relief and Drainage……. 7

1.4 Climate and Vegetation…… 7

1.5 People, Settlement and Land Use…… 9

1.6 Previous Work…….. 9

1.7 Research Problem, Objectives and Scope of the Study…… 15

CHAPTER TWO: GEOLOGICAL SETTING

2.1 Introduction……..…….. 17

2.2 Precambrian Basement Rocks…….. 17

2.2.1 Granulite – perknite – granite association…….. 17

2.2.2 Monzodiorite and granodiorite association……..……. 18

2.2.3. Post-magmatic rocks……..…….…… 18

2.3 Cretaceous Sedimentary Rocks……. 18

2.3.1 Origin of the Benue Trough……. 18

2.4 Tectono-Sedimentary Evolution of the Lower Benue Trough…... 22

2.4.1 Tectonic evolution…… 23

2.4.2 Sedimentary evolution and stratigraphy……. 24

CHAPTER THREE: METHODOLOGY

3.1 Desk Study…….. 30

3.2 Field Mapping…… 30

3.3 Laboratory Sample Preparation and Analysis……. 30

3.3.1 Petrographic Study..…….. 30

3.3.2 Geochemical Analysis…… 31

3.3.3 Geotechnical Study..……. 31

3.3.4 X-Ray Diffraction (XRD) Analysis…… 34

3.4 Data Handling and Presentation of Results…….. 34

CHAPTER FOUR: RESULTS

4.1 Introduction…….…. 35

4.2 Basement Rocks……..... 35

4.2.1 Gneiss…….. 35

4.2.2 Granite…… 37

4.2.3 Pegmatite…… 41

4.3 Sedimentary Rocks…… 42

4.3.1 Sandstone..…….. 42

4.3.2 Shale…… 44

4.4 Quartz Vein....…… 45

4.5 Laterites…….. 46

4.6 Superficial Deposits……... 47

4.7 Structures…… 47

4.7.1 Faults…..…… 47

4.7.2 Joints…… 49

4.8 Baryte Mineralization…… 50

4.8.1 Field Occurrence……..……..…… 50

4.9 Mineralogical and Petrographic characteristics…..…… 54
4.10 Geochemical Data…….. 60
4.11 Geochemistry of Basement Rocks…… 65
4.12 Geochemistry of Lessel Sandstone and Shale……. 73
4.13 Geochemistry of Baryte……. 80
4.14 Geotechnical Characteristics of Barytes……..…….……. 92

CHAPTER FIVE: DISCUSSION, CONCLUSION & RECOMMENDATIONS

5.1 Discussion……..…… 97
5.1.1 Granitic rocks in Lessel-Ihugh area……. 97
5.1.2 Sedimentary rocks in Lessel-Ihugh area…….. 100
5.1.3 Field occurrence and mineralogical features of Lessel-Ihugh barytes... 103
5.1.4 Geochemistry of baryte in Lessel-Ihugh area…….. 105
5.1.5 Geotechnical attributes of baryte in Lessel-Ihugh area..…… 113
5.1.6 Economic geology…… 114
5.2 Conclusion…… 118
5.3 Recommendations…… 122
Contributions to Knowledge……... 123
References……. 124
Appendices…….. 142

LIST OF FIGURES

Figure 1.1: World distribution of major baryte deposits (Bonel, 2005)…… 1

Figure 1.2: Location map of the study area…… 8

Figure 1.3 : Inferred baryte resource estimate of some states in Nigeria (MMSD, 2008)…… 10

Figure 1.4: Distribution of lead-zinc-barite and salt mineralization along the Benue Trough (source: Ene *et al.,* 2012)..…… 12

Figure 2.1: Outline geological map of the Benue Trough and adjacent areas (Zaborski, 1998)……..... 21

Figure 2.2: Proposed stages in the tectonic evolution of the Benue Trough involving active mantle upwelling (Olade, 1975)……... 22

Figure 2.3: Geological map of the Lower Benue Trough region and adjoining areas (Zaborski, 1998)……. 24

Figure 2.4: Generalized stratigraphic subdivisions of the Gboko area in the Lower Benue Trough (Najime, 2010)……. 28

Figure 2.5: The Stratigraphy of the Lower Benue Trough region (Najime, 2010)……. 29

Figure 4.1: Geological map of Lessel and Ihugh area…… 36

Figure 4.2: Rose diagram showing the general structural trend of lineaments in (a) granitic rocks (b) sedimentary rocks ……...……. 47

Figure 4.3: Idealized vertical section of baryte mineralization in basement, sandstone and weathered overburden in Lessel-Ihugh area…… 52

Figure 4.4: Total alkali-silica plot of granitic rocks in the area (Middlemost, 1997)…….. 66

Figure 4.5: A/CNK versus A/NK plot granitic rocks in the area (Maniar and Piccoli, 1989)……..…….. 67

Figure 4.6: Bivariate plot of SiO_2 (wt. %) versus major oxides……..…….. 68

Figure 4.7: Bivariate plot of SiO_2 (wt. %) versus trace elements..…….…….. 69

Figure 4.8: Multi-element spider diagram in granitic rocks from the study area (chondrite normalizing values, Thompson, 1982). ……..... 71

Figure 4.9: Y+Nb versus Rb discrimination diagram for granitic rocks of the area (Pearce *et al*., 1984)…… 71

Figure 4.10: REE distribution pattern in granitic rocks from the study area (chondrite normalizing values, Nakamura, 1974)…….. 73

Figure 4.11: Chemical classification diagram for sandstone samples based on log SiO_2/Al_2O_3 versus log Fe_2O_3/K_2O diagram of Herron (1988)…….. 75

Figure 4.12: CIA ternary diagram, $Al_2O_3 – (CaO + Na_2O) – K_2O$ of sandstones Samples (Nesbitt and Young, 1982)……. 76

Figure 4.13: Multi-element spider diagram in shale and sandstone from the study area (chondrite normalizing values, Taylor and McLennan, 1995)..…….. 77

Figure 4.14: Provenance discriminant function plot of the Lessel Sandstones and Shale (Roser and Korsch, 1988)…….. 78

Figure 4.15: REE distribution pattern of average sandstone and Granitic rocks from the study area (chondrite normalizing values,Nakamura, 1974…... 79

Figure 4.16: REE plot of shale and sandstone from the study area (chondrite normalizing values, Wakita *et al.,* 1971)……. 80

Figure 4.17: Multi-element spider diagram in baryte from Lessel-Mbagwa, Bunde and Ihugh (chondrite normalizing values, Taylor and McLennan, 1981) 83

Figure 4.18: Trace element variations in baryte vein, wall rock and barren host Rock from (a) Lessel-Mbagwa (b) Bunde (c) Ihugh (normalizing values are those of Taylor and McLennan, 1981)……..…… 84

Figure 4.19: REE plot in baryte from Lessel-Mbagwa, Bunde and Ihugh (chondrite normalizing values, Nakamura, 1974)…….…….. 87

Figure 4.20: Comparison of the rare earth elements profiles of average baryte in this study with the surrounding rocks from Lessel-Ihugh area…..…… 89

Figure 4.21: Comparison of the rare earth elements profiles of average baryte with lead-zinc from Lessel-Ihugh area ……...…….. 89

Figure 4.22: Comparison of the rare earth elements profiles of barytes from the study area with seawater dominated hydrothermal fluid……..…….. 90

Figure 4.23: The distribution of rare earth elements in marine baryte, low temperature hydrothermal baryte compared with baryte from Lessel-Ihugh area …….. 90

Figure 4.24: Comparison of the rare earth elements profiles of average baryte in the study area with barytes from marine, diagenetic and hydrothermal environments ……. 91

Figure 4.25: Binary plot of Ce_N/Sm_N against Ce_N/Yb_N showing distribution of baryte, lead-zinc sulphide veins, granitic rocks and sandstones of Lessel-Ihugh area along with various hydrothermal fluids and baryte occurrences in the world……. 92

LIST OF TABLES

Table 1.1: Physical properties of baryte…….. 1

Table 1.2: Ionic radii / electronegativity of selected cations (Griffith and Paytan, 2012)…….……. 2

Table 1.3: Location of baryte resources and their current status of exploration In some parts of Nigeria……... 12

Table 4.1: Major oxides composition in granitic rocks from the study area (all values in weight percent [wt. %] except the ratio)……. 60

Table 4.2: Trace elements concentration in granitic rocks from the study area (all values in parts per million [ppm] except the ratios)……... 61

Table 4.3: Rare earth elements concentration in granitic rocks from the study area (all values in ppm except the ratios)……..….. 62

Table 4.4: Major oxides concentration in sedimentary rocks from the study area (all values in ppm except the ratios)…… 63

Table 4.5: Trace elements concentration in sedimentary rocks from the study area (all values in ppm except the ratios)…..…… 64

Table 4.6: Rare earth elements concentration in sedimentary rocks from the study area…….…… 65

Table 4.7: Average chemical composition of shale and sandstone from the study area compared to those from other sedimentary basins in Nigeria and worldwide……. 74

Table 4.8: Major oxides concentration in mineralized host rocks, baryte vein and lead-zinc vein from the area of study (all values are in wt. %)……. 81

Table 4.9: Trace elements concentration in mineralized host rocks, baryte vein and lead-zinc vein from the area of study (all values are in ppm except the element ratios)……. 82

Table 4.10: Rare earth elements concentration in mineralized host rocks, baryte vein and lead-zinc vein from the area of study (all values are in ppm except the element ratios)…….. 86

Table 4.11: REEs comparison of Lessel-Ihugh baryte against barytes and hydrothermal systems in some parts of the world ……. 88

Table 4.12: Result for moisture content, uniaxial compressive strength and specific gravity in baryte from the study area…… 94

Table 4.13: Major oxides and some selected trace elements in barytes from Lessel-Ihugh area compared with those in other parts of Nigeria …..... 94

Table 4.14: Mineralogical and physical characteristics of Lessel-Ihugh barytes compared with Azara barytes.....…… 96

Table 5.1: Specifications and end uses for barytes…….. 116

LIST OF PLATES

Plate I: Photograph of baryte from (a) Tasmania, Australia (b) Dareta, Anka District, Northwestern Nigeria……...…… 1

Plate II: Uniaxial compressive strength testing of baryte block using the Denison Compression Testing Machine…….…… 33

Plate III: Photomicrograph of banded gneiss from Mbatoo area in (a) plane polarized light (PPL) and (b) crossed polarized light (XPL)..…..…….. 37

Plate IV: (a) Granite exposure in a mining pit at Bunde (N 07°09'28.1", E 009°01'34.9") (b) Granite exposure in Mtema stream channel, southwest of Ihugh Town (N 07°00'30.3", E 008°58'40.8")…….…. 38

Plate V: Photomicrograph of coarse-grained biotite muscovite granite from Mbaakase in (a) PPL and (b) XPL ……. 40

Plate VI: Photomicrograph of medium-grained muscovite granite southwest of Ihugh in (a) PPL and (b) XPL ……..… 40

Plate VII: Photomicrograph of medium-grained muscovite granite from Mbatoo in (a) PPL and (b) XPL …….…… 41

Plate VIII: Pegmatite vein at Mbason area (N 07°00'48.3", E 009°01'22.4")..…. 41

Plate IX: Sandstone exposure northeast of Mtema stream (N 07°00'33.8", E 008°55'43.0")……. 43

Plate X: Sandstone exposure at Mbason, northwest of Ihugh (N 07°00'42.2", E 009°01'25.6")…….. 43

Plate XI: Massive boulders of sandstone at Ajun stream (N 07°00'45.5", E 009°02'02.9")…….. 44

Plate XII: Photograph of Shale outcrop at Kase, northeast of Ihugh (N 07°00'45.0", E 009°02'02.9")……..……. 45

Plate XIII: Quartz vein (in dash lines) at Lessel Mbagwa (N 07°07'58.2", E 009°00'59.4")…… 46

Plate XIV: Photomicrograph of quartz vein from Lessel-Mbagwa area (a) PPL and (b) XPL…….. 46

Plate XV: Slickenside surface on quartz vein (N 07°07'58.2", E 009°00'59.4")... 48

Plate XVI: Sandstone lamina in Shale at Kase, northeast of Ihugh displaced by a fault (N 07°00'45.0", E 009°02'02.9")……...…… 49

Plate XVII: Cross-cutting joints in quartz vein at Lessel-Mbagwa (N 07°08'00.5", E 009°01'03.2")…… 50

Plate XVIII: Baryte mineralization at Tarzoho-Mbaakase, Ihugh (N 06°59'53.6", E 008°59'35.2")…… 51

Plate XIX: Baryte mining pit in Basement Gneiss at Lessel-Bunde (N 07°09'28.1", E 009°01'34.9")…..…..…… 52

Plate XX: (a) Vertical baryte vein in gneiss (b) Baryte vein in gneiss……..…. 53

Plate XXI: (a, b) Vug in baryte sample from Lessel-Bunde with shiny black crystals of galena, greenish-yellow coloured crystals of sphalerite and reddish grains of iron oxide crystals…….. 54

Plate XXII: Photographs of baryte samples from (a) Lessel-Mbagwa (sample NM) (b) Lessel-Bunde (sample NO5) (c) Tarzoho-Mbaakase, Ihugh (sample NQ2) (d) and galena from Lessel-Mbagwa…….…. 55

Plate XXIII: Photomicrograph of baryte mineralized gneiss from Bunde area in (a) PPL and (b) XPL …….. 56

Plate XXIV: Photomicrograph of baryte mineralized gneiss from Bunde area in (a) PPL and (b) XPL…. ……..…… 57

Plate XXV: Photomicrograph of baryte mineralized gneiss from Bunde area in (a) PPL and (b) XPL ……..…..… 58

Plate XXVI: Photomicrograph of baryte mineral in (a) PPL and (b, c) XPL… 59

Plate XXVII: Baryte heap at (a) Lessel-Mbagwa (b) Bunde (c) Tarzoho-Mbakase, Ihugh areas (d) Gullies produced during mining activities…. 118

LIST OF APPENDICES

Appendix I: X-Ray diffraction (XRD) sample identification: NM (Lessel-Mbagwa baryte)…….…… 142

Appendix II: XRD sample identification: NQ2 (Ihugh baryte)…….. 143

Appendix III: XRD sample identification: NO5 (Bunde baryte)……..….. 144

Appendix IV: Provenance Discriminant Function Values……..…… 145

Appendix V: Scatterplot of La/Ce, La/Pr, Ce/Nd and Ce/Pr ratios…… 145

Appendix VI: Standard sedimentary composition used for normalizing the REE concentrations (ppm) in sedimentary rocks…… 146

APPENDIX VII: Lineament trends in granitic rocks and sandstones…… 147

CHAPTER ONE

INTRODUCTION

1.1 GENERAL INTRODUCTION

Baryte is the principal mineral of barium with chemical formula $BaSO_4$ in the proportion of 66% BaO and 34% SO_3**.** The mineral is sometimes referred to as "heavy spar" or "spar", meaning a transparent or translucent, readily cleavable, crystalline mineral having a vitreous luster (Thrush, 1968). Baryte is a relatively dense mineral with specific gravity of about 3.0 - 4.4 g/cm^3 which is its most distinct feature. Other physical properties of baryte are presented in Table 1.1.

Table 1.1: Physical properties of baryte (modified from Harben, 1999)

Property	**Description**
Colour	Pure baryte appears white to transparent but depending on the impurities (strontium and iron oxides) present in the mineral, the colour may vary from light shades of grey – blue – yellow – brown. (Plate I)
Hardness	2.5 – 3.5
Habit	The crystals commonly appear as tabular or leaf-like aggregates with edges projecting into crest-like or rosette forms and also as prismatic, compact (which may have the appearance of massive gypsum) or grainy masses.
Cleavage	Perfect cleavage

a)  b) 

Plate I: Photograph of baryte from (a) Tasmania, Australia (b) Dareta, Anka District, Northwestern Nigeria.

Baryte rarely exists in nature as a pure end member but rather as solid solutions. Solid solution appears to be continuous between baryte and celestine ($SrSO_4$) (Hanor, 2000; Zhu, 2004; Monnin and Cividini, 2006) but discontinuous with anhydrite ($CaSO_4$). The substitution of Ba in baryte ($BaSO_4$) with other cations (such as K^+, Mg^{2+}, Ca^{2+}, Sr^{2+}, Ra^{2+}, Pb^{2+}, La^{3+}, Ce^{3+}, Lu^{3+}, Eu^{2+}) depends on its degree of similarity in ionic charge, ionic radius and electronegativity (Hanor, 2000) (Table 1.2).

Table 1.2: Ionic radii / electronegativity of selected cations (Griffith and Paytan, 2012).

Cation	Ionic radius (Angstroms)	Electronegativity (Pauling Scale)
K^+	1.33	0.82
Mg^{2+}	0.72	1.31
Ca^{2+}	1.00	1.00
Sr^{2+}	1.16	0.95
Ba^{2+}	1.36	0.89
Ra^{2+}	1.43	0.90
Pb^{2+}	1.18	2.33
La^{3+}	1.05	1.10
Ce^{3+}	1.01	1.12
Lu^{3+}	0.85	1.27
Eu^{2+}	1.17	1.20

Baryte occurs in diverse geological environments in a host of sedimentary, metamorphic and igneous rocks which span from Early Archean to Late Phanerozoic (Bonel, 2005). Most of the baryte in the Earth's crust has been formed through mixing of fluids, one containing Ba leached from silicate minerals and the other fluid containing sulphate (Hanor, 2000). Baryte is usually associated with one or more of the following minerals: Celestine ($SrSO_4$), galena (PbS), sphalerite (ZnS), pyrite (FeS_2), quartz (SiO_2), calcite ($CaCO_3$), dolomite ($Ca,Mg(CO_3)$), marcasite (FeS_2), chalcopyrite ($CuFeS_2$), fluorite (CaF_2), siderite ($FeCO_3$) and witherite ($BaCO_3$). China is the leading producer of baryte in the world followed by India with the Mangampet deposit in Cuddapah district of Andhra

Pradesh being the single largest deposit in the world. The distribution of major baryte deposits in some parts of the world is presented in Figure 1.1.

1.1.1 Types of Baryte Deposit

Baryte deposits can be classified based on the mode of occurrence into the following:

a. Bedded and Residual Deposits

b. Veins and Cavity Filling Deposits

a. Bedded and Residual Deposits

Bedded deposits are those formed by the precipitation of barytes at or near the sea floor of sedimentary basins. The ore fluid is generated by migration of reduced saline fluids and are concentrated by major basin controlling faults. Baryte may occur either as a principal mineral or cementing agent associated with stratiform massive sulphide deposits (Harben and Kužvart, 1996). Most bedded deposits occur in sequences of sedimentary rocks characterized by abundant chert, black siliceous shale and siltstone referred to as 'black bedded baryte'. Bedded deposits of baryte are associated with rocks of age ranging from Precambrian to Tertiary (especially from Early to Mid-Paleozoic) (Ramos and de Brodtkorb, 1989). Individual beds are fine-grained, massive to laminated and may contain about 50 – 95% baryte. The bedded deposits are the most valuable and economically most important deposit type because they are usually large and have higher grades (Lorenz and Gwosdz, 2003). Residual deposits are derived from the weathering of baryte-bearing rocks in which baryte is present as loose fragments embedded within residual soil or clay e.g. Georgia and Missouri baryte deposits (Bonel, 2005). Clark *et al.* (1990) further subdivided the bedded baryte deposits into five groups based on its depositional environment as follows:



Figure 1.1: World distribution of major baryte deposits (after Bonel, 2005)

i. Bedded deposits with base-metal sulphides (cratonic rift type) associated with alkali volcanic rocks, e.g. Meggen and Rammelsberg, Germany; Ballynoe and Silvermines, Ireland; Selwyn Basin, Canada and Red Dog, Alaska.

ii. Bedded deposits without base-metal sulphides (continental margin type), e.g. Arkansas and Nevada deposits, USA; Jiangnan and Qinling deposits in China.

iii. Bedded deposits associated with volcanic series, e.g. Kuroko type ore, Japan; Buchans deposit, Canada.

iv. Stratiform baryte deposits e.g. Mangampet deposit in Andhra Pradesh, India.

v. Exogenetic baryte deposits: These are unconsolidated alluvial or residual deposits formed by erosion or weathering processes occurring on or near the surface of the earth e.g. Krakow deposit, Poland.

b. Veins and Cavity Fillings

These are epithermal deposits which form by the precipitation of hot barium-enriched fluids in faults, joints, bedding planes, breccia zones, solution channels and cavities as a result of fluid mixing or reduced pressure and/or temperature. In some cases, the ore fluid dissolves the surrounding host rocks (especially limestone and dolomite) and baryte is deposited in its stead, thus forming replacement deposits. The resulting veins are characterized by sharp contacts, extensive pinching and swelling, and extreme variations in length and depth. The veins consist predominantly of barytes (80% $BaSO_4$ and <5% $SrSO_4$), sulphides (galena, pyrrhotite [FeS_2 – magnetic pyrite]), iron, manganese oxides as well as fluorite, calcite and quartz. This type of deposits are generally smaller than the bedded deposits, examples include Dreislar and Rhineland-Palatinate vein deposits in

Germany; Les Arcs deposit in France and Pennine ore fields in the United Kingdom (Lorenz and Gwosdz, 2003).

1.1.2 Uses of Baryte

1. The high density, non-corrosive, non-abrasive, chemical inertness and non-toxic nature of baryte makes it a suitable weighting agent or drilling mud which is used in drilling shafts of gas and oil wells. Baryte makes the mud dense and therefore prevent blow-up ensuing from oil and gas pressure.
2. Baryte is a raw material used in the production of barium chemicals such as:

   Ba-metal which is used to remove traces of gases in vacuum tubes. $BaCO_3$, $BaCl_2$, Ba(OH) are used to control efflorescence and scum from forming on brick and ceramic materials during its manufacture.
3. Baryte is also used as an additive in the manufacture of plastics, paper, paints, enamels and leaded glass.
4. Baryte significantly blocks x-rays and gamma rays hence; it is used as a contrast medium in medical x-ray examination and an aggregate in high density concrete to shield against radiation.

1.2 LOCATION AND ACCESSIBILITY

The study area lies within two quarter sheets: 271 Gboko SE and 272 Katsina-Ala SW in the southeastern part of the present Benue State, north-central Nigeria. It is bounded by latitudes $7^o00'00"$ and $7^o10'00"$ N and longitudes $8^o58'00"$ and $9^o03'00"$ E and covers an area of about 171 km^2 (Fig. 1.2).

The major road in the area runs from Gboko through Lessel, Ge to Ihugh. This road together with a network of footpaths make the area generally accessible.

1.3 RELIEF AND DRAINAGE

The study area is generally an undulating lowland. The eastern half of the area shows gradual rise from plains and is characterized by gently sloping highlands that are about 220 to 236 m above sea level. The terrain on the western half of the area is dominated by low lands with elevation well below 150 m.

Most of the rivers in the area are ephemeral and usually dry up during the dry season; very few of them flow all year round. The Nienga, Ukyohav and Umaa streams which are tributaries of the Konshisha River flow in a southeasternly direction. Agbudu and Ingye streams are tributaries of the Katsina-Ala River and runs in a southwesternly direction. Other streams such as Mtema, Uire and Kpa flow in a northeastern direction. These rivers as well as their tributaries make up the drainage system in the area and display a dendritic pattern of flow.

1.4 CLIMATE AND VEGETATION

The project area lies in north-central Nigeria, which has Tropical Savannah Climate with distinct wet and dry seasons. Rainfall is concentrated in the wet season, which extends from April to October with an annual rainfall of about 1000 – 1500 mm. The dry season begins in November and ends in March is characterized by high mean temperatures of about 32º C. A large diurnal variation in temperature due to the harmattan is experienced between December and January during which temperature may fall below 28ºC (Bunnett and Okunrotifa, 1984).

The vegetation type in the study area is typically the Guinea Savannah and is characterized by scattered trees, shrubs and dense growth of tall grasses. Trees common in the area include; raffia palm, locust bean, shea butter, doka, cashew.

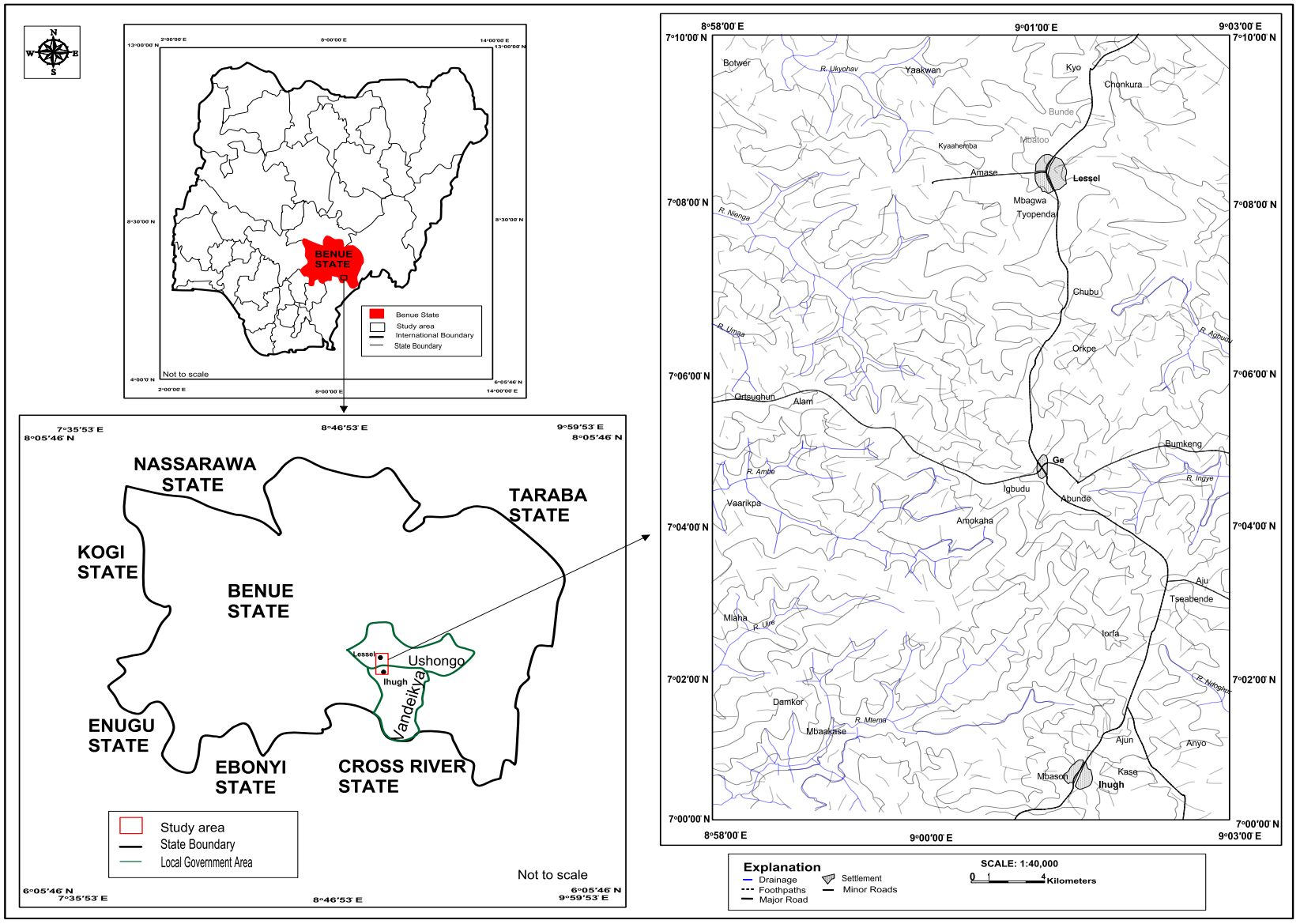


Figure 1.2: Location map of the study area

1.5 PEOPLE, SETTLEMENT AND LAND USE

The inhabitants of the area are basically the Tiv ethnic group. The Tiv people are hospitable and have a rich and diverse cultural heritage which finds expression in music, dance and clothing. The area is a fertile grassland and for the most part suitable for agriculture (arable, citrus and pastoral farming) which is the backbone of the local economy. A great majority of the populace are farmers; producing yam, cassava, groundnut, rice, oranges and mangoes. In areas where there is an appreciable amount of mineral deposit (baryte), the people are engaged in artisanal mining activities.

The key settlements in the study area are Lessel and Ihugh. Other minor nucleated settlements are Ge and numerous smaller villages.

1.6 PREVIOUS WORK

Earlier works on the Nigerian baryte indicate that baryte occur as gangue in galena and sphalerite veins (Farrington, 1952; McConnel, 1949). The baryte resource of Nigeria started gaining recognition as from 1951. Bogue (1951) presented a report of baryte prospect near Gabu in Ogoja Province in the present Cross River State. Occurrences of baryte have been reported in 1957 edition of the "Minerals and Industry in Nigeria" yearbook at Lefin in Ogoja Province; Aba-Gbandi, Keana and Akiri in Benue Province and Dumgel in Adamawa Province (Oden, 2012). The Geological Survey of Nigeria in 1959 estimated baryte reserve to be 41,000 tonnes at a depth of 20 meters for the Benue Valley deposits in the Azara locality.

In 2008, the Nigerian Geological Survey Agency embarked on the evaluation of newly reported deposits in the present Cross Rivers, Benue, Nassarawa, Plateau and Taraba States (Table 1.3). The inferred resource of baryte in these states was put at

21,123,913 metric tons (Fig. 1.3). Further exploration activities revealed additional areas with favourable geological setting for baryte mineralization namely: Liji Hill, Gombe Town, Ganye, Suwa and Sabin areas northeast Nigeria in addition to Dareta, Tofa Forest Reserve, Rebeku and Yarkatsina areas in northwestern Nigeria (Table 1.3).

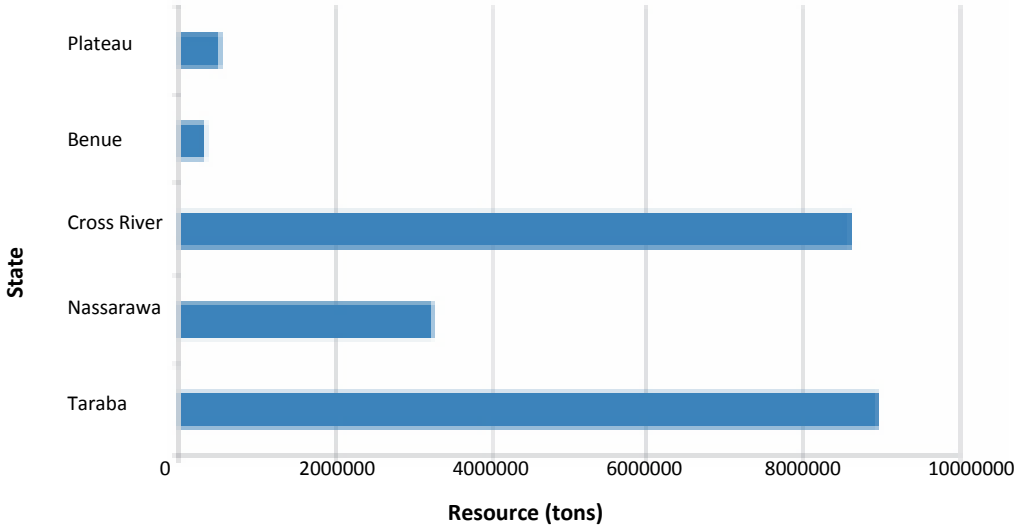


Figure 1.3 : Inferred baryte resource of some states in Nigeria (Source: MMSD, 2008).

Daspan and Imagbe (2010) reported the occurrence of baryte veins corresponding to the major Anka fault system in metasedimentary rocks at Dareta-Tungan Kudaku area, northwest Nigeria. According to Akpeke *et al.* (2006), MMSD (2008) and Ekwueme and Akpeke (2012) baryte mineralization in southeastern Nigeria (Obubra, Yakur, Akamkpa, Biase, Nkarasi, Okpoma and Omoji areas of Cross River state) is localized mostly along the boundary between the Basement rocks (migmatite, gneiss, granite), Cretaceous sediments (sandstone) and also in dolerite. Edu (2006) also observed that baryte is hosted in basement gneisses, porphyritic and fine grained granite in some parts of the present Taraba State, northeastern Nigeria.

Akande *et al.* (1989) and Oden (2012) reported that most baryte mineralization in Nigeria are hosted in the Cretaceous sediments of the Benue Trough and are associated with lead-zinc-flourite vein ore bodies and occasionally with salt deposits (Fig. 1.4)**.** Oden (2012) further documented the occurrence of baryte across eight major areas within the Benue Trough (Adamawa, Benue, Cross River, Ebonyi, Gombe, Nassarawa, Taraba and Plateau States) (Table 1.3). The geology and stratigraphy of the Lessel and Ihugh areas have been captured in the works of Reyment (1965), Murat (1972), Nwachukwu (1972), Dandume (1978), Kogbe (1989), Najime (2010) and Obiora (2012). The field occurrence, mineral association and paragenesis of baryte in some parts of the Benue Trough have been documented by Farrington (1952), Omada (1985, 1987), Akande *et al.* (1989, 1992), Omada and Ike (1996), Ekwueme and Akpeke (2012) and Oden (2012). Nwafor *et al*. (1997), Ministry of Mines and Steel Development (2008) and Najime (2010) reported the occurrence of baryte at Lessel. In a more recent study, Oden (2012) also described their field characteristics and quality of baryte occurrences in Ihugh and Lessel areas.

Ajayi (1987) carried out gravity survey of the Middle Benue Trough and proposed that baryte occurrence in this part of the trough was most probably formed as a result of the interplay of volcanic intrusions with brine water from buried salt domes. Oladapo and Adeoye-Oladapo (2011) recorded high gravity and low conductivity values influenced by the density of concealed baryte veins at Tunga in the Middle Benue Trough.

Several models have been suggested for the origin of baryte in the Benue Trough; Farrington (1952) suggested a magmatic hydrothermal origin for the lead-zinc-baryte mineralization in the Benue Trough. Ofoegbu and Odigi (1989) suggested that Pb-Zn

sulphide, baryte and other ore mineralizations in the Benue Trough are closely associated with magmatic episodes and are mainly localized in steeply dipping faults and fracture systems of predominantly N-S, NE-SW trend. Hot mantle materials involved in the rifting of the Trough provided the thermal energy needed for upward movement of ore fluids (Ofoegbu and Odigi, 1989).

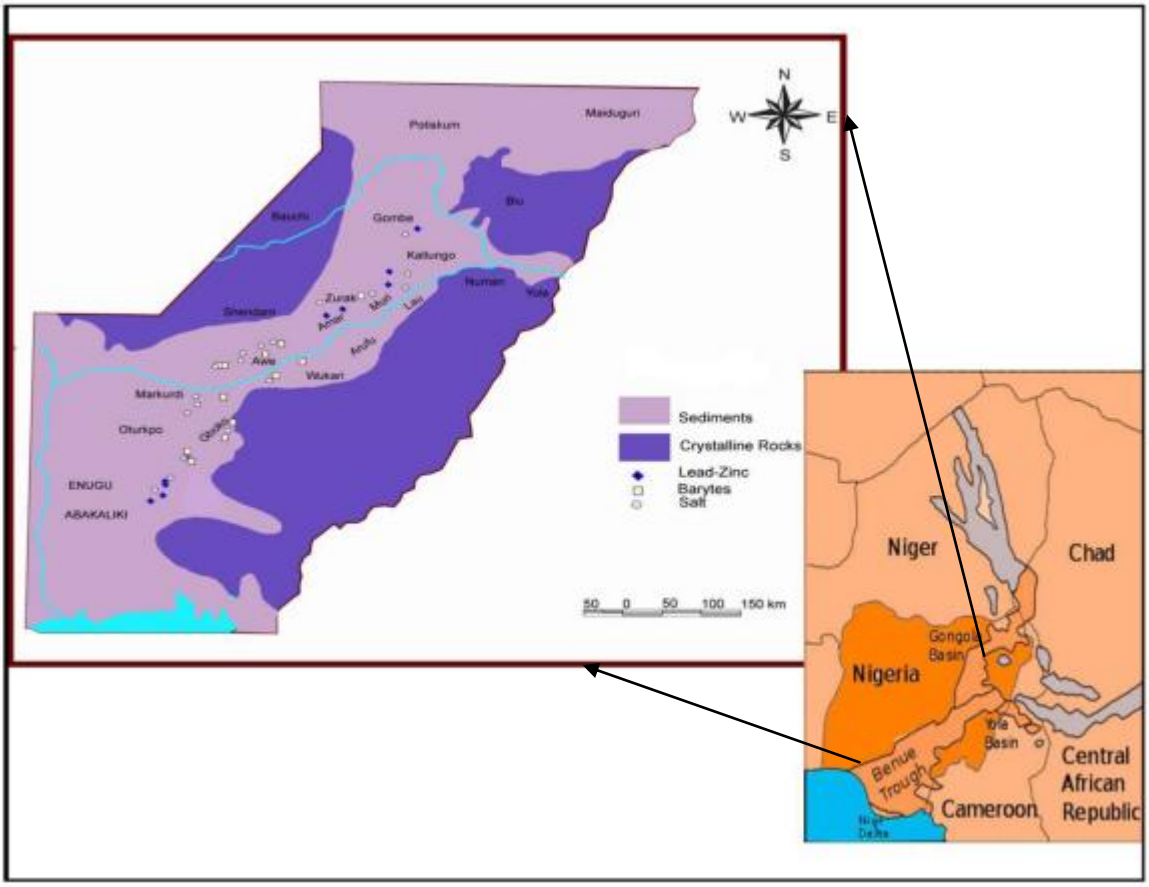


Figure 1.4: Distribution of lead-zinc-barite and salt mineralization along the Benue Trough (Inset sketch map of Nigeria showing the Benue Trough) (source: Ene *et al.*, 2012).

Reyment (1965) alleged that volcanic rocks generated the hydrothermal fluids from which the ore was deposited. Orajiaka (1964) considered both sedimentary and igneous rocks to be possible sources of the mineralizing fluid. Omada (1985) stated that Ba (barium) was mobilised from the host rock and then concentrated in fractures with the aid

of hydrothermal fluids. Omada and Ike (1996) further reported that the geochemical signature of baryte in the Middle Benue Trough was derived from hydrothermal fluids of igneous origin.

Table 1.3: Location of baryte resources and their current status of exploration in some parts of Nigeria.

STATE	LOCATION	RESERVE ESTIMATION (TONES)	STATUS	REMARK
1. Nassarawa*	Azara, Akiri, Aloshi, Chiata, Gidan Bera, Gidan Tailor, Wuse Kuduku, Ribi	730,000 recorded by NMC at Azara, Akiri and Wuse alone (5 veins)	Mining in progress by private companies and artisanal miners. NMC has divested	Very rich state, grade ranges from poor to good, reserve could be improved through further exploration
2. Plateau	Panyam (Wase), Faya	Yet to be determined	Registered companies and artisanal miners at work	Further exploration could increase stok of veins
3. Taraba*	Mbanga Petel, Mbanga 3 corner, Juo, Gidan Waya, Kauyen Isa, Bakuyu, Ibua, Kumar, Pupule, Apawa 1 & 2, Didango, Suwa	Yet to be determined	Active informal and some organized mining in progress	Further exploration necessary to improve the known stock of veins and boost reserve
4. Benue*	Ambua, Torkula, Makurdi, Kaseyo, Yandev, Orgba, Ihugh, Lessel, Tombu, Korinya, Iye, Zanzan, Logo	Yet to be determined	Active informal and organized mining in progress	Exploration work necessary to improve the known stock of veins and boost reserve
5. Adamawa	Ganye, Suwa, Sabin Village	Yet to be determined	Only Suwa and Sabin deposits are currently mined	Further exploration necessary
6. Cross River*	Okumurutet, Okangha, Agoi Ekpo, Agoi Ibami, Akept1, Akpet Central, Okurike, Lefin, Bitol, Ugbem	Yet to be determined	Enormous informal and organized mining in progress	Large scale operators needed and further exploratory work very necessary in this state with the highest prospect
7. Gombe	Liji Hill, Gombe Town	Yet to be determined	Mining activity started here recently	Requires further exploration
8. Ebonyi	Ishiagu	Yet to be determined	No mining activity is going on	Requires further exploration

* Major producing states (Source: Oden, 2012)

Ezepue (1984), Uma and Leohnert (1992), Tijani, *et al.* (1996) believed that igneous intrusions caused changes (pressure and temperature conditions probably entrained precipitation and concentration from fluids to form the ore) in the geochemistry of the surrounding rocks thus releasing important masses of volatiles. Juvenile and connate brine origin was proposed by Offodile (1976a) advocating that the brines evolved from connate water by osmotic filtration or from meteoric water by solution of evaporites in the course of sinking to great depth in the sedimentary basin. Russell (1978) put together a circulating brine convection model for Irish base metal mineralization whose mineralization is almost similar to that of the Benue Trough. Olade and Morton (1985) suggested that brine circulation was driven by magmatic intrusions.

Basinal brine source was adopted by Akande *et al.* (1989) who carried out fluid inclusion and isotope studies on barytes in the Middle and Lower Benue Trough. These authors noted that the mineralizing fluids were saline brines (14 to 21 equiv. wt% NaCl) containing hydrocarbons with fluid temperatures of between 95 and 200^{o} C. Their Sr and Pb isotopic data indicated that the metal ore components were sourced from the Lower Paleozoic gneisses and migmatites while sulphur data suggested that sulphur was derived from Cretaceous evaporite source within the trough. Sulphur isotope values reported by Akande *et al.* (1989) matches that of the Lower Cretaceous seawater sulphate of Lieben *et al.* (2000) which have been interpreted by Grandia *et al.* (2003) to be consistent with mixing of metal-rich brine with sulphur-rich fluid of Upper Cretaceous and Lower Paleocene age.

Similarly, lower temperatures and salinities of fluid inclusions in baryte from Alston Block of the North Pennine Orefields indicate that baryte was deposited during the waning stages of hydrothermal circulation, under cooler conditions when sources of metals within the basement and/or igneous intrusions became depleted (Bouch *et al.*, 2008). The study of Bozkaya and Gokce (2004) on the rare earth element geochemistry of Karalar baryte veins (Southern Turkey) showed that baryte precipitated from seawater dominated hydrothermal fluids.

1.7 RESEARCH PROBLEM, OBJECTIVES AND SCOPE OF THE STUDY

Since the Federal Government banned importation of baryte in 2003, high priority has been placed on exploration and exploitation of the baryte deposits in the country. The bulk of the baryte mined in Nigeria are used as heavy mud in oil-well drilling. Hitherto, the demand for oil and gas remains strong and demand for baryte may probably continue to grow giving the fact that further exploration and development of wells will consequently boost baryte consumption.

So far, as can be ascertained, there has not been any detailed work on geochemistry and genesis of baryte mineralisation in the Lessel and Ihugh areas. There is therefore, a need to characterize the baryte mineralization in the area using major oxides and trace elements composition and other physical parameters which will serve as guide to further exploratory work. This research work focuses on the geological and geochemical factors controlling baryte mineralization in the area. The objectives of this study, therefore, are:

i. To produce a geological map of the study area on a scale of 1:40,000

ii. To establish the origin of the baryte mineralisation based on petrographic and geochemical attributes of the baryte veins, host rocks and barren rocks.

iii. To determine the variety (or varieties) of the baryte and its quality with respect to standard quality specifications.

In line with the set objectives, this research work essentially involved elaborate desk study to review the existing literature on the area. Field mapping commenced with reconnaissance survey followed by detailed mapping. Rock and baryte vein samples were collected during field mapping and subjected to laboratory analyses. The results obtained were interpreted based on background geological knowledge of the area and geochemical behaviour of elements in geological systems with the aid of variation, classification, geotectonic, discrimination, spider and rare earth elements diagrams. The nature of the mineralization and geotechnical attributes was established by comparing barytes from Lessel-Ihugh area with similar studies on baryte mineralization in parts of Nigeria and else where in the world.

CHAPTER TWO

GEOLOGICAL SETTING

2.1 INTRODUCTION

The Benue Trough is a linear northeast-southwest trending basin about 800 km long and 90 km wide on the average. The Benue Trough is considered to have originated as an aulacogen on the Precambrian shield resulting from the separation of the African and South American continents in the Early Cretaceous (King, 1950 and Olade, 1975). The Cretaceous rocks filling the trough are bordered on either side by the basement complex rocks of ages ranging from Precambrian to Early Paleozoic (Ofoegbu, 1985).

2.2 PRECAMBRIAN BASEMENT ROCKS

The Precambrian geology of southeast Nigeria is folded with northerly (NNE to NNW) axes, comprising parts of Gboko, Katsina-Ala, Takum and Obudu and bordered to the west by the Benue Trough. The igneous bodies recognized are of granulite – perknite – granite association, monzodiorite – granodiorite association and post-magmatic rocks (Umeji

, 1981).

2.2.1 Granulite – Perknite – Granite Association

The ultramafic perknite forms a NNW-SSE aligned ridge within the enderbitic granulite southwest of Obudu. The Obudu Massif forms part of the western part of the Bamenda Massif which underwent Pan-African polyphase deformation and polymetamorphism, producing N-S trending belt of migmatites, gneisses, schists, amphibolites and quartzites (Rahaman *et al.*, 1981; Ukaegbu and Ekwueme, 2005).

2.2.2 Monzodiorite and Granodiorite Association

Hypersthene-quartz monzodiorite and hornblende-pyroxene granodiorite plutons form isolated domes and high rugged relief often having discordant contact relations with the granulite. The monzodiorite forms NNE-SSW oriented elongate hills east of Katsina-Ala River. The granodiorite is exposed between Gboko and Katsina-Ala. Outcrops of these rocks make up the Mkar Hill and other low land mound exposed along the Yandev – Katsina-Ala road cutting (Umeji, 1981). Obiora (2012) documented the Precambrian Basement rocks around Ityowanye and Katsina-Ala to comprise of banded gneiss intruded by non-porphyritic and porphyritic hornblende-biotite granitoids. Umeji and CaenVachette (1983) gave the Rb/Sr isochron ages of these granitoids to be 540 $\pm$ 86 Ma.

2.2.3. Post-magmatic Rocks

The pyroclastics and lavas associated with volcanic activities are scarce in other parts of the Benue Trough but in the Gboko area however, these post-magmatic rocks form the NE-SW trending Gboko Hill and Ikyuen Hill (Umeji, 1981). Najime (2010) and Nwajide (2012) documented the post Pan-African rocks at Gboko to comprise of basalts, trachy-andesites, dacites, syenites, gabbros and quartz diorite which exhibit conspicuous NE-SW lineament parallel to the Benue Trough.

2.3 CRETACEOUS SEDIMENTARY ROCKS

2.3.1 Origin of the Benue Trough

The Benue Trough is a sediment filled NE-SW trending structure (Cratchley and Jones, 1965; Burke and Whiteman, 1970). Benkhelil (1982) also described it as an

elongated sedimentary basin extending over 800 km from the Niger Delta Basin in southern Nigeria to northeastern Nigeria where it bifurcates into an E-W trending Yola Basin and a northeast trending Gongola Basin (Fig. 2.1).

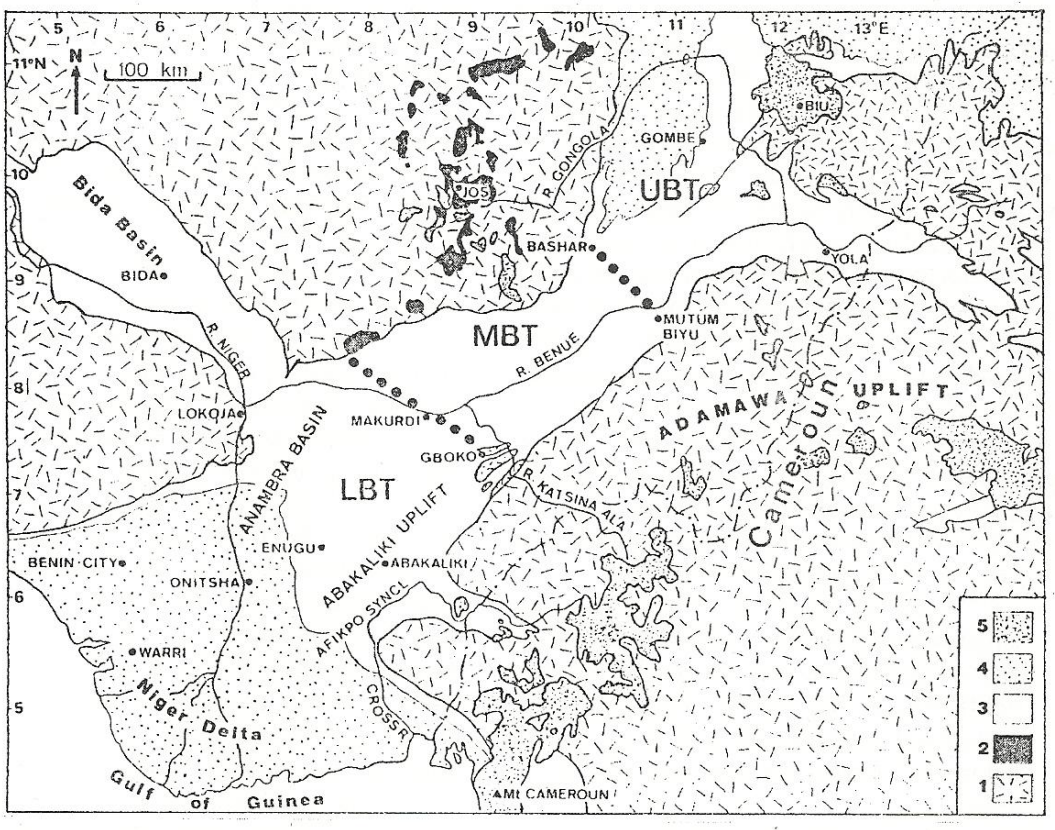


Figure 2.1: Outline geological map of the Benue Trough and adjacent areas. Lower Benue Trough (LBT), Middle Benue Trough (MBT) and Upper Benue Trough (UBT). (1) Precambrian rocks (2) Mesozoic (Anorogenic) Granites (3) Cretaceous sedimentary rocks (4) Post-Cretaceous sediments (5) Cenozoic-Recent basalts including those of the Cameroun line (after Zaborski, 1998).

The origin of the Benue Trough is intricately linked to the opening of the Atlantic Ocean in the Early Cretaceous and several models have been proposed to explain its origin. King (1950) regarded the Benue Trough, Bida Basin/Gao Trough as extensions of the rift which produced the Equatorial and South Atlantic oceans respectively. Lees (1952) described the trough to be a compressional downwarp induced by deep seated

basement contraction. Cratchley and Jones (1965) are of the opinion that the Benue Trough was a rift and on the basis of gravity data inferred marginal faulting along most of its middle and upper parts, the faults being concealed by Cretaceous sediments. Stoneley (1966), Uzuakpunwa (1980), Hoque (1981, 1984) attributed the origin of the trough to rifting. Wright (1968) related the opening and slight Santonian closure of the trough to the separation of the Africa and South America which resulted to wave-like folding event propagating from south-west to north-east along the Benue Trough. Burke *et al.* (1971, 1972) (Fig. 2.2b), Burke and Whiteman (1973), Burke and Dewey (1974), Olade (1975, 1979) and Wright (1981, 1989) associated the formation of the trough with the breakup of the Afro-Brazillian plate in the Early Cretaceous and thus regarded it as a failed arm of the triple rift junction developed over a Cretaceous hotspot located beneath the present day Niger Delta.

Illies (1970) and Wright (1981) associated the rifting along the Benue Trough to doming and volcanism. Grant (1971) proposed a rift-rift-fault triple junction with the faulted arm along the Benue Trough representing an aulacogen. Nwachukwu (1972) regarded the Benue folding as caused by the collision of continental plates during the Cenomanian and Santonian thereby producing two folding phases. However, Olade (1975, 1976, 1979) related the Early Cretaceous magmatism to hotspot activity and interpreted the Benue Trough as an aulacogen related to intermittent mantle upwelling (Fig. 2.2a). Burke and Dewey (1973) and Ofoegbu (1984a, 1984b, 1984c, 1988) suggested that evolution of the trough involved the rise of a mantle plume, followed by updoming and development of lines of weakness marginal to the plume.

Freeth (1978a, 1978b, 1979a, 1979b, 1990) suggested a subduction model for the present-day Lower Benue Trough which he believed to be floored by oceanic crust. Benkhelil (1982), Benkhelil and Robineau (1983) and Maurin *et al.* (1986) proposed a strike-slip model for the Benue Trough which developed as extension of equatorial oceanic fracture zones (Romanche, Chain and Charcot fractures) onto the African continent. Benkhelil (1989) retreated slightly from a pure strike-slip model regarding the evolution of the Benue Trough as best explained by a combination of extensional and strike-slip movements. Fairhead (1988a, 1988b) (Fig. 2.2c), Fairhead and Green (1989), Fairhead and Binks (1991), Binks and Fairhead (1992) and Genik (1993) matched the separation of Africa and South America with its effects on the African plates and the development of a closely linked rift system known as the West and Central Africa Rift System (WCARS).

The WCARS developed within Pan-African lines of weakness (Maurin and Guiraud, 1993) weakened by the underlying St. Helena hotspot (Morgan, 1983; O'Connor and Duncan 1990). According to Guiraud and Maurin (1991, 1992) the Benue Trough and the Central African Shear Zone (CASZ) are regarded as ancient shear zones reactivated during the Cretaceous times with crustal thinning and ultimately sedimentation extending over a wider area than the actual zone of faulting. Shear movements originating along the transform faults of the Equatorial Atlantic due to differential opening between the Central and South Atlantic Oceans were transmitted into the African plate as sinistral and dextral strike-slip movement along the Benue Trough and the CASZ respectively.

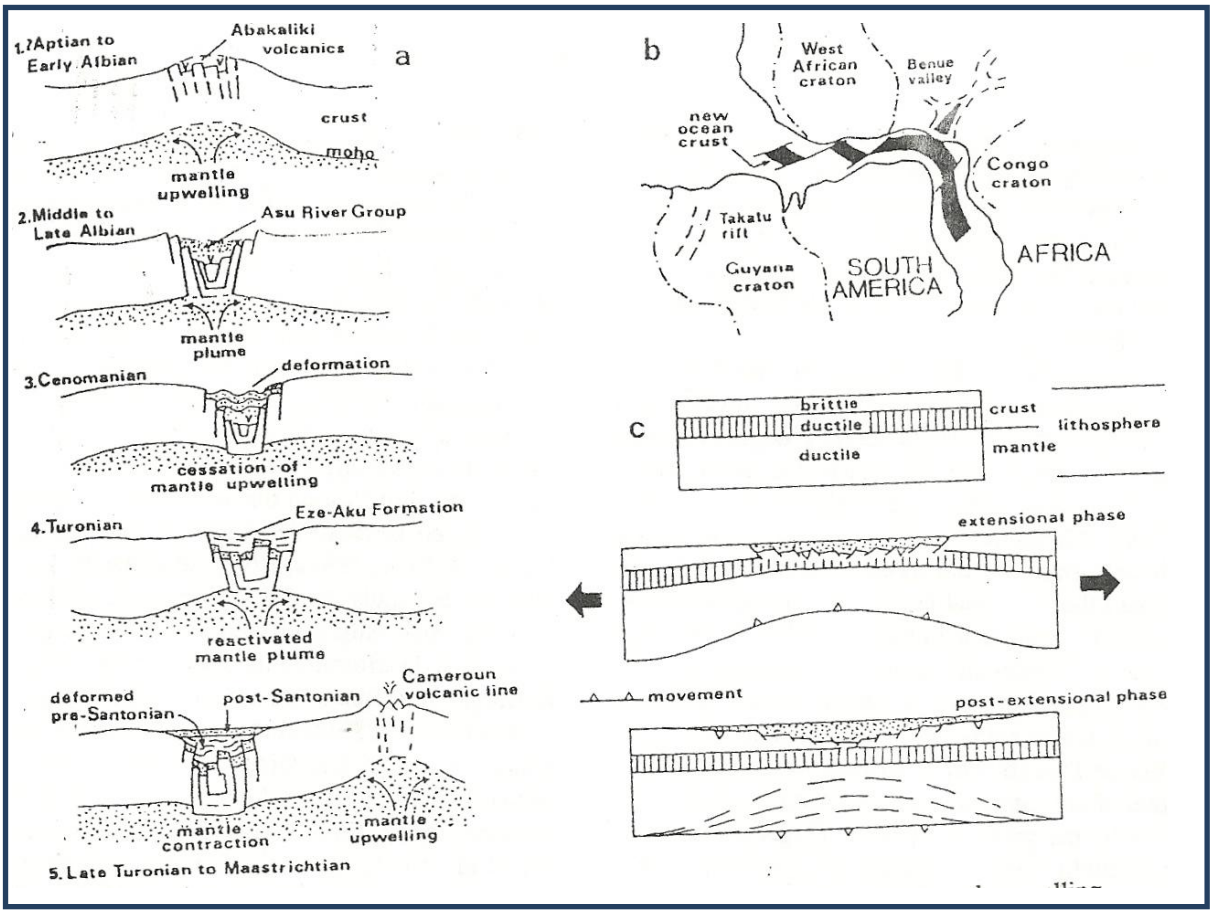


Figure 2.2: (a) Proposed stages in the tectonic evolution of the Benue Trough involving active mantle upwelling (after Olade, 1975). (b) Sketch map of the Gulf of Guinea area in the Early Cretaceous with the Lower Benue Trough floored by oceanic crust (after Burke *et al.*, 1971, 1972). (c) Lithospheric model for the WCARS basins involving extension and passive upwelling (after Fairhead, 1988b).

2.4 TECTONO-SEDIMENTARY EVOLUTION OF THE LOWER BENUE TROUGH

The Lower Benue Trough extends roughly as far north as a line running through Makurdi and along the course of the Katsina-Ala River. The line corresponds to the "Gboko line" of Whiteman (1982) across which the pre-Santonian depocentres of the Lower and Middle Benue Trough are offset (Fig. 2.3).

2.4.1 Tectonic Evolution

The tectonic evolution of the Lower Benue Trough was controlled by three major tectonic phases (Murat, 1972). The first phase commenced during the Albian and is characterized by movements along major NE-SW trending faults resulting in the formation of the rift-like Abakaliki-Benue Trough. To the northwest, the limit of the basin was the Benin-Benue Hinge Line (fault zone) beyond which no pre-Upper Santonian sediments have been reported. Between the hinge line and the Abakaliki Trough, shelf deposits were laid down on the Anambra Platform. On the Calabar Flank, sedimentation was governed by major SE trending faults.

The second phase (Upper Santonian to Lower Campanian) was characterized by compressional movements along the established NE-SW trend which resulted in folding and uplifting of the Abakaliki-Benue Folded Belt. The Abakaliki uplift coincided with the subsidence of Anambra Platform and the axis of the basin was displaced to a position SW of the Benue Folded Belt and NW of the Abakaliki Uplift. A new structural unit, the relatively shallow Dahomey Embayment appeared to the west of the Benin Hinge Line as a result of an active NNE-SSW fault system. With the onset of the Abakaliki folding phase, a large number of intermediate to basic intrusions occurred accompanied by lead-zinc mineralization (Farrington, 1952).

The third phase occurred towards the end of the Eocene. Periods of erosion and non-deposition during the Middle and Upper Eocene were experienced in the eastern part of the Niger Delta downdip of the Abakaliki Plunge and the Calabar Flank whereas a large deltaic complex was deposited in the downdip Anambra Basin. These positive movements of blocks bounded by NE-SW and NW-SE trending faults, preceded the

subsidence of the Oligocene and Younger Niger Delta Basin along the NW-SE fault trend.

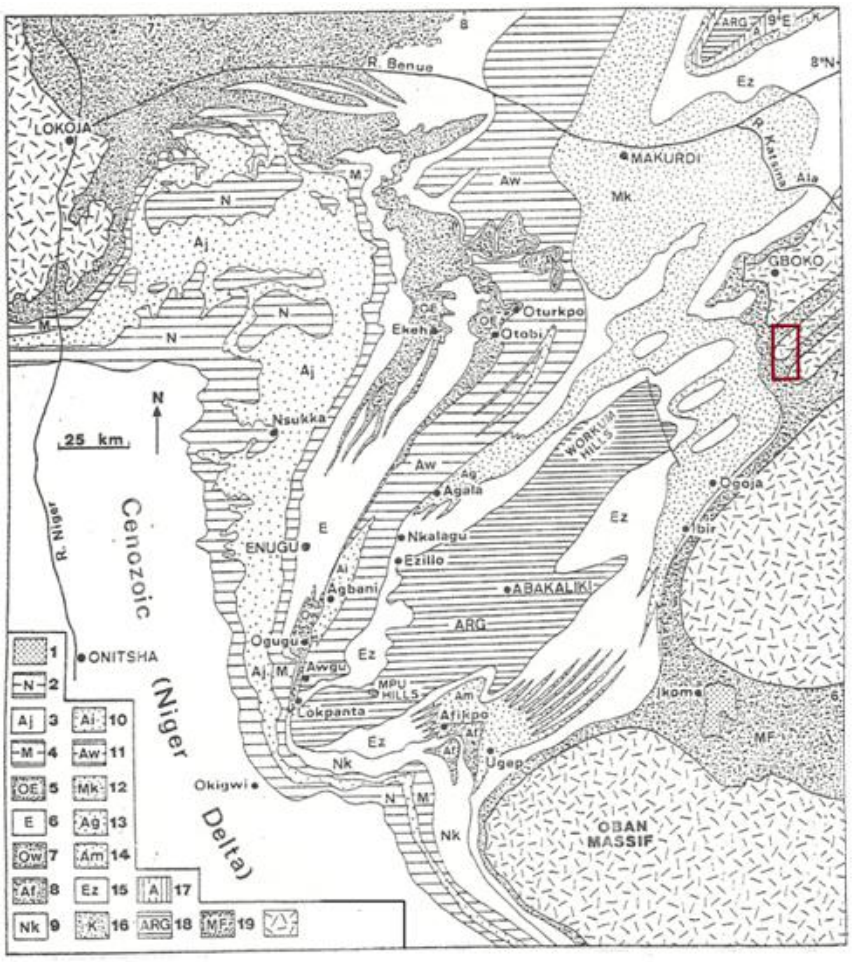


Figure 2.3: Geological map of the Lower Benue Trough region and adjoining areas. (1) Cenozoic basalt (2) Nsukka Formation (3) Ajali Sandstone (4) Mamu Formation (5) Otobi/Ekeh Sandstone (6) Enugu Shale (7) Owelli Sandstone (8) Afikpo Sandstone (9) Nkporo Shale (10) Agbani Sandstone (11) Awgu Formation (12) Makurdi Formation (13) Agala Sandstone (14) Amaseri Sandstone (15) Eze-Aku Formation (16) Keana Sandstone (17) Awe Formation (18) Asu River Group (19) Mamfe Formation and lateral equivalents (20) Precambrian (after Zaborski, 1998).

2.4.2 Sedimentary Evolution and Stratigraphy

The sedimentary fill of the successive basins was controlled by tectonic events and by epeirogenic movements which resulted in major transgressive-regressive cycles.

Murat (1972) identified four Cretaceous cycles of transgression and regression in the Lower Benue Trough namely Middle Albian to Cenomanian, Early Turonian to Middle Turonian, Late Turonian to Early Santonian and Late Campanian to Maastrichtian. These cycles display a remarkably constant depositional pattern. Shales were deposited in the structural depressions whereas shoal (shallow water) carbonates developed on submerged structural highs protected from clastic influx during the transgressive phases. The regressive phases are characterized by extensive deltaic sediments, filling the subsiding basins and by fine clastics deposited over the structural highs.

Murat (1972) described pre-Albian deposits in the Anambra and Calabar areas as "basal grits". In the Ogoja area, Uzuakpunwa (1980), Hoque and Nwajide (1984) described arkosic conglomerates overlying the basement complex as the Ogoja Sandstone. According to Benkhelil *et al.* (1989) similar deposits recorded east of Gboko are believed to be lateral equivalents of the Mamfe Formation of the Calabar Flank and Mamfe Basin. The sedimentation in the Gboko area started with the clastic continental deposits of the Agyaku Sandstone from Aptian to Middle Albian (Najime, 2010) (Fig. 2.4).

The Mid-Albian to Late Cenomanian transgressive phase which resulted from subsidence within the trough and eustatic sea level rise coincided with the global sea level rise (Kominz, 1984) and deposited the first marine sediments known as the Asu River Group (Simpson, 1954). The Asu River Group, the "Lower Limestone" was deposited on the Calabar Flank (Murat, 1972). The Gboko Formation, Akpagher Formation, Ikumbur Limestone and Mayange Limestone were deposited during the Middle to Late Albian. The transgression was followed by a regressive phase in the Mid

Cenomanian during which the Gbemacha Sandstone and the Nienga Sandstone were deposited (Najime, 2010). The Albian sedimentation was accompanied by igneous activity, such as in the Wanakum Hill area and the Mt. Ikyuyen rhyolitic dome in the Gboko area associated with NE-SW trending rhyolitic dykes.

The Late Cenomanian to Lower Santonian succession was deposited during the second cycle of marine transgression. Murat (1972) recognized two cycles of sedimentation separated by a middle Turonian regression. Simpson (1954) referred to these sediments as the Lower Eze-Aku Shales and an Upper "Awgu-Ndeaboh Shales" whereas Reyment (1965) and Murat (1972) referred to them as the "Awgu Shale" and "Ezeaku Shale Group" respectively. Reyment (1965) regarded the former as Lower Turonian and the latter as Upper Turonian to Coniacian with the Makurdi Formation representing the middle part of the Turonian. According to Simpson (1954), the Eze-Aku Formation consists mainly of hard, flaggy, dark grey to black calcareous shales and siltstones with minor sandstones and the Awgu Formation mainly bluish-grey shales with intercalated fine-grained sandstones and thin shelly limestones. Petters and Ekweozor (1982) proposed Nkalagu Formation for the Cenomanian to Santonian shale-limestone-minor sandstone succession in the Lower Benue Trough along with the Amaseri, Makurdi, Agala and Agbani sandstones. This unit made up the Cross River Group. The Tse-Agberagba Sandstone and Lessel Sandstone were also deposited during this interval (Late Cenomanian to Turonian) (Najime, 2010).

The Campano-Maastrichtian cycle began with Late Campanian transgression during which the lower parts of the Nkporo Shale and its northerly lateral equivalent the Enugu Shale were deposited in the Anambra Basin, Afikpo Syncline and the Calabar

Flank (Zaborski, 2000). A regressive phase in the Anambra basin, deposited the Mamu, Ajali and the Nsukka Formations of Reyment (1965), Murat (1972) and Petters and Ekweozor (1982).

The final transgression occurred during the Late Paleocene. During this event, the Imo Shale was deposited in the Anambra Basin and eastern Benin Basin. A subsequent prolonged regressive phase is represented by the Ameki Formation and the Eocene to Recent Niger Delta.

Several lithostratigraphical subdivisions for the Cretaceous rocks of the Lower Benue Trough have been proposed by Simpson (1954); Reyment (1965); Murat (1972); Petters and Ekwezor (1982); Agagu *et al.* (1985); Agumanu (1989) and Ojoh (1990) (Fig. 2.5).

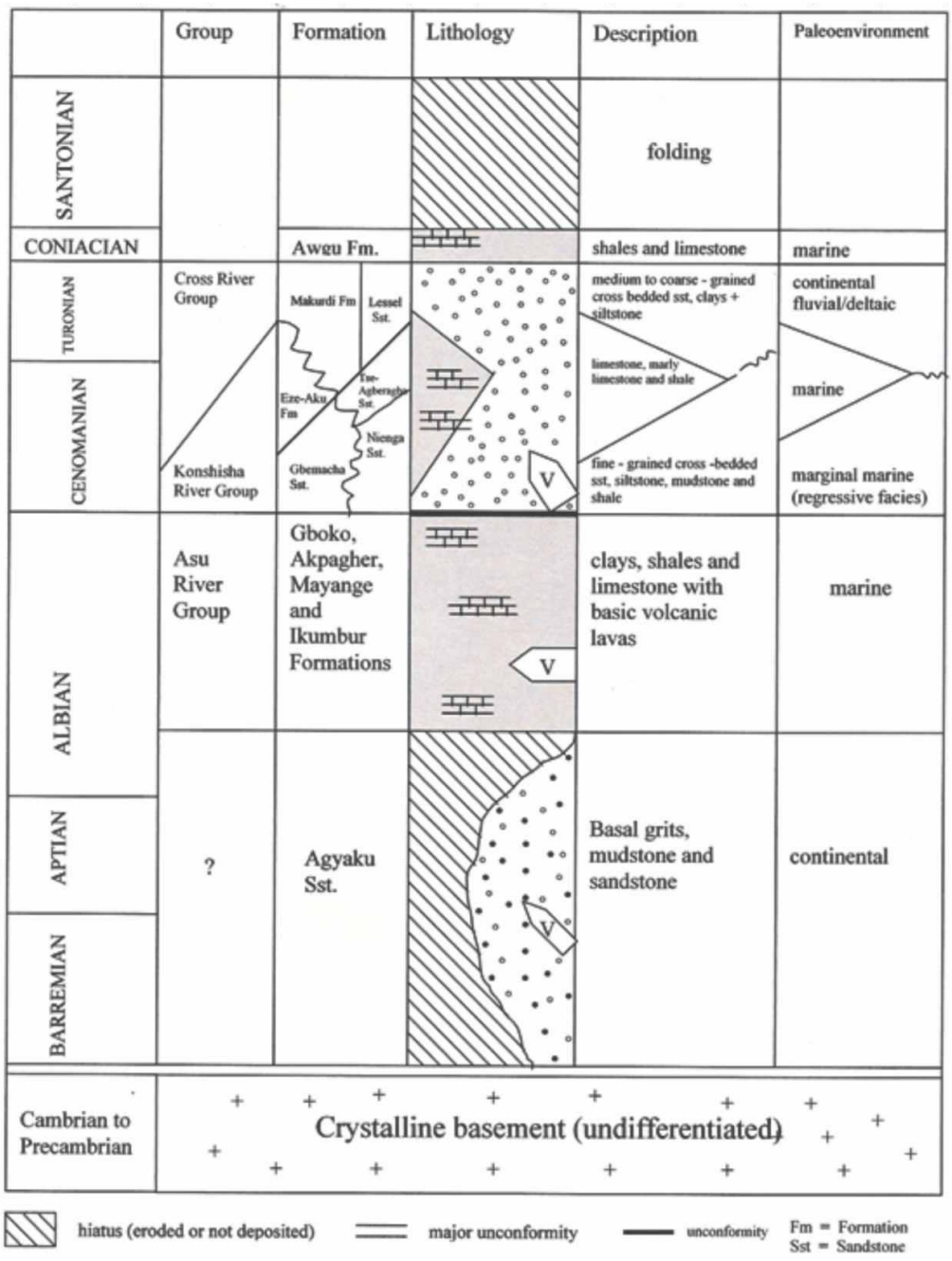


Figure 2.4: Generalized stratigraphic subdivisions of the Gboko area in the Lower Benue Trough (after Najime, 2010)

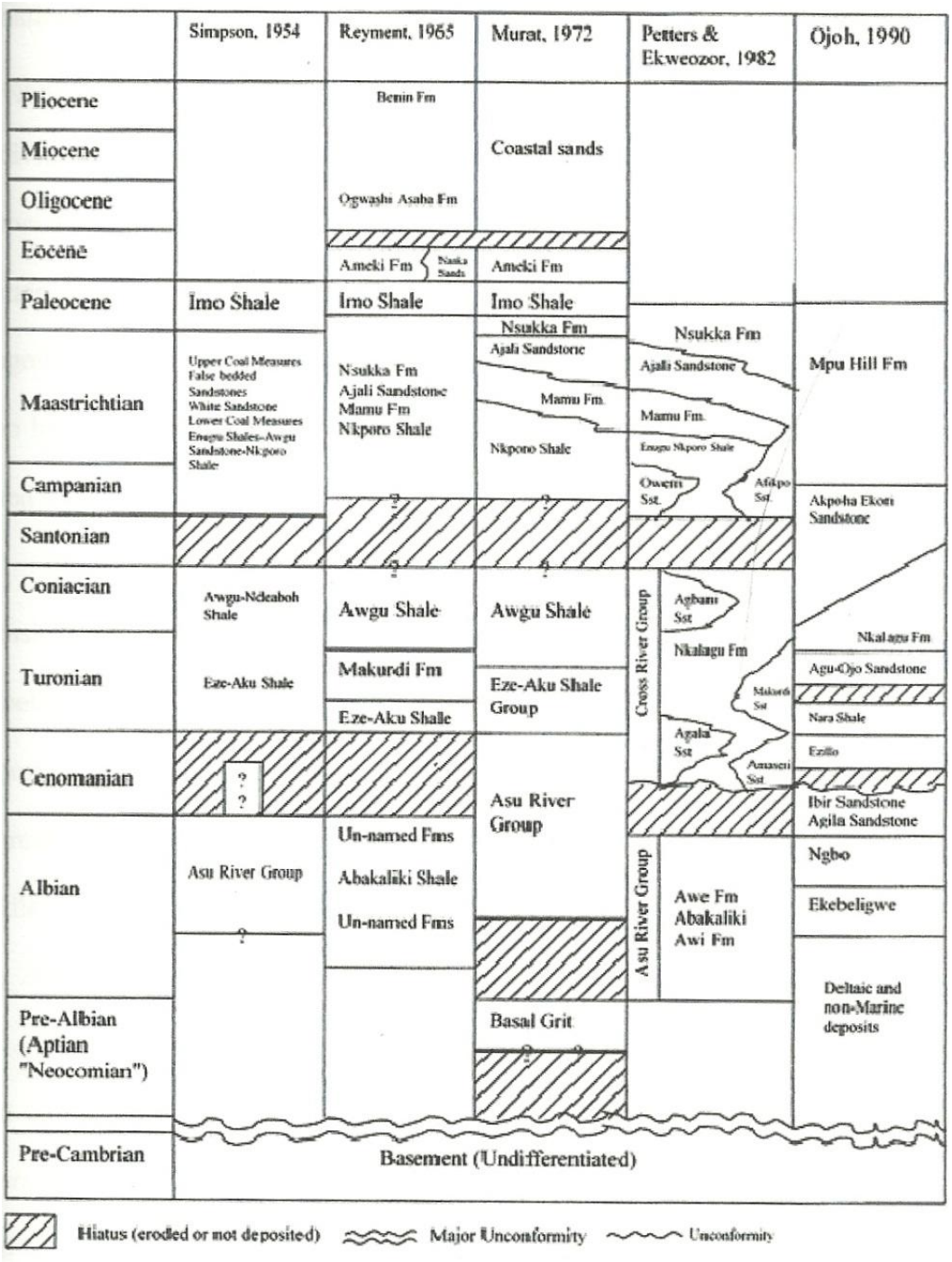


Figure 2.5: The Stratigraphy of the Lower Benue Trough region (after Najime, 2010).

CHAPTER THREE

METHODOLOGY

3.1 DESK STUDY

The desk study involved in-depth and extensive review of previous published and unpublished works on the area of study.

3.2 FIELD MAPPING

The first phase of the field mapping involved reconnaissance survey which was carried out in order to have a broad overview of the geology of the area on a scale of 1:50,000. Areas of interest with respect to baryte mineralization were delineated from the reconnaissance survey and mapped on a scale of 1:10,000. The area was traversed via the major roads, footpaths and stream channels. Global positioning system (GPS) was used to locate outcrops in the area. Compass clinometer facilitated traversing and was also used to take strike and dip measurements of the various lithologies. Linear measurements were taken with the aid of meter rule. Rock samples were collected from the outcrops with the aid of a hammer and examined using hand lens.

3.3 LABORATORY SAMPLE PREPARATION AND ANALYSIS

3.3.1 Petrographic Study

Barren granitic rocks, mineralized rocks and baryte samples obtained from the study area were prepared into thin sections to understand their mineralogical variation. This was carried out using the Meiji transmitted light microscope at the Thin Section Laboratory, Department of Geology, Ahmadu Bello University, Zaria.

3.3.2 Geochemical Analysis

A total of twenty (20) selected samples were analysed. Three (3) representative samples of baryte and seventeen (17) rock samples were pulverized to –150 μm in a tungsten carbide mill at the Department of Geology, Ahmadu Bello University, Zaria. The samples were thereafter packaged and transported to Acme Laboratory, Vancouver, Canada for whole-rock analysis of major oxides and trace elements. The major oxides in the samples were analysed using Inductively Coupled Plasma Atomic Emission Spectrometry (ICP-AES) following a lithium borate fusion and dilute acid digestion of a 0.2 g sample pulp. Trace element analyses required 5 g of sample pulp subjected to lithium borate decomposition for rare earth/refractory elements and aqua-regia digestion for base metals using Inductively Coupled Plasma Mass Spectrometry (ICP-MS) to give total abundances.

3.3.3 Geotechnical Studies

In order to ascertain the quality, baryte samples from Lessel-Mbagwa, Bunde and Ihugh areas were subjected to three distinct geotechnical tests namely density, moisture content and uniaxial compressive strength at the Concrete Laboratory and Soil Mechanics Research Laboratory, Department of Civil Engineering, Ahmadu Bello University, Zaria.

Moisture Content Test

The three samples were first weighed and oven dried at a temperature of 110^{o} C. These samples were removed after 48 hours, cooled at room temperature and weighed using a D and G JJ3000 Electronic Scale. The process was repeated until a constant

weight was attained. The moisture content of each sample was calculated using the following equation:

$$\%W = \frac{(A - B)\ 100}{B} = \frac{\text{Weight of water}}{\text{Weight of dry sample}} \times 100$$

Where:

%W - Percentage of moisture in the sample

A - Initial weight of sample (wet sample in kg)

B - Final weight of sample (dry sample in kg)

Density and Specific Gravity

Baryte samples were cut into rectangular blocks (cuboid) and the length, breadth and height of the each baryte block measured with a vernier caliper. Each block was then weighed on the D and G electronic scale and the desnity calculated. The density of each sample is calculated as the mass of a material per unit volume.

$$\text{Density} = \frac{\text{Mass of sample (g)}}{\text{Volume of sample (cm}^3\text{)}}$$

Where: Volume = length x breadth x height

The specific gravity is therefore derived by substituting the density values into the specific gravity formula.The specific gravity is a dimensionless unit defined as the ratio of the density of a substance to the density of water at a specified temperature. Mathematically, this can be written as:

$$\text{Specific Gravity} = \frac{\text{Density of sample}}{\text{Density of equal volume of water}}$$

Where:

Density of water = $1 g/cm^3$ at $4\ ^oC$

Uniaxial Compressive Strength (UCS) Test

Uniaxial compression test is a conventional method often used to investigate the strength, deformation behavior and failure characteristics of materials, including rocks (Yang *et al.*, 2012).

Sample preparation and test procedure follow the methods prescribed by the American Society for Testing and Materials Standards (ASTM D7012, 2007) and the International Society for Rock Mechanics (ISRM) (Brown, 1981).

The rock samples were cut into regular rectangular block and compressed by the Denison Compression Testing Machine model TIB/MC 29206 with capacity of 2500 kN (Plate II)**.** The sample was loaded axially under a constant stress until failure occurred. The post-failure characteristics were observed and recorded.

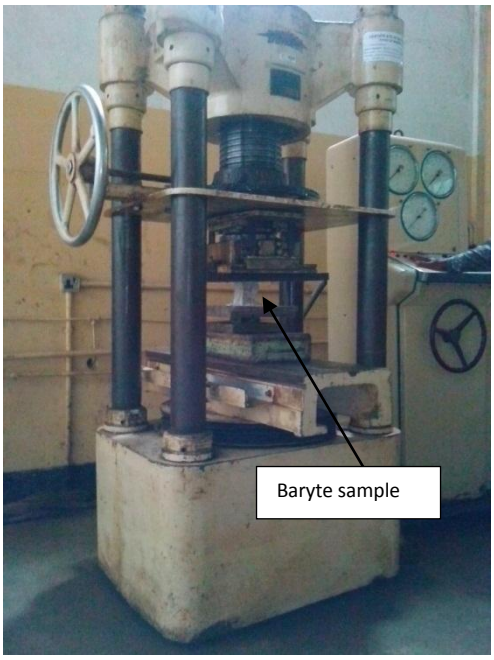


Plate II: Uniaxial compressive strength testing of baryte block using the Denison Compression Testing Machine

Uniaxial compressive strength (σ_C) was calculated as the failure load (P) divided by the initial cross sectional area (A) of the sample. This can be written mathematically as:

$$\sigma_C = \frac{P\ (kN)}{A\ (mm^2)}$$

kN - KiloNewton

3.3.4 X-Ray Diffraction Analysis

The X-Ray diffraction technique was employed to identify the mineralogical components of the baryte samples using the Empyrean x-ray diffractometer and was carried out at Nigerian Geoscience Research Laboratories, Kaduna.

3.4 DATA HANDLING AND PRESENTATION OF RESULTS

Data derived from field work and laboratory analyses were subjected to statistical analysis using statistical, mapping and geo-analytical computer softwares namely Microsoft Excel, Minitab, Rose Net, Surfer, Petrograph and Geochemical Data Tool Kit (GCDKit). The results obtained were presented as tables, figures, plates and interpreted based on geological knowledge.

CHAPTER FOUR

RESULTS

4.1 INTRODUCTION

The area of study is covered by Cretaceous sediments mainly sandstones and underlain by basement rocks consisting of granites and gneiss. Sandstones make up about 90% while gneiss and granites constitute only about 10% of the rocks in the area (Fig. 4.1). Macroscopic and microscopic descriptions, structural characteristics and field relationships, geochemical variation of these rocks / baryte veins as well as geotechnical attributes of barytes in this area are presented in the following sections.

4.2 BASEMENT ROCKS

4.2.1 Banded Gneiss

Exposure of banded gneiss is poor and it is generally observed in mining pits. The banded gneiss is exposed at Mbatoo and Bunde and for the most part is greatly weathered. Outcrops of this rock are oriented predominantly in a NW-SE direction. In hand specimen it is medium-grained with minor mafic/felsic layering, which confers weak foliation on the rock. The foliation is defined by streaks of biotite having narrow bands of about 0.1 cm. The quartz and K-feldspar – rich streaks have wider thickness between 0.2 cm and 0.3 cm. Quartz is observed in the banded gneiss as subhedral colourless crystals exhibiting undulose extinction and conchoidal fracture (Plate III). Plagioclase is cloudy forms subhedral grains and displays polysynthetic twinning. Conchoidal fracture filled with well formed intergrowths of quartz can be observed in most parts of the section.

Alteration of plagioclase to sericite is observed in the central and top right part of the field of view. Biotite is pale brown in colour and also exhibits pleochroism from pale brown to dark brown. It has moderate relief, the crystals are elongate and subhedral exhibiting one directional cleavage.

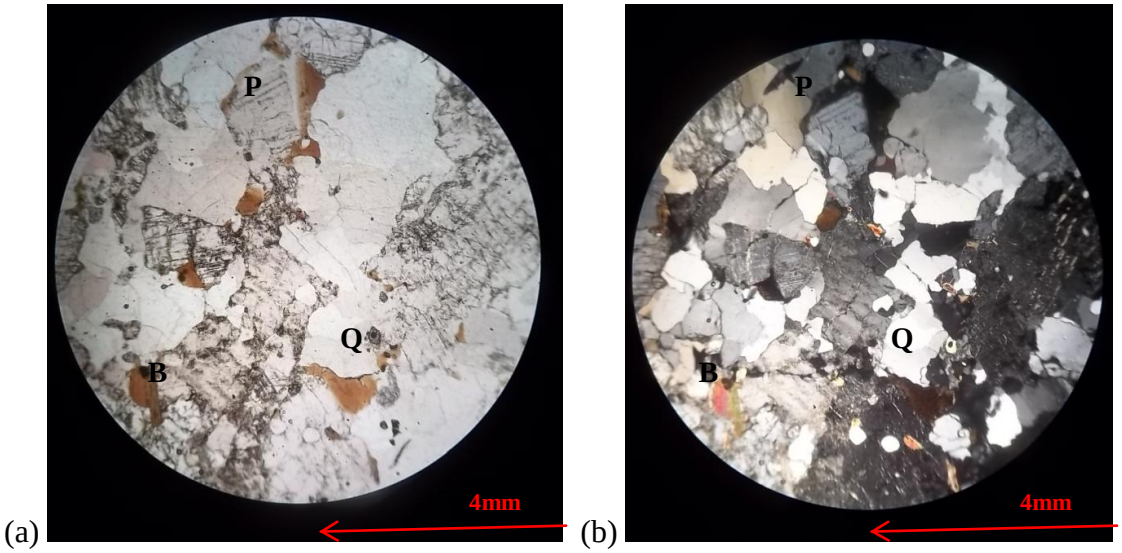


Plate III: Photomicrograph of banded gneiss from Mbatoo area in (a) plane polarized light (PPL) and (b) crossed polarized light (XPL) (Q-Quartz, P-Plagioclase, B-Biotite)

4.2.2 Granite

Medium grained-muscovite granite was observed in a mining pit at Bunde northwest of Lessel. The granitic rocks are highly fractured, trending NE-SW and dipping 10^{o} to 50^{o}E (Plate IVa). The rock is medium-grained, pale grey to white in colour largely due to the abundance of quartz and felsic minerals. The coarse grained-biotite-muscovite granite exposure at Mbaakase (southwestern part of the study area) is a low lying dome-shaped outcrop and it is coarse-grained in texture. For most part, it is covered by the Mtema stream (Plate IVb). The granite exposure at Akaajime (southwest of Ihugh) is

medium-grained trending NW-SE and is grey in appearance due to the presence of muscovite.

a.  b. 

Plate IV: (a) Granite exposure at Bunde (N 07^{o}09'28.1", E 009^{o}01'34.9") (b) Granite exposure in Mtema stream channel, Mbaakase (N 07^{o}00'30.3", E 008^{o}58'40.8").

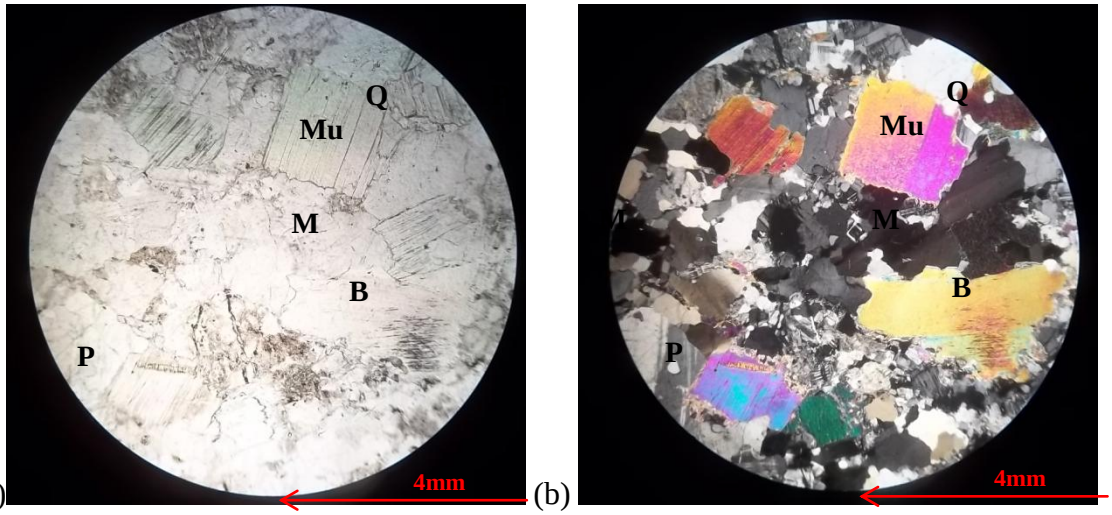
The coarse grained-biotite-muscovite granite at Mbaakase is composed mainly of quartz (40%), plagioclase (30%), microcline (5%) while biotite and muscovite constitute about 10 – 15%. Quartz forms colourless anhedral crystals and exhibits non-uniform extinction. Subhedral crystals of quartz occur as intergrowths in plagioclase (Plate V). Plagioclase is observed as subhedral grains some of which are fractured and also show well developed polysynthetic twinning. Microline is seen to occur as interstitial grains around plagioclase feldspars and quartz. Tartan twinning is also exhibited by microcline. The pale green colour of muscovite stands out in relief relative to quartz and plagioclase. One directional cleavage is well displayed in the muscovite crystals. Slight alteration is noticed along the rims of the muscovite crystals and birefringence colours of pink and blue are common in crossed polarized light (Plate IX). Biotite appears pale brown in

colour with pleochroism from pale brown to yellowish brown. Alteration in biotite is observed along the crystal edges leaving greenish patches of chlorite.

In thin section, the granite at Akaajime is composed of quartz (30%), plagioclase (30%), muscovite (20%) and orthoclase (10%) (Plate VI). Quartz is colourless, polycrystalline, cracked and exhibits wavy extinction. Plagioclase is subhedral and lamellar twinning is common. The section shows alteration of plagioclase to sericite and black blebs of opaque mineral enclosed in plagioclase. Orthoclase is euhedral to subhedral in form, cleaved in one direction and displays carlsbard twinning. Muscovite is pale green in colour under plane polarized light. It is subhedral to euhedral in shape with perfect cleavage in a common direction. In crossed polarized light it shows birefringence colours of dark green, blue and pink. (Plate VI).

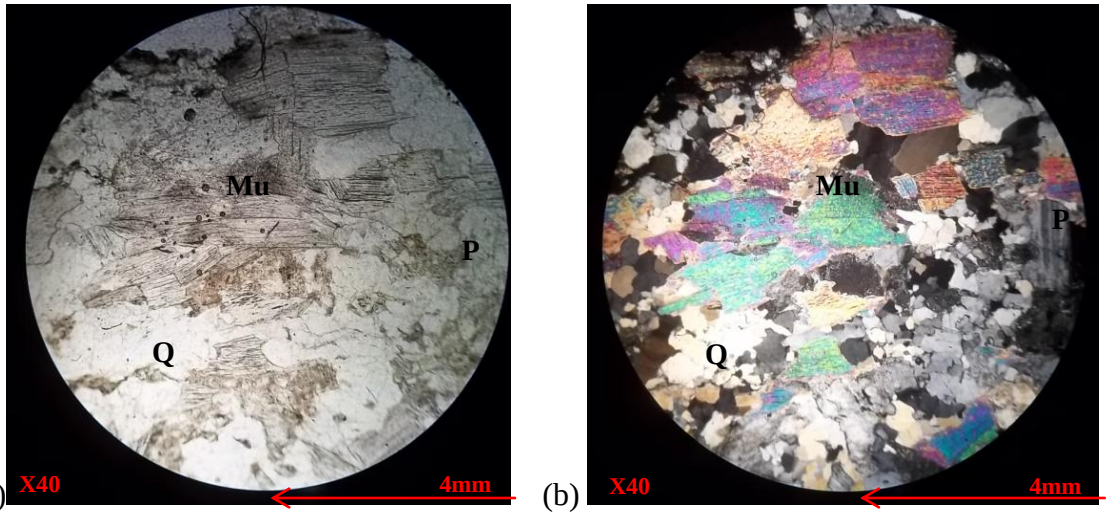
The granite from Mbatoo is composed of quartz (40%), plagioclase (35%), microcline (10%), muscovite (7%), biotite (5%) and opaque minerals (3%). Quartz crystals are subhedral and exhibit undulose extinction. Plagioclase is cloudy, subhedral with poor relief and intergrown with quartz. It is slightly altered and exhibits lamellar albite twinning. Microcline is subhedral with its characteristic cross-hatch twinning. Muscovite is pale green in colour, anhedral in shape with one-directional cleavage. Biotite appears green in colour, pleochroic, with moderate-high relief and characteristic cleavages. The edges of some of the biotite crystals have been altered to chlorite (Plate VII).

Based on the textural characteristics and mineralogical composition, the granite in the study comprises of medium-grained muscovite granite and coarse-grained biotite muscovite granite.



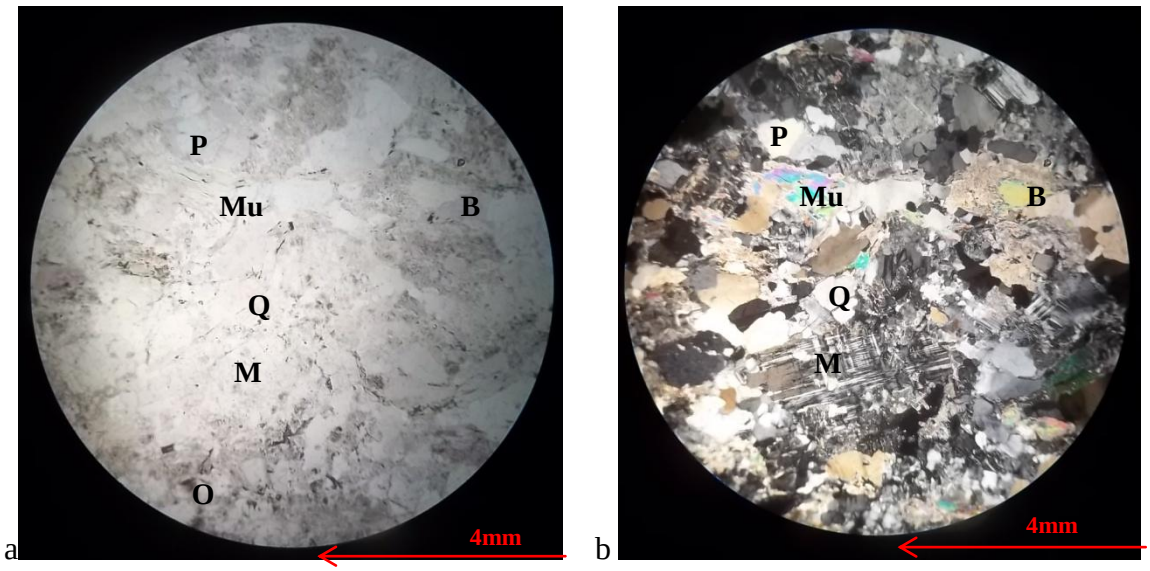
(a) (b)

Plate V: Photomicrograph of coarse-grained biotite muscovite granite from Mbaakase in (a) PPL and (b) XPL (Q- Quartz, P-Plagioclase, M-Microcline, B-Biotite, Mu-Muscovite)



(a) (b)

Plate VI: Photomicrograph of medium-grained muscovite granite at Akaajime in (a) PPL and (b) XPL (Q-Quartz, P-Plagioclase, Mu-Muscovite)



a b

Plate VII: Photomicrograph of medium-grained muscovite granite from Mbatoo in (a) PPL and (b) XPL (Q- Quartz, P-Plagioclase, M-Microcline, Mu-Muscovite, B-Biotite, Opaque minerals)

4.2.3 Pegmatite

A pegmatite vein trending NE-SW is exposed along Mbason stream channel (northwest of Ihugh) where it intrudes the medium-grained-muscovite granite. It is weathered (the feldspars have been altered to clay) and fractured. Muscovite flakes and large angular crystals of quartz of about 1 – 6 cm wide are very common (Plate VIII).



Plate VIII: Pegmatite vein along Mbason stream channel (N 07^{o}00'48.3", E 009^{o}01'22.4").

4.3 SEDIMENTARY ROCKS

The Cretaceous sediments comprising of Lessel Sandstone, Ezeaku Formation and Makurdi Sandstone is collectively called the Cross River Group. The Cross River Group (Late Cenomanian to Early Santonian) was proposed by Petters and Ekweozor (1982) to include shales, limestones and sandstones previously assigned to the Ezeaku and Awgu Formations and marginal inter-tonguing regressive sandstones such as the Makurdi, Agala, Amaseri and Agbani Formations of Murat (1972), Offodile (1976b) and Banerjee (1980).

4.3.1 Sandstone

The study area is covered in large part by the "Lessel Sandstone" which is Turonian in age. Najime (2010) described the Lessel Sandstone as poorly bedded conglomeratic sandstones outcropping along River Nienga near Abuul and extending eastward to Lessel Town and southwestward to Ikyobo and Agbeede areas (southwest of Gboko). The sandstones consist of angular to rounded pebbles of mainly polycrystalline quartz scattered in a matrix of coarse to medium-grained sand and clay. The sandstones are whitish in Lessel area and laterally change to reddish or brownish varieties (ferruginous sandstones) towards Ikyobo (southwest of Gboko).

The sandstone bed northeast of Mtema stream is fine grained, reddish brown in colour comprising basically of quartz, iron oxides and micaeous minerals. The sandstone beds trend NE-SW with near vertical dip along the Mtema stream (Plate IXa). Thick sandstone beds are observed southwest of the Mtema stream dipping 40^{o}W.



a b

Plate IX: (a, b) Sandstone exposure northeast of Mtema stream (dash lines show beds with vertical dip) (N 07^{o}00'33.8", E 008^{o}55'43.0").

An exposure of the sandstone observed in a drainage channel northwest of Ihugh along Mbason stream has been affected by various degree of jointing (NE-SW and NW-SE joint sets) and as a result has been shattered into medium to large angular bodies of rock (Plate X). The sandstone is medium-grained, rusty brown in colour with about 50% quartz.



Plate X: Sandstone exposure along Mbason stream, northwest of Ihugh (N 07^{o}00'42.2", E 009^{o}01'25.6").

An outcrop of the sandstone was observed along the Ajun Stream channel. The outcrop is fractured and fragmented into thick massive boulders (Plate XI).



Plate XI: Massive boulders of sandstone at Ajun stream (N 07^{o}00'45.5", E 009^{o}02'02.9").

At Lessel-Mbagwa, the Lessel Sandstone appears reddish-grey in colour. The topmost layer is medium-grained composed of angular fragments of quartz. In contrast, the bottom layer is fine to medium-grained with reddish-brown tint. In hand specimen, the sandstone is composed predominantly of quartz (> 40%), feldspars (20%), micas (10%) and iron oxides (10 - 15%). The feldspars are altered to clay minerals.

The gritty and friable nature of the sandstones did not allow thin section studies to be carried out on them.

4.3.2 Shale

Shale outcrops in a stream channel southwest of Kase has a NW-SE trend and dip of 12^{o} E. It is thinly laminated and intercalated with sandstone (Plate XII). The shale is very fine grained, fissile and appears dark grey to greenish brown in colour.

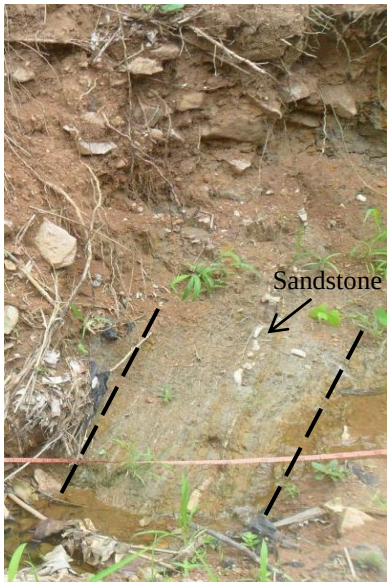


Plate XII: Outcrop of Shale (in-between dash lines) at Kase, northeast of Ihugh (N 07°00'45.0", E 009°02'02.9").

4.4 QUARTZ VEIN

The quartz vein cross-cuts the Lessel Sandstone at Lessel-Mbagwa about 50 meters to a baryte mining pit (Plate XIII). The exposed portion of the vein is about 9.1 m in length and 3.0 m wide. It is massive, highly fractured and trends in NW-SE direction. In hand specimen it appears glassy, whitish to bluish grey in colour with a tint of red.

In plane and crossed polarized light, the crystals of quartz are submicroscopic and indistinguishable from one another. In a higher magnification (X100) boundaries of some quartz crystals are partially visible and the crystals appear compact. This character suggests that of cryptocrystalline quartz that is crystals that are too small to be identified with the microscope**.** The most distinct feature of the quartz vein is the presence of numerous micro-fractures although; there are other micro-fractures which are perpendicular to the former. These microfractures are infilled with opaque minerals likely to be iron oxide. Under crossed polars, the crystals display a host of birefringence colours of pink-blue-green to blue (Plate XIV).

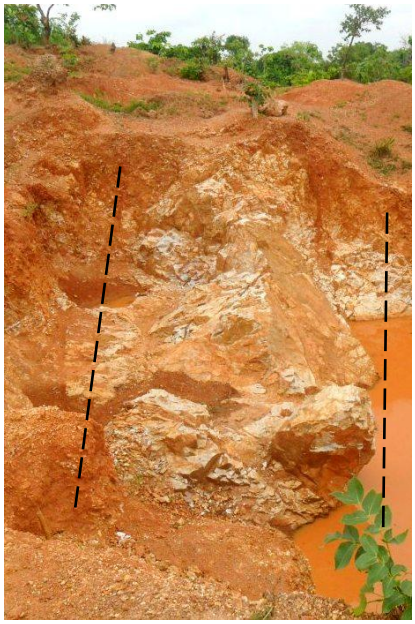
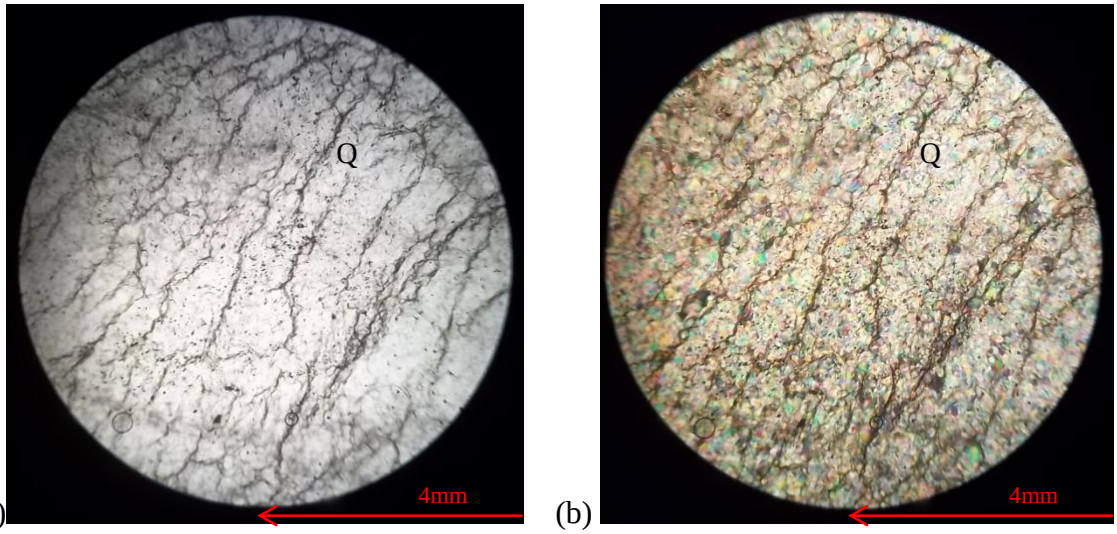


Plate XIII: Quartz vein (in-between dash lines) at Lessel Mbagwa (N 07°07'58.2", E 009°00'59.4").



(a) (b)

Plate XIV: Photomicrograph of quartz vein rock from Lessel-Mbagwa area (a) PPL and (b) XPL (Q- Quartz Mag. 40)

4.5 LATERITES

Laterite is a residual ferruginous rock which occurs in most parts of the study area. It is particularly widespread in the western half of the area. It is reddish brown in colour, hard and sometimes appears earthy and porous.

4.6 SUPERFICIAL DEPOSITS

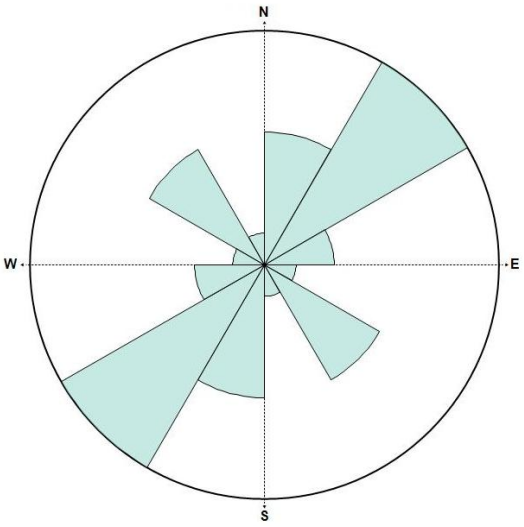
Superficial deposits are unconsolidated soil cover or regolith derived from the weathering of the underlying bedrock. Sandstone regolith is loose, pebbly containing sub-rounded to angular pebbles of quartz about 0.5 – 5 cm and has been affected by laterization giving it a reddish colouration.

4.7 STRUCTURES

Structures in the study area comprise of joints and faults majority of which have a NE-SW trend (Fig. 4.2a, b) (Appendix VII). Other minor trend direction is NW-SE.

4.7.1 Faults

The quartz vein at Lessel-Mbagwa (Plate XV) is characterized by intensive degree of fracturing with visible fault surface. The medium-grained muscovite granite at Bunde has been affected by NE-SW trending sinistral strike-slip fault (Plate VIII). A minor shift of sandstone lamina in shale at Kase trending NW-SE shows a vivid dextral displacement of about 4 cm (Plate XVI).



a.

b.

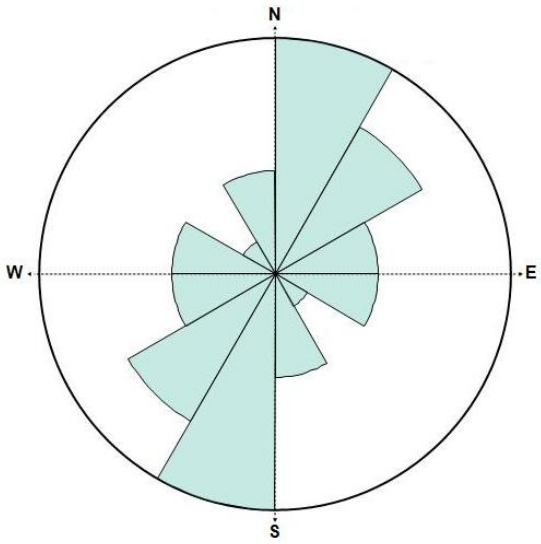


Figure 4.2: Rose diagram showing the general structural trend of joints in (a) granitic rocks (b) sedimentary rocks

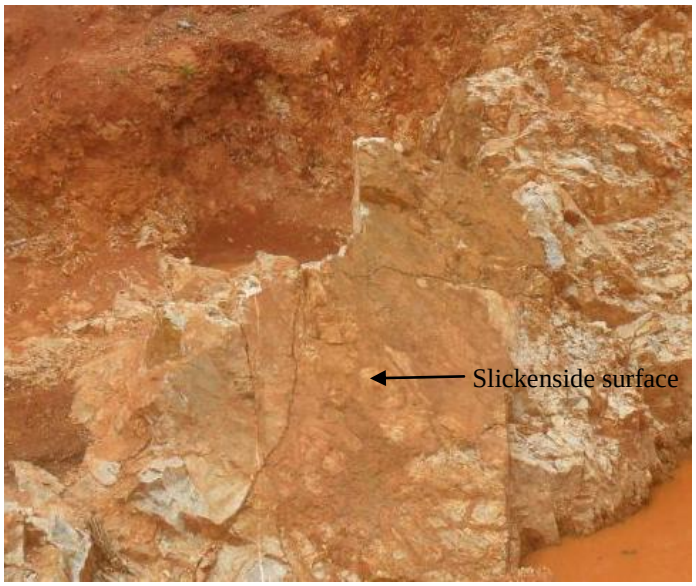


Plate XV: Slickenside surface on quartz vein (N 07^{o}07'58.2", E 009^{o}00'59.4").



Plate XVI: Sandstone lamina in shale at Kase, northeast of Ihugh displaced by a fault (N 07°00'45.0", E 009°02'02.9").

4.7.2 Joints

Joints are fractures that cut across a rock and do not show any discernible displacement of one side of the fracture relative to the other. The cross-cutting joint system with NE-SW and NW-SE trends is particularly intense in the quartz vein (Plate XVII). The outcrops of sandstone at Mbason and Ajun (presicely at N 07°00'42.2", E 009°01'25.6" and N 07°00'45.5", E 009°02'02.9" respectively) are fractured by NE-SW trending joints. The former is broken into small rock fragments (Plate IV) and the later into thick massive boulders (Plate V).



Plate XVII: Cross-cutting joints in quartz vein at Lessel-Mbagwa (N 07^{o}08'00.5", E 009^{o}01'03.2").

4.8 BARYTE MINERALIZATION

Several baryte mining pits are scattered over the study area. The vein system is guided by fractures and joint patterns in the country rocks trending NE – SW in addition to the minor veins characterized by NW – SE trend**.** Baryte is the the primary ore mineral while galena and sphalerite are minor minerals.

4.8.1 Field Occurrence

4.8.1.1 Ihugh Area

Baryte occurs as thin whitish NE-SW trending lenses and varies in thickness from 0.5 – 1 cm within the ferrugenised Lessel Sandstone overburden (Fig. 4.3). The lenses can be traced from pit to pit, pinching in and out of the wall-rock over a distance of about 30 meters (Plate XVIII). The lateritic sandstone overburden has concealed these mineralized zones. At greater depth (greater than 3 meters), baryte appears much clearer and denser.The reddish tint observed on the baryte and surrounding host rock is due to

the presence of iron minerals, typical of sandstones in the area. Baryte in this area is massive, cleaved and appears yellow in colour.



Plate XVIII: Baryte mineralization at Tarzoho-Mbaakase, Ihugh (N 06^{o}59'53.6", E 008^{o}59'35.2").

4.8.1.2 Lessel Area

The highest concentration of baryte mining pits are located in Lessel area. Lessel-Mbagwa, Bunde and Mbatoo are the focal points. Mining in this area is both manual and mechanized as major mining pits have reached depth greater than 40 meters. At Lessel, baryte mineralization occurs within the banded gneiss and in the Lessel Sandstone. Baryte veins trending NE-SW and dipping 65^{o} E at Lessel-Mbagwa are hosted in the sandstones whereas at Bunde and Mbatoo, the baryte veins are hosted by banded gneiss (Plate XIXb) (Fig. 4.3).

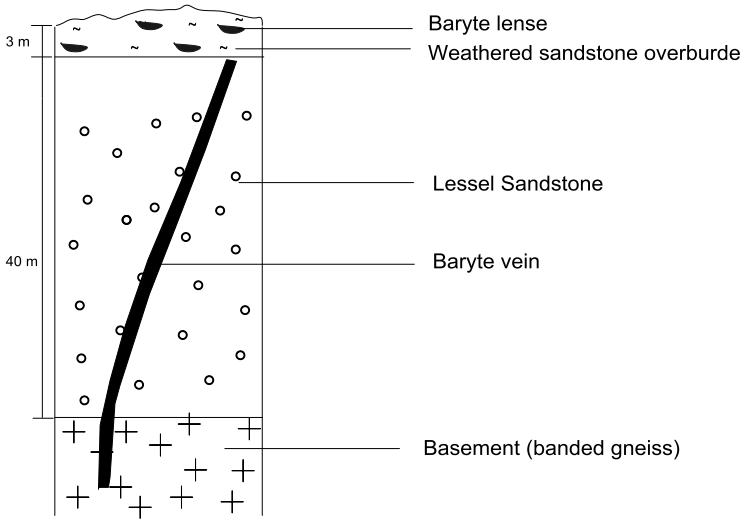


Figure 4.3: Idealized vertical section of baryte mineralization in basement, sandstone and weathered overburden in Lessel-Ihugh area

b. 

Plate XIX: Baryte mining pit in Basement Gneiss at Bunde (arrow shows the vein trend) (N 07°09'28.1", E 009°01'34.9").

At Lessel Mbagwa, the host sandstone appears to have been altered as it displays gradational changes in colour varying from pink to white and to green. In hand specimen, the sandstone has greater percentage of micas and less of quartz, feldspars. The major

baryte vein exposed in a mine pit cuts through the Lessel Sandstone and stretches over a length of over 150 m. Baryte mineralization is widespread in this area and occurs as NE-SW fracture infilling. Smaller veins have an average width of about 1.8 to 2.2 cm and larger veins about 0.8 to 4 m. A thick fractured quartz vein (Plate XIV) trending NW-SE cuts across the former NE-SW trend of sandstone and baryte vein. Lead-zinc suphide veins with an average width of 2 cm have been observed in the sandstones. Baryte in Lessel-Mbagwa area occur as bladed to tabular compact masses and appears off-white with reddish tint.

At Bunde and Mbatoo, baryte veins are hosted in the banded gneiss (Plate XX). The banded gneiss is more dense, massive and pale green to slightly dark green in colour than a typical gneissic rock.

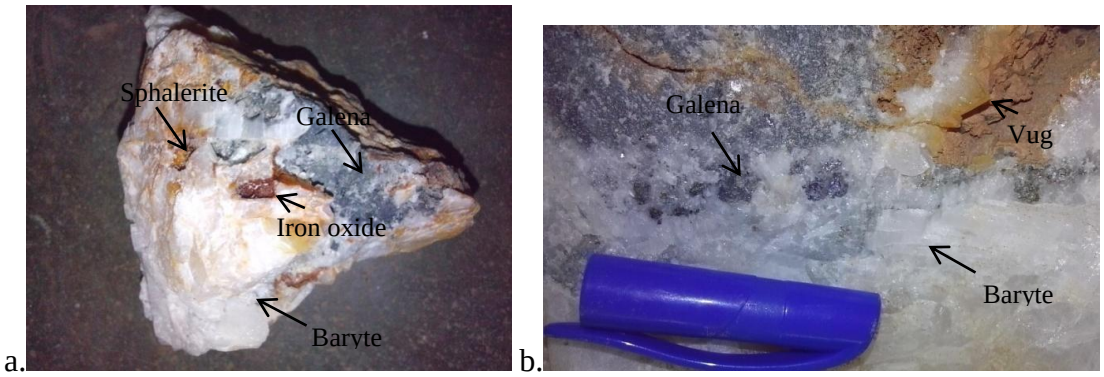


a b

Plate XX: (a) Vertical baryte vein in banded gneiss at Bunde (b) Baryte vein in banded gneiss (notice the pale green colour of the host rock)

This colouration of the banded gneiss is an indication of wall-rock alteration while the foliated character appears to be masked. The length of the larger vein is about 100 - 200 m. The minor veins however, have an average width of 4.5 - 20 cm, thickness of 15 cm with a near vertical dip. Veinlets are also common having an average width of about 0.4 cm. Medium sized vugs are common in the vein. These vugs present suitable

environment for the development of external crystals of galena, sphalerite and iron oxide (Plate XXI a, b). Baryte in this area is massive, cleaved and appears white in colour. Though its colour may also vary from white to grey depending on whether baryte is intermixed with sulphide ores (PbS, ZnS).



a. b.

Plate XXI: (a, b) Vug in baryte sample from Bunde with shiny black crystals of galena, greenish-yellow coloured crystals of sphalerite and reddish grains of iron oxide.

4.9 MINERALOGICAL AND PETROGRAPHIC CHARACTERISTICS

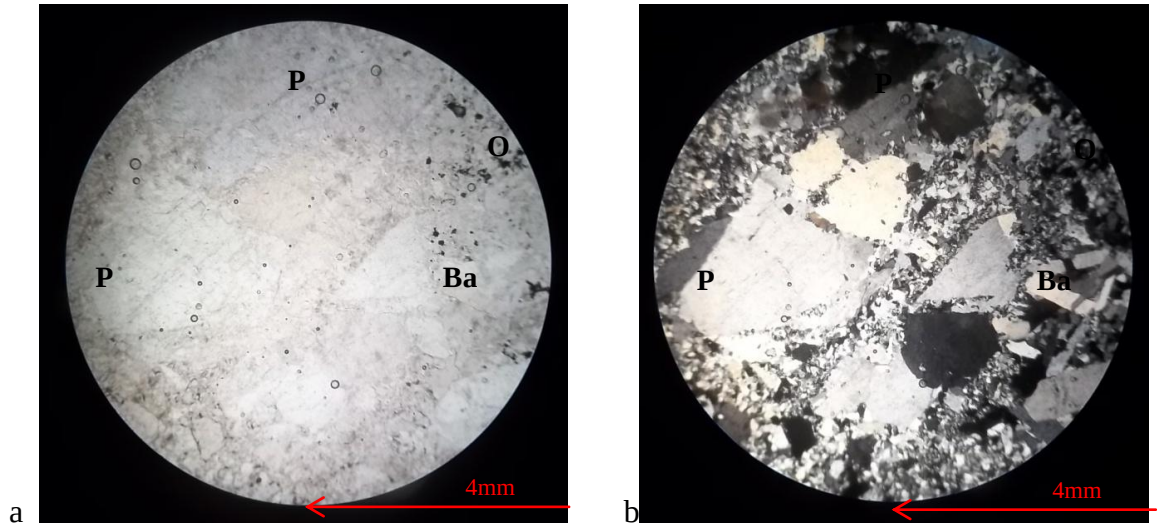
Barytes from Lessel-Ihugh area is dense, and composed of tabular crystals (Plate XXII a, b, c). It is clear white to pinkish white in colour (Plate XXII a, b, c). The deviation in colour from clear white is probably due to incorporation of iron in the lattice structure of baryte. X-ray Diffraction (XRD) was used to identify and characterize the mineralogical forms of baryte and the associated minerals. The result obtained shows that baryte pattern masks the weak lines of the small amounts of the associated minerals. It however reveals that quartz is the major associated mineral present (Appendix I-III). Galena occurs as small cubic crystals or tiny grains in vugs as recorded in the baryte from Bunde (Plate XXI a, b). Sphalerite occurs as patchy coatings in vugs associated with iron oxide and galena. Its colour varies from pale green to yellow and is not as widespread as galena (Plate XXI b).

a.  b. 

c.  d. 

Plate XXII: Photographs of baryte samples from (a) Lessel-Mbagwa (sample NM) (b) Bunde (sample NO5) (c) Tarzoho-Mbaakase, Ihugh (sample NQ2) (d) and galena from Lessel-Mbagwa.

The baryte-mineralized banded gneiss is a medium-coarse grained rock (Sample NO3) composed of plagioclase (40%), quartz (30%) and opaque minerals (10%). Coarse-grained plagioclase crystals are embedded in equigranular plagioclase and quartz groundmass (Plate XXIII)**.** The plagioclase crystals exhibits lamellar twinning and are slightly altered in some places to sericite. Baryte mineral constitutes about 20% and occurs as colourless tabular or lath shaped crystals.

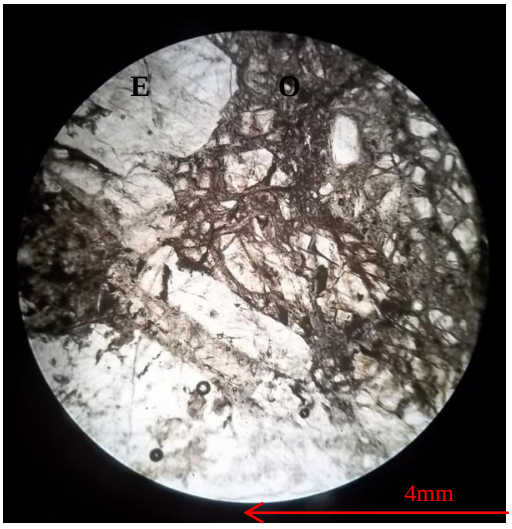


a b

Plate XXIII: Photomicrograph of baryte-mineralized banded gneiss from Bunde area in (a) PPL and (b) XPL (Q-Quartz, P- Plagioclase, Ba- Baryte, O- Opaque minerals)

Optical analyses of the baryte-mineralized banded gneiss (Sample NO2) revealed that plagioclase crystals are pale white, anhedral in shape with irregular cracks (Plate XXIV). Intergrowth and inclusion of quartz are common in some of the large crystals of plagioclase. In plane polarized light, whitish to pale green euhedral crystals of epidote with moderate relief were observed. By contrast the crystals of epidote exhibit pinkish-blue third order birefringence colours in crossed polarized light. Epidote is cracked having numerous cross-cutting micro-fractures. The micro-fractures are characteristic of rocks that have been affected by intense tectonism. Opaque minerals appear as swarms of micro-veins which cut through quartz, plagioclase and epidote crystals (Plate XXIV).

A section of baryte vein cutting through the banded gneiss shows medium-grained quartz and baryte crystals in fine grained matrix of plagioclase, quartz, biotite and opaque mineral (Plate XXV). The right hand field of view stretching from top to bottom in both plane and crossed polars shows subhedral bladed quartz grains. Quartz has cloudy to pale brown colour, subhedral crystals with bladed edges and exhibits undulose extinction.

a 

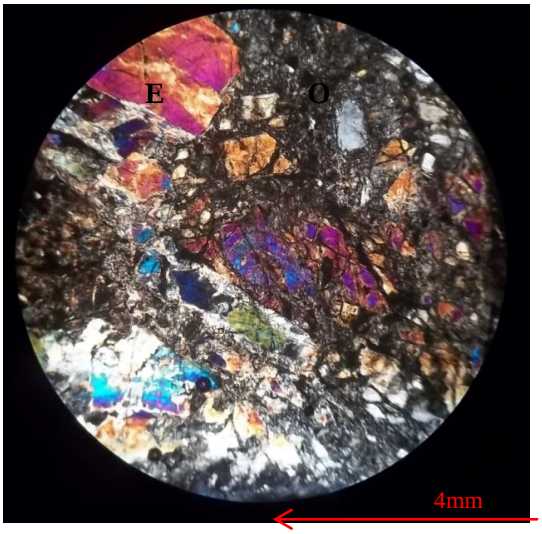
b 

Plate XXIV: Photomicrograph of baryte-mineralized banded gneiss from Bunde area in (a) PPL and (b) XPL (E-Epidote, O-Opaque mineral)

The contact between quartz and baryte crystals show interference colours of yellowish-brown and pink (Plate XXV). Baryte crystals bordering the bladed quartz crystals also appear to be well formed but strained, thus indicating that it has been subjected to stress (Plate XXV b). The early stage baryte crystals at the upper region of the section are cleaved and micro-fractures are also evident. Baryte crystals (that is the late stage baryte) at the lower region of the section appear colourless, with low to moderate relief and exhibit one-directional cleavage in plane polarized light. In crossed polarized light, outlines of individual crystals are visible and the contact between each crystal appears sharp giving it a compact outlook. The crystal form, size and contact relationship between quartz and baryte indicate that there are at least two stages of crystallization of baryte.

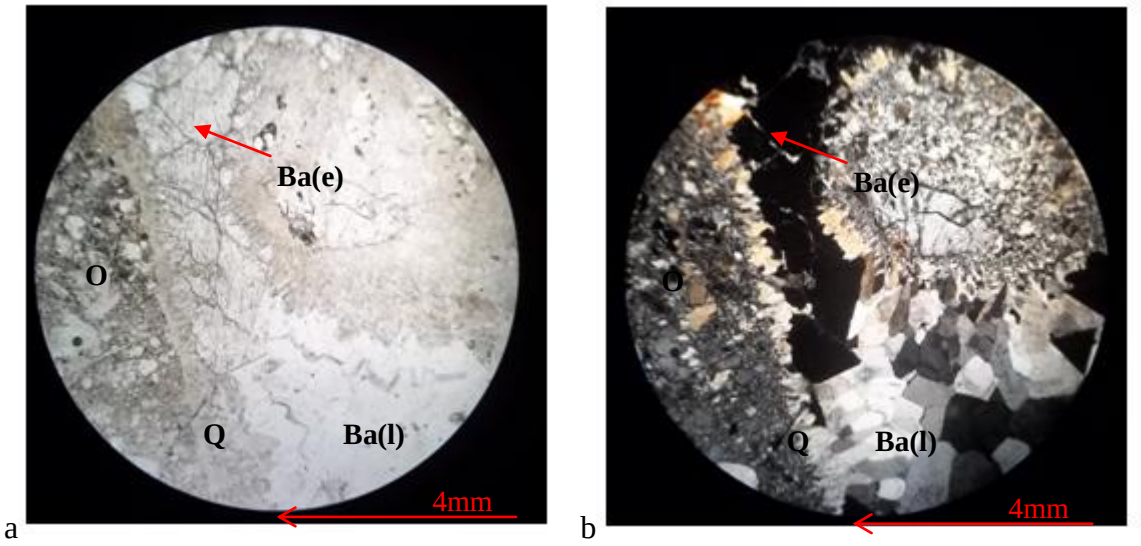
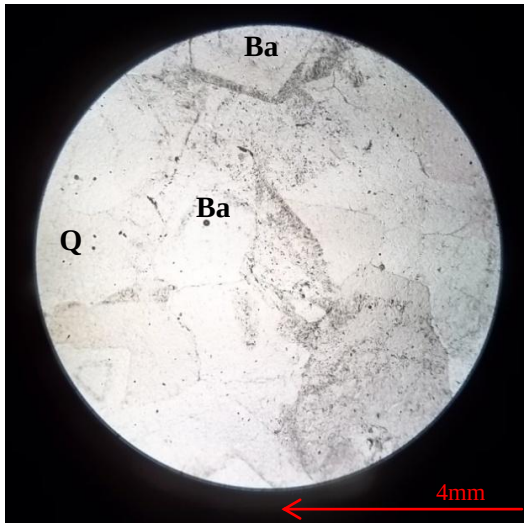
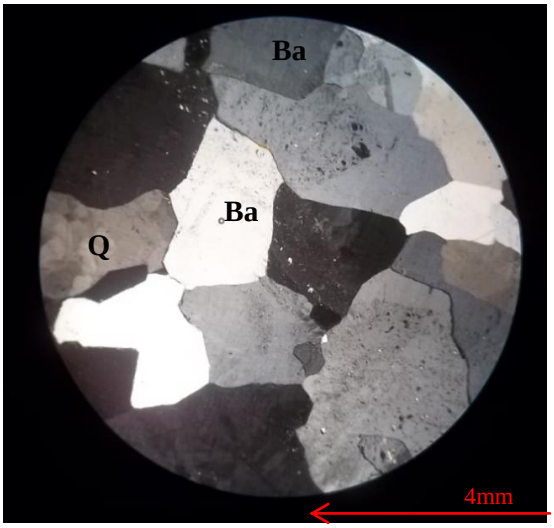


Plate XXV: Photomicrograph of baryte-mineralized banded gneiss from Bunde area in (a) PPL and (b) XPL (Q-Quartz, Ba(e)-Early Baryte, Ba(l)-Late Baryte, O-Opaque mineral).

Another view of the section in crossed polarized light show well developed granoblastic texture of baryte and quartz (Plate XXVI b). Quartz is colourless having subhedral to euhedral crystals. The non-uniform shadowy extinction and strained nature of quartz suggests that the banded gneiss has been subjected to tectonic deformation. Baryte is predominant relative to quartz. It is cloudy, with clear to unclear crystal boundaries and has low relief in plane polarized light. In crossed polarized light, baryte commonly displays various shades of grey. The crystals are well formed, highly compact and exhibit straight extinction. Inclusions of quartz, baryte and opaque minerals are present (Plate XXVI a, b). The larger tabular crystals of baryte had enough time to grow and consequently, exerted some pressure against the quartz grains, therefore their elongated shape (Plate XXVI c).

a 

b 

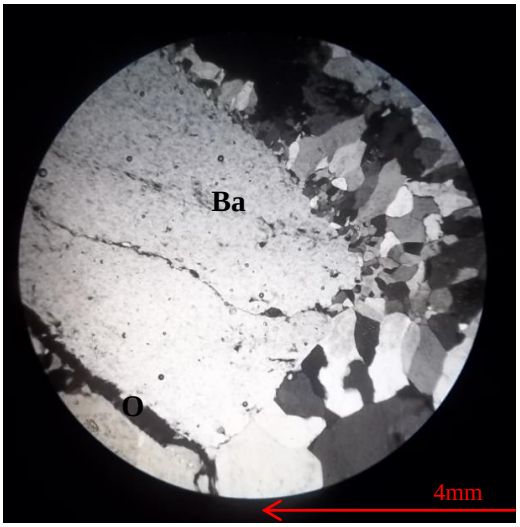
c. 

Plate XXVI: Photomicrograph of baryte vein rock (a) PPL and (b, c) XPL (Q-Quartz, Ba-Baryte, O-Opaque mineral)

4.10 GEOCHEMICAL DATA

The geochemical data comprising major oxides and trace including rare earth elements concentration in the basement and sedimentary rock samples are presented in Tables 4.1 to 4.6.

Table 4.1: Major oxides composition in granitic rocks from the study area (all values in weight percent [wt. %] except the ratio)

Major Oxides	Pegmatite	Granite					Banded Gneiss	
		MGMG*				CGBMG†		
	NJ	NI	NW1	NX	NW2	NT2	NX2	NX3
SiO_2	80.9	79.7	81.1	75.6	75.04	85.5	77.7	74.5
TiO_2	0.01	0.01	0.01	0.2	0.1	0.1	0.01	0.01
Al_2O_3	11.6	10.6	12	13.9	15.5	7.1	13.9	14.7
Fe_2O_3	0.6	1.3	0.2	0.4	1.2	2.5	0.7	0.9
MnO	0.03	0.1	0.01	0.01	0.03	0.1	0.03	0.03
MgO	0.1	0.3	0.03	0.2	0.2	0.6	0.1	0.2
CaO	0.03	0.3	0.2	0.2	0.4	0.2	0.4	0.2
Na_2O	2.8	4.5	2.5	2.2	1.7	3.6	3	2.1
K_2O	3.7	3.5	4.1	5.9	3.3	0.4	4.2	5.4
P_2O_5	0.1	0.04	0.1	0.1	0.2	0.04	0.04	0.1
TOTAL	100.00	100.00	100.00	98.70	97.4	100.0	100.0	98.0
Ratio K_2O/Na_2O	1.3	0.8	1.7	2.65	1.9	0.1	1.4	2.6

*MGMG – medium-grained muscovite granite
†CGBMG – coarse-grained biotite muscovite granite

Table 4.2: Trace elements concentration in granitic rocks from the study area (all values in parts per million [ppm] except the ratios)

Trace Elements	Pegmatite	Granite					Banded Gneiss		Average Granite**
		MGMG*				CGBMG†			
	NJ	NI	NW1	NX	NW2	NT2	NX2	NX3	
Ni	1	1.8	0.4	20	20	10.4	20	20	0.5
Sc	1.6	0.6	0.6	2	2	1.3	1	0.6	5
Ba	132	44	64	787	314	277	806	743	600
Be	2	2	1	3	4	1	3	2	5
Co	29	25	28.7	32	20.7	42.5	40	29	1
Cr	4.4	6.1	4.4	29.2	14.6	29.2	4.4	1.5	4
Cs	1.7	2.5	3.6	2.5	2.8	0.3	2.1	2.5	5
Ga	21.4	26.4	14.7	22.5	27	7.8	20.9	25	18
Hf	5.1	7.8	1.1	3.5	1.6	1.6	4.6	2	4
Nb	0.6	2.13	0.4	16.2	10.2	0.3	16.5	12	20
Rb	163	378.9	241.6	313.8	162	14.4	287	195	150
Sn	2.2	4.8	1.3	4	5	0.4	0.7	0.8	3
Sr	42	4	19	74.7	37.9	108	32	40	285
Ta	0.8	1.4	0.4	1.2	1.6	0.4	1.4	1.1	3.5
Th	1.6	2.1	0.9	22.7	4.8	4.2	18.7	20.4	17
U	0.6	1.8	0.8	3.6	1.8	0.5	3.4	6.1	4.8
V	2	5	1	8	8	10	8	8	20
W	186.3	164.7	187.1	195.6	139.7	200	190.4	195	2
Zr	9.4	28.9	7.7	95.4	36.7	8.9	74	82	180
Y	1.9	3	1.6	6.7	6.9	10.4	7	6.9	40
Mo	0.1	0.1	0.1	0.1	0.1	0.1	0.11	0.1	2
Cu	1.2	2.36	0.5	0.5	0.1	4.9	0.8	0.3	10
Pb	438	15.3	57.09	22.8	3.2	3.2	30	37	20
Zn	5.4	27.3	2.3	150	3	44.9	131.2	110	40
As	0.2	0.2	0.2	0.5	0.5	0.2	0.5	0.5	1.5
Cd	0.1	0.1	0.1	0.1	0.1	0.03	0.1	0.1	nd
Ag	20	0.1	20	0.1	0.1	20	0.1	0.1	0.04
Au	0.1	0.1	0.1	1.3	2.6	0.1	0.1	0.1	nd
Ratios									
Ba/Rb	0.8	0.1	0.3	2.5	1.9	19.2	2.8	2.8	0.5
Ba/Sr	3.1	11	3.4	10.5	8.3	2.6	6.6	6.5	4

*MGMG – medium-grained muscovite granite
†CGBMG – coarse-grained biotite muscovite granite
**Average Granite (Taylor, 1965)
nd – not detected

Table 4.3: Rare earth elements concentration in granitic rocks from the study area (all values in ppm except the ratios)

Rare Earth Elements	Pegmatite	Granite					Banded Gneiss	
		MGMG*				CGBMG†		
	NJ	NI	NW1	NX	NW2	NT2	NX2	NX3
La	3.5	1.9	0.7	28.1	10.7	14.5	26.2	40.3
Ce	8.3	3.8	1.9	62	23.3	29.9	51.1	82.5
Pr	1.1	0.6	0.2	7.3	2.7	3.8	5.25	9.35
Nd	3.3	1.4	0.8	25	9.9	13.5	17.7	34.1
Sm	0.8	0.3	0.5	5.4	2.3	2.7	3.5	6.3
Eu	0.3	0.1	0.1	0.4	0.2	0.9	0.4	0.2
Gd	0.6	0.4	0.4	3.3	1.9	2.5	2.3	4
Tb	0.1	0.1	0.1	0.4	0.3	0.5	0.3	0.7
Dy	0.5	0.5	0.3	1.7	1.4	2.1	1.1	3.1
Ho	0.1	0.1	0.1	0.2	0.2	0.3	0.2	0.5
Er	0.2	0.3	0.1	0.5	0.5	0.8	0.4	1.4
Tm	0.1	0.1	0.1	0.1	0.1	0.1	0.1	0.2
Yb	0.1	0.3	0.2	0.5	0.4	0.7	0.4	1
Lu	0.1	0.1	0.1	0.1	0.1	0.1	0.1	0.1
ΣREE	19.1	10	5.6	134.8	53.8	72.4	109.1	183.7
Ratios								
ΣLREE/ΣHREE	8.1	4	2.7	18.2	9.8	8.1	20	15.4
$(La/Yb)_N$	23.3	4.2	2.3	41.6	16.9	13.8	43.7	26.9
$(Ce/Yb)_N$	21.1	3.2	2.4	35	13.8	10.9	32.5	21
$(La/Sm)_N$	2.7	3.9	0.9	3.2	2.8	3.3	4.6	3.9
Eu/Eu*	1.3	0.9	0.7	0.3	0.3	1.1	0.4	0.1

*MGMG – medium-grained muscovite granite †CGBMG – coarse-grained biotite muscovite granite

Table 4.4: Major oxides concentration in sedimentary rocks from the study area (all values in ppm except the ratios)

Major Oxides	Shale	Lessel Sandstone			
	NF	NH	NK	NN3	NT1
SiO_2	77.6	97.2	96.3	73.7	65.3
TiO_2	0.8	0.1	0.1	0.7	1
Al_2O_3	14.4	1.4	2.2	13	16.1
Fe_2O_3	4	0.2	0.7	7.0	8.9
MnO	0.1	0.1	0.1	0.1	0.3
MgO	1.1	1.1	0.1	1.5	2.4
CaO	0.4	0.1	0.2	0.2	0.7
Na_2O	0.1	0.1	0.1	0.1	1.5
K_2O	1.5	0.1	0.4	3.8	3.7
P_2O_5	0.2	0.1	0.01	0.2	0.2
TOTAL	100.0	100.0	100.0	100.0	100.0
Ratios					
K_2O/Na_2O	15	1	4	38	2.5
SiO_2/Al_2O_3	5.4	69.4	44	5.67	4.1
CIA*	88	80.4	76.69	76.68	73.18
AI_2O_3/TiO_2	18.5	20.7	43.78	19.92	16.04

*CIA - Chemical Index of Alteration

Table 4.5: Trace elements concentration in sedimentary rocks from the study area (all values in ppm except the ratios)

Trace Elements	Shale	Lessel Sandstone			
	NF	NH	NK	NN3	NT1
Ni	18.6	1.9	2	40.1	54.5
Sc	10.4	0.8	0.6	19.5	15.1
Ba	822	210	171	857	1097
Be	2	1	1	1	6
Co	14.8	80.7	80.3	30.9	41.1
Cr	146.1	10.2	10.2	146.1	146.1
Cs	3.6	0.3	0.3	7.1	7
Ga	22.1	1.6	2.8	20.8	27.5
Hf	15.2	1.1	0.6	6.3	14.3
Nb	1.91	0.3	0.4	0.1	1.3
Rb	67.1	3.5	12.9	140.3	159.5
Sn	3	0.3	0.1	0.7	3
Sr	327	58	23	12	135
Ta	1.1	0.4	0.1	0.5	1
Th	12.4	2.1	3	3.8	14.6
U	2.3	0.7	0.4	0.6	2.4
V	93	4	5	135	103
W	43	200	200	116.2	32.3
Zr	61.1	9.9	11.3	2.4	41.3
Y	18.4	4.8	2.3	5.7	44.8
Mo	0.6	0.4	0.3	0.05	0.13
Cu	20.4	1.4	1.7	37.1	7.82
Pb	27.4	5.6	6.2	2625.3	29.0
Zn	37.8	3.1	5.6	301	140.2
As	2	0.2	0.2	0.5	0.2
Cd	0.1	0.1	0.1	0.4	0.1
Ag	22	20	20	22	20
Au	0.1	0.1	0.1	0.1	0.1
Ratios					
Th/U	5.4	3	7.5	6.3	6.1
La/Co	2.8	0.1	0.3	1.6	0.2
Th/Co	0.8	0.1	0.1	0.1	0.4
Ba/Sr	2.5	3.6	7.4	71	8.1

Table 4.6: Rare earth elements concentration in sedimentary rocks from the study area (all values in ppm except the ratios)

Rare Earth Elements	Shale NF	Lessel Sandstone NH	NK	NN3	NT1
La	40.7	13.4	8.1	8.8	65
Ce	97.6	29.4	19.3	22.5	135
Pr	12.9	3.8	1.6	2.8	19.2
Nd	42.9	14.1	5.1	11.4	65
Sm	8	2.5	0.9	2.3	13.7
Eu	1.5	0.6	0.1	0.5	37
Gd	6.1	1.9	0.8	2	12.6
Tb	0.9	0.3	0.1	0.3	2.1
Dy	4.4	1.2	0.4	1.6	9.5
Ho	0.9	0.2	0.1	0.3	1.8
Er	2.1	0.4	0.2	0.8	3.8
Tm	0.3	0.1	0.1	0.1	0.6
Yb	1.9	0.3	0.1	0.6	3.1
Lu	0.3	0.1	0.1	0.1	0.5
ΣREE	220.5	63.2	36.5	54	335.6
Ratios					
ΣLREE/ΣHREE	11	12.9	23.3	7.7	7.9
$(La/Yb)_N$	13	27.1	49.1	8.9	12.7
$(La/Sm)_N$	2.8	2.9	4.9	2.1	2.6
$(Gd/Yb)_N$	2.6	5.1	6.4	2.7	3.2
Eu/Eu*	0.7	0.9	0.4	0.7	0.9

4.11 GEOCHEMISTRY OF BASEMENT ROCKS

The oxides composition of the granites shows that SiO_2 varies from 75 to 85.5 wt. %, Al_2O_3 ranges from 7.1 to 15.3 wt. % while the concentration of Fe_2O_3, MgO, CaO, Na_2O, K_2O, P_2O_5 and TiO_2 varies from 0.2 to 2.5 wt. %, 0.03 to 0.6 wt. %, 0.03 to 0.4 wt. %, 1.7 to 4.5 wt. %, 0.4 to 5.9 wt. %, 0.04 to 0.2 wt. % and 0.01 to 0.2 wt. % respectively (Table 4.1).

In the gneissic rocks, the average concentration of SiO_2 is about 76.1 wt. % and 14.3 wt. % for Al_2O_3 while average concentration of Fe_2O_3, MgO, CaO, Na_2O, K_2O, P_2O_5

and TiO_2 are 0.8 wt. %, 0.2 wt. %, 0.3 wt. %, 2.5 wt. %, 4.8 wt. %, 0.1 wt. % and 0.01 wt. % respectively.

The total alkali-silica (TAS) plot is a useful tool for classification of igneous rocks and for distinguishing between two types of magmatic series: alkaline series and calc-alkaline/tholeiitic series. The analyzed rocks plot within the calc-alkaline/tholeiitic magma series (Fig. 4.4).

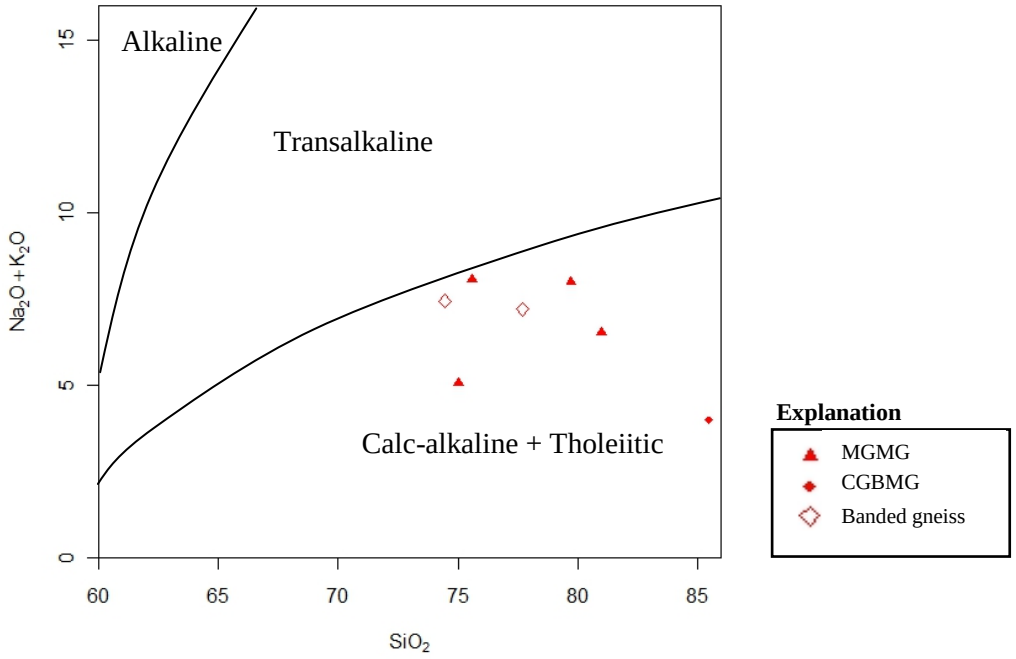


Figure 4.4: Total alkali-silica plot of granites (banded gneiss included) in the area (after Middlemost, 1997) [MGMG – medium-grained muscovite granite, CGBMG – coarse-grained biotite muscovite granite]

Alumina saturation is based on comparing the mole proportions (mole proportion = weight percentage of oxide/molecular weight of the oxide) of the alkalis to alumina in the rock. In order to determine the petrogenetic trait, the samples were plotted on an A/CNK

versus A/NK (where A/CNK = molar Al_2O_3/ [CaO+Na_2O+ K_2O] and A/NK = molar Al_2O_3/ [Na_2O+K_2O]) diagram of Maniar and Piccoli (1989) (Fig. 4.).

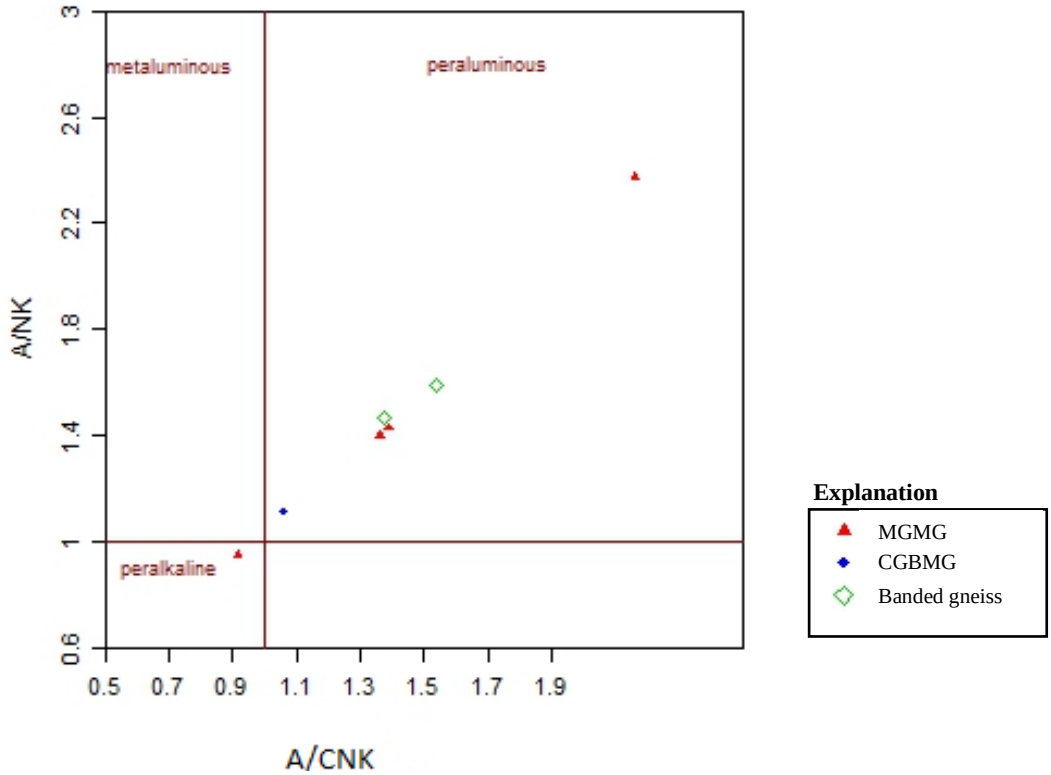


Figure 4.5: A/CNK versus A/NK plot of granites (banded gneiss included) in the area (after Maniar and Piccoli, 1989). [MGMG – medium-grained muscovite granite, CGBMG – coarse-grained biotite muscovite granite]

The granitic rocks plot within the peralkaline and peraluminous field (Fig. 4.5). The granites are peraluminous while medium-grained muscovite granite (NI) appears to be slightly peralkaline. An overall peraluminous character is inferred from the A/NK and A/CNK ratios.

The plot of SiO_2 against Al_2O_3, Na_2O, K_2O, MgO, CaO, Fe_2O_3, P_2O_5 and TiO_2 is used as an index of differentiation. The plot shows that SiO_2 is negatively correlated with Al_2O_3, K_2O, CaO, P_2O_5 while Na_2O is positively correlated. Fe_2O_3, MgO shows both positive and negative correlation with SiO_2 whereas TiO_2 shows no correlation (Fig. 4.6).

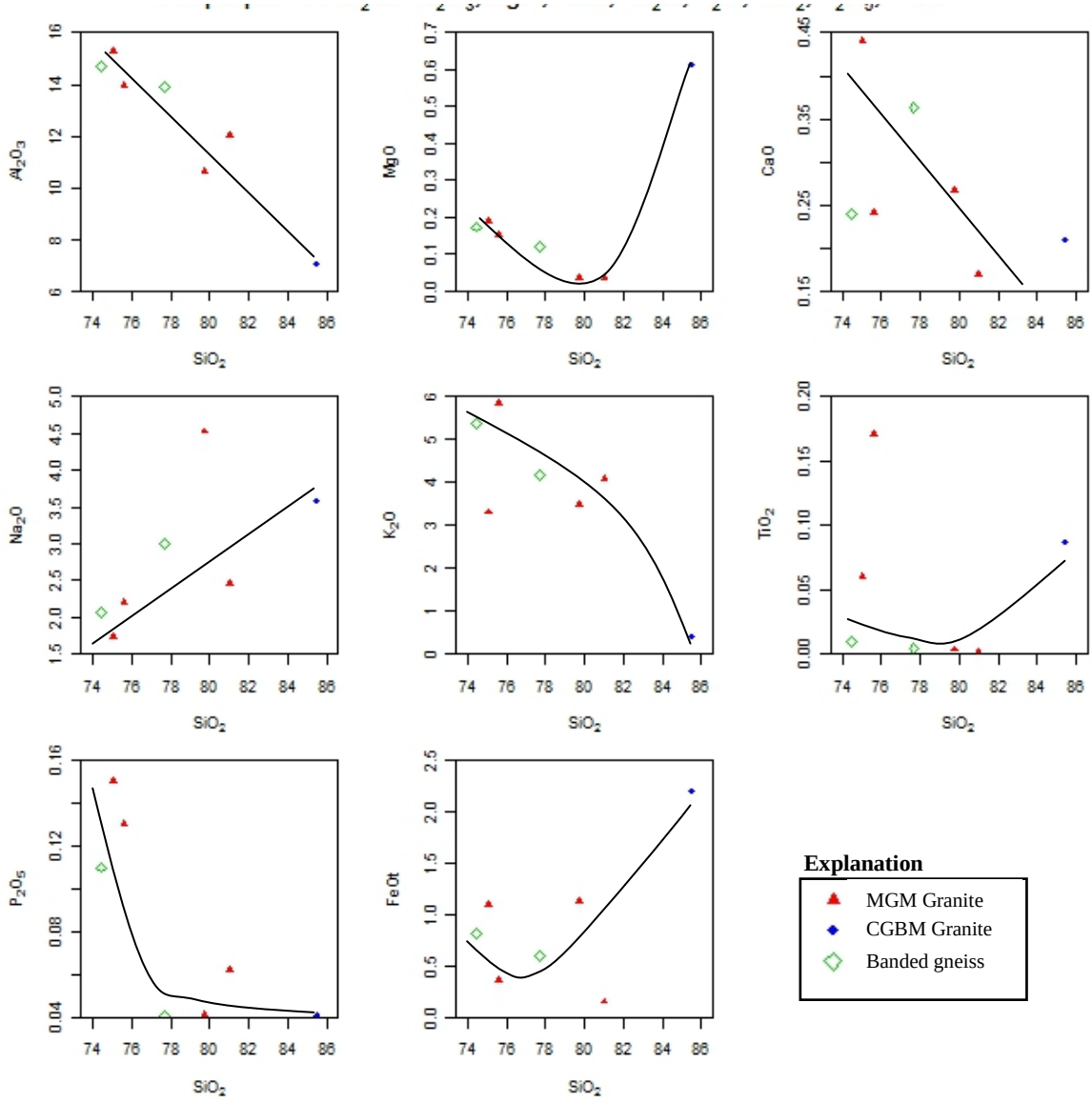


Figure 4.6: Bivariate plot of SiO_2 (wt. %) versus Al_2O_3, Na_2O, K_2O, MgO, CaO, Fe_2O_3, P_2O_5 and TiO_2 in granitic rocks. [MGMG – medium-grained muscovite granite, CGBMG – coarse-grained biotite muscovite granite]

The trace elements have good correlation with SiO_2. Ni, Ba, Rb, Zr, Zn, Pb are negatively correlated with SiO_2 whereas Sr, Cu, Co display positive correlation with SiO_2 (Fig. 4.7).

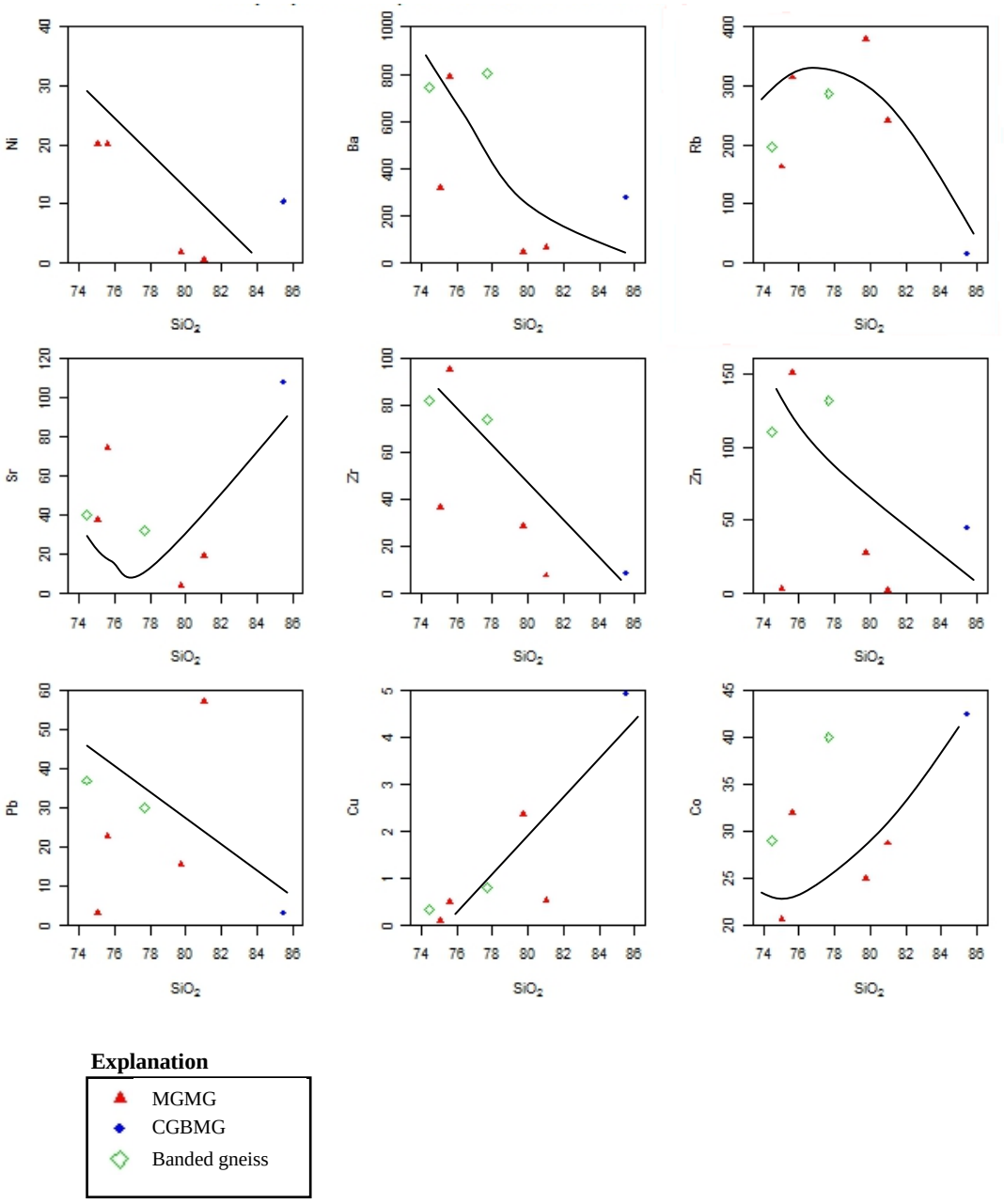


Figure 4.7: Bivariate plot of SiO_2 (wt. %) versus Ni, Ba, Rb, Sr, Zr, Zn, Pb, Cu and Co in granitic rocks. [MGMG – medium-grained muscovite granite, CGBMG – coarse-grained biotite muscovite granite]

The banded gneiss and medium-grained muscovite granite at Mbatoo contains the highest concentration of Ba, Th, Zn compared with the other granitic rocks in the area and the average granite value of Taylor (1965) (Table 4.2). The concentration of Ni (0.5 – 20

ppm), V (1 – 10 ppm), Zr (7.7 – 95.4 ppm) are low whereas Co (20.7 – 42.5 ppm) is high in the granitic rocks compared with the average granite values of Taylor (1965) **(**Table 4.2**)**. Copper (Cu) and Pb contents in the granitic rocks are low relative to values reported by Taylor (1965) for granite. By contrast, the concentration of Pb in pegmatite is high (438 ppm)**.** Ag content in the pegmatite, coarse-grained biotite muscovite granite and medium-grained muscovite granite (NW1) also appears to be high (20 ppm).

Trace element data normalized to chondrite values of Thompson (1982) and the multi-element spider plot show that the large lithophile elements (LILE) are generally enriched relative to the high field strength elements (HFSE) (Fig. 4.8). The large lithophile elements (LILE) Rb, K are enriched while Sr is depleted in the rocks. The high field strength elements Nb, Zr, Y are slightly depleted while Ti is strongly depleted in the granitic rocks.

The ratio of Ba/Rb ranges from 0.1 to 2.5 in the granitic rocks increasing to 2.8 in banded gneiss and much higher value in coarse-grained biotite muscovite granite (19.2). Ba/Sr ratios are higher in the granites relative to the gneissic rocks and Ba/Rb ratios are higher in the gneissic rocks relative to the granites.

On the Y+Nb versus Nb discrimination diagram (Fig. 4.9) the banded gneiss (NX3) is straddled on the boundary line between the syn-collision (syn-COLG) and volcanic arc granite (VAG) fields. The medium-grained muscovite granite (NI) and coarse-grained biotite muscovite granite plot in volcanic arc granite field while the other medium-grained muscovite granite and banded gneiss (NX2) plot within the syn-COLG field.

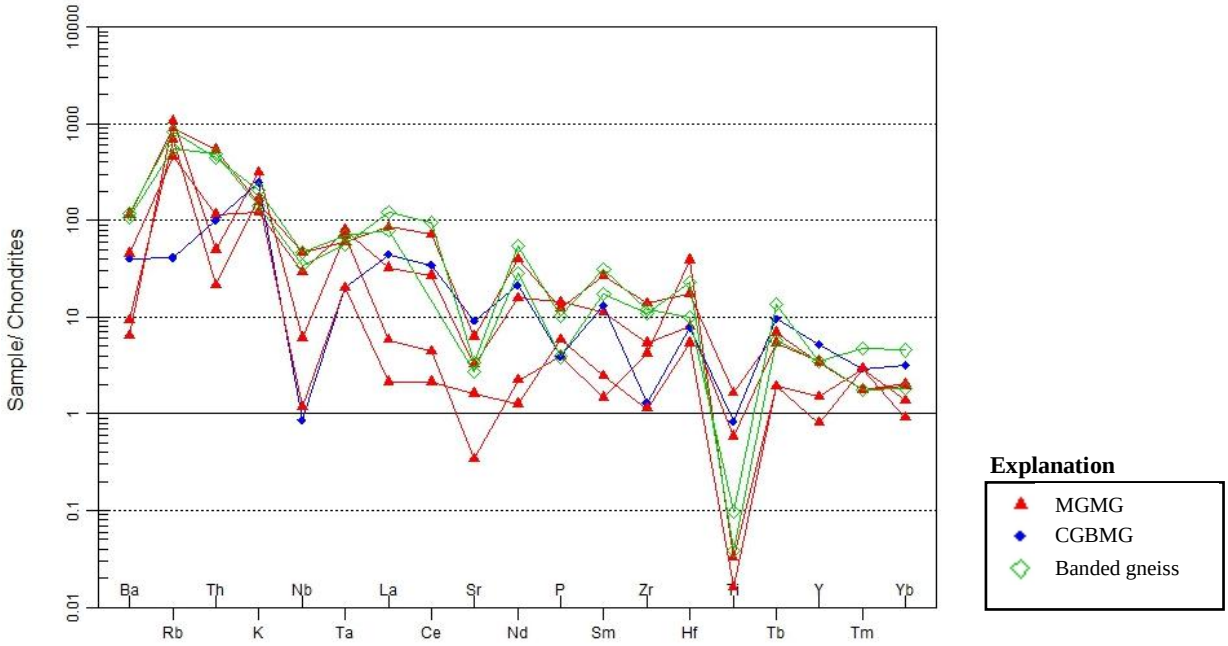


Figure 4.8: Multi-element spider diagram in granitic rocks from the study area (chondrite normalizing values, Thompson, 1982). [MGMG – medium-grained muscovite granite, CGBMG – coarse-grained biotite muscovite granite]

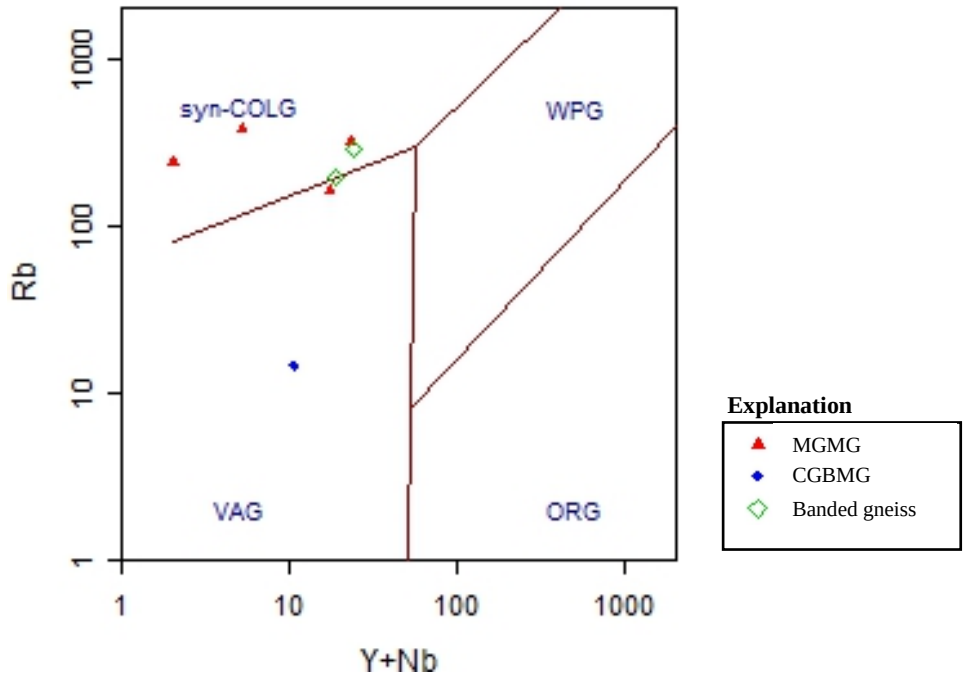


Figure 4.9: Y+Nb versus Rb discrimination diagram for granites (banded gneiss included) in the area (after Pearce *et al*., 1984) [Syn-COLG = Syn-collision granite; VAG = Volcanic arc granite; WPG = Within plate granite; ORG = Ocean ridge granite]

The rare earth elements (REE) are usually sub-divided into the light rare earth element (LREE) and heavy rare earth element (HREE) classes. The LREE consist of La to Sm (atomic numbers 57 – 62) and the heavy REE are Gd to Lu (atomic numbers 64 – 71). The REE data on granitic rocks in the area is presented in Table 4.3. The ΣREE varies from 5.6 to 183.74 ppm. The medium-grained muscovite granite from Ihugh (NI, NW1) has the lowest ΣREE of 5.6 ppm and 10 ppm whereas the highest ΣREE values were recorded in banded gneiss (109.1 ppm, 183.7 ppm) and medium-grained muscovite granite from Mbatoo (134.8 ppm). The ratio of light rare earth element to heavy rare earth element (ΣLREE/ΣHREE) varies from 2.3 to 20. Negative europium anomaly (Eu/Eu*) relative to chondrite is present in banded gneiss and medium-grained muscovite granite and ranges from 0.1 – 0.9 while a positive anomaly is observed in coarse-grained biotite muscovite granite (1.1) and pegmatite (1.3) (Table 4.3).

Rare earth elements data are normalized to chondrite values of Nakamura (1974) (Fig. 4.10). The REE pattern of banded gneiss (NX2, NX3), medium-grained muscovite granite (NX, NW2) displays a steep slope from the LREE to the HREE and a negative Eu anomaly. The banded gneiss, medium-grained muscovite granite (NX, NW2) and coarse-grained biotite muscovite granite have generally similar REE pattern while the other medium-grained muscovite granite (NI, NW1) show dissimilar irregular REE pattern. The normalized La/Yb ranges from 2.3 - 41.6 in the granites and 26.9 – 43.7 in banded gneiss. Normalized Ce/Yb in the granitic rocks ranges from 2.4 - 35 and 21 – 32.5 in banded gneiss. In granite, $(La/Sm)_N$ varies from 0.9 - 3.9 and in banded gneiss is is about 3.9 – 4.6. These ratios are generally low in the medium-grained muscovite granites (Table 4.3).

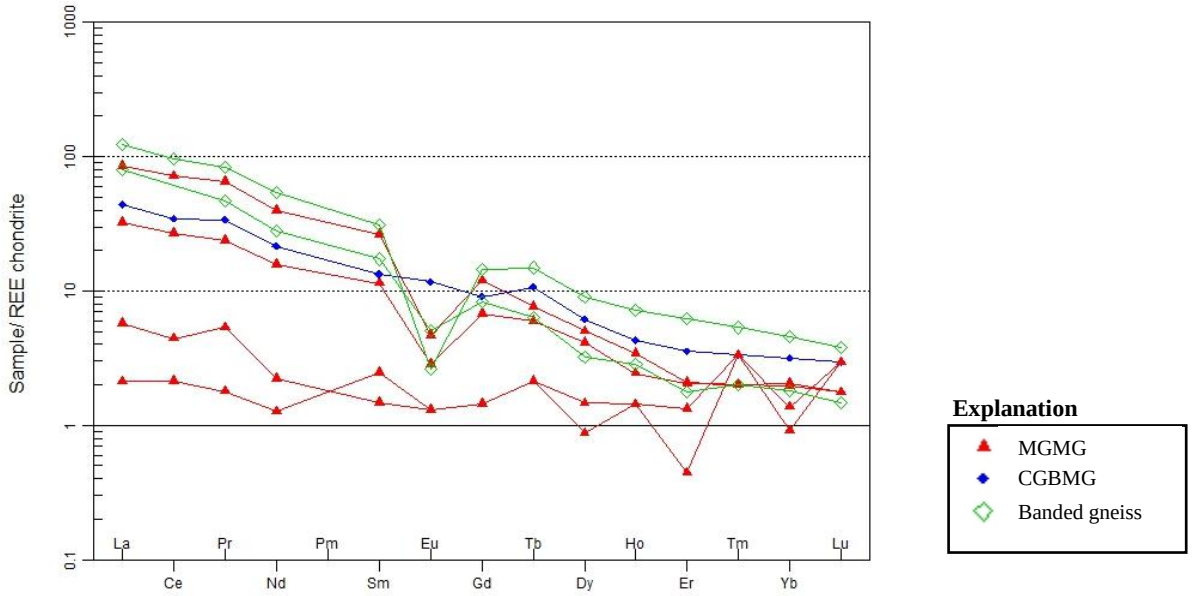


Figure 4.10: Rare earth elements distribution pattern in granitic rocks from the study area (chondrite normalizing values, Nakamura, 1974). [MGMG – medium-grained muscovite granite, CGBMG – coarse-grained biotite muscovite granite]

4.12 GEOCHEMISTRY OF LESSEL SANDSTONES AND SHALE

SiO_2 ranges from 73.7 – 97.2 wt. %, Al_2O_3 ranges from 1.4 to 16.1, Fe_2O_3 varies from 0.7 to 8.9, MgO ranges from 0.05 to 2.4 wt. % in the Lessel sandstones. In addition, the concentration of CaO, Na_2O, K_2O, MnO, TiO_2 and P_2O_5 in the sandstones also varies from 0.03 to 0.7 wt. %, 0.01 to 1.5 wt. %, 0.04 to 3.7 wt. %, 0.01 to 0.3 wt. %, 0.1 to 1.0 wt. % and 0.01 to 0.2 wt. % respectively (Table 4.4). There is a positive correlation existing between Al_2O_3 and K_2O, Na_2O, MgO, CaO, Fe_2O_3, TiO_2 (Table 4.4). SiO_2 is in abundance compared to the average Upper Continental Crust value (66%) of Taylor and McLennan (1985). Fe_2O_3, MgO, MnO concentration is slightly high in sandstones around Lessel and Ihugh areas whereas CaO content is low compared to values reported by Adeigbe and Jimoh (2013) for the Cross River Group (Table 4.7).

Table 4.7: Average chemical composition of shale and sandstone from the study area compared to those from other sedimentary basins in Nigeria and worldwide.

Major Oxides	Present Study: Shale	NASC[a]	PAAS[b]	Present Study: Average Sandstone	Cross River Group[c]
SiO_2	77.6	64.2	62.4	83.1	79.6
TiO_2	0.8	0.8	1	0.4	0.4
Al_2O_3	14.4	17.1	18.8	8.2	7.7
Fe_2O_3	4	5.7	7.2	4.2	1.4
MnO	0.1	-	-	0.1	0.1
MgO	1.1	2.8	2.2	1.2	0.4
CaO	0.4	3.5	1.3	0.3	1.5
Na_2O	0.1	1.1	1.2	0.4	0.3
K_2O	1.5	3.9	3.7	2	2.0
P_2O_5	0.1	0.2	0.2	0.1	0.1
Total	100.0	99.4	97.9	100.0	93.4

a. NASC (North American Shale Composite) - Haskin *et al.* (1966)
b. PAAS (Post Archean Australian Shale) - Taylor and McLennan (1985)
c. Cross River Groups - Adeigbe and Jimoh (2013)

The chemical composition of shale relative to global average for shale shows that the shale in the study area is rich in SiO_2 and poor in CaO content. Al_2O_3, Fe_2O_3, MgO, Na_2O, K_2O contents are fairly low relative to NASC (Haskin *et al.,* 1966) and PAAS (Taylor and McLennan, 1985). P_2O_5 and TiO_2 concentration are similar to NASC and PAAS.

Silica enrichment is a measure of the maturity of sandstone. It reflects the duration, intensity of weathering and destruction of other minerals during transportation. The ratio of SiO_2 and Al_2O_3 can therefore be used to determine whether a rock is enriched or depleted in silica. In the area of study, SiO_2 content is low (4.1 to 5.7) in some of the sandstones (NF, NN3, NT1) whereas it is high (44 - 70.5) in the other sandstones (NK, NH) (Table 4.4).

According to Crook (1974), K_2O/Na_2O ratio > 1 indicates quartz-rich sandstones, while K_2O/Na_2O ratio < 1 is an indication of quartz-poor sandstones. In Lessel-Ihugh area, the ratio of K_2O/Na_2O ranges from 1 – 38, indicating that the sandstones are quartz-rich.

Employing the plot of log SiO_2/Al_2O_3 versus log Fe_2O_3/K_2O as proposed by (Herron, 1988), sedimentary rocks are classified as shale (NF), wacke (NT1), litharenites NN3), sub-litharenite (NK) and quartz-arenite (NH) (Fig. 4.11). The average composition of the Lessel sandstones in the study area plot within the sub-litharenite field (Fig. 4.11).

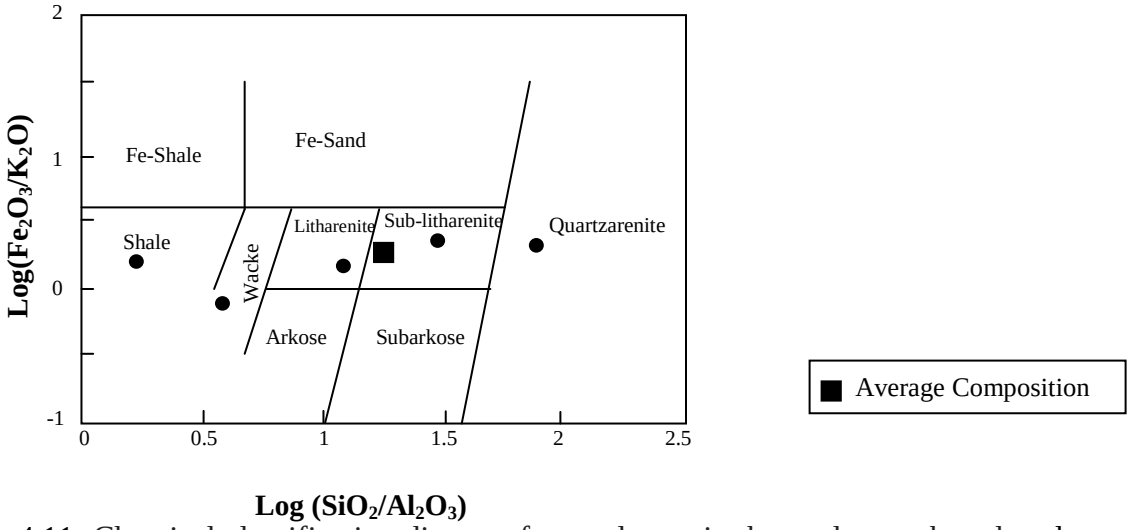


Figure 4.11: Chemical classification diagram for sandstone in the study area based on log SiO_2/Al_2O_3 versus log Fe_2O_3/K_2O diagram of Herron (1988).

As proposed by Nesbitt and Young (1982) chemical index of alteration (CIA) is a measure of the degree of weathering in the source region. It records also the progressive alteration of plagioclase and K-feldspars to clay minerals (Rahaman and Suzuki, 2007). The CIA is calculated as shown in the following the equation: CIA = [Al_2O_3 / (Al_2O_3 + CaO* + Na_2O + K_2O)]100 (in molecular proportion) where CaO* represents the amount of CaO incorporated in the silicate phase. Lime (CaO) values are accepted only if CaO $\leq$

Na_2O; consequently, when CaO is > Na_2O it is assumed that the concentration of CaO equals that of Na_2O (Bock *et al.,* 1998).

Nebitt and Young (1982) suggested CIA values of 100 for kalonite and chlorite and 70 - 75 for average shales. High values of 76 - 100 indicate intensive chemical weathering in the source areas whereas values <50 indicate unweathered source areas. CIA values for the sedimentary rocks in the study area vary from 73.2 - 88 (Table 4.4). Shale (NF) has a CIA of 87.9. The sub-litharenite (NK), litharenites (NN3), wacke (NT1) and quartz arenite (NH) have CIA values of 76.7, 76.7, 73.2 and 80.4 respectively (Table 4.4) thus indicating that an intensive chemical weathering occurred in the source area (Fig. 4.12).

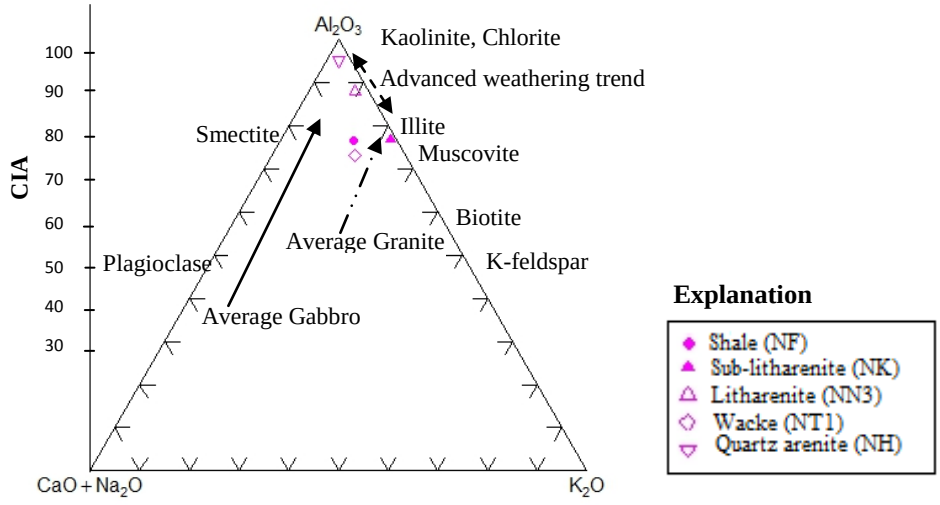


Figure 4.12: Chemical Index of Alteration (CIA) ternary diagram of sandstones in the study area (after Nesbitt and Young, 1982).

According to McLennan *et al.* (1993), the ratio of Th/U in sedimentary rocks can be used to determine the degree of weathering and recycling of sedimentary rocks. During weathering U is lost leading to an increase in the Th/U ratio. Th/U ratio in most upper continental crust rocks ranges from 3.5 to 4.0 (McLennan *et al*., 1993). Th/U values > 4.0

may indicate intense weathering in source area or sediment recycling (Rahaman and Suzuki, 2007). Th/U ratio in shale and sandstones in the study area ranges from 3.0 – 7.5 (average of 5.7) (Table 4.5) thus implying a moderate to intense weathering in the source area.

Trace element concentrations are normalized to average upper continental crust (UCC) values of Taylor and McLennan (1995). The trace element concentration in shale, litharenite and wacke sandstones have compositions almost similar to those of the average upper continental crust though with depletion in Zr and Nb (Fig. 4.13)**.** Pb is strongly enriched in litharenite but strongly depleted in Sr, Zr, Nb than in the other sandstones. The concentration of the trace elements in sub-litharenite and quartz-arenite sandstones are generally lower than the average UCC (Fig. 4.13) except for their high Co content.

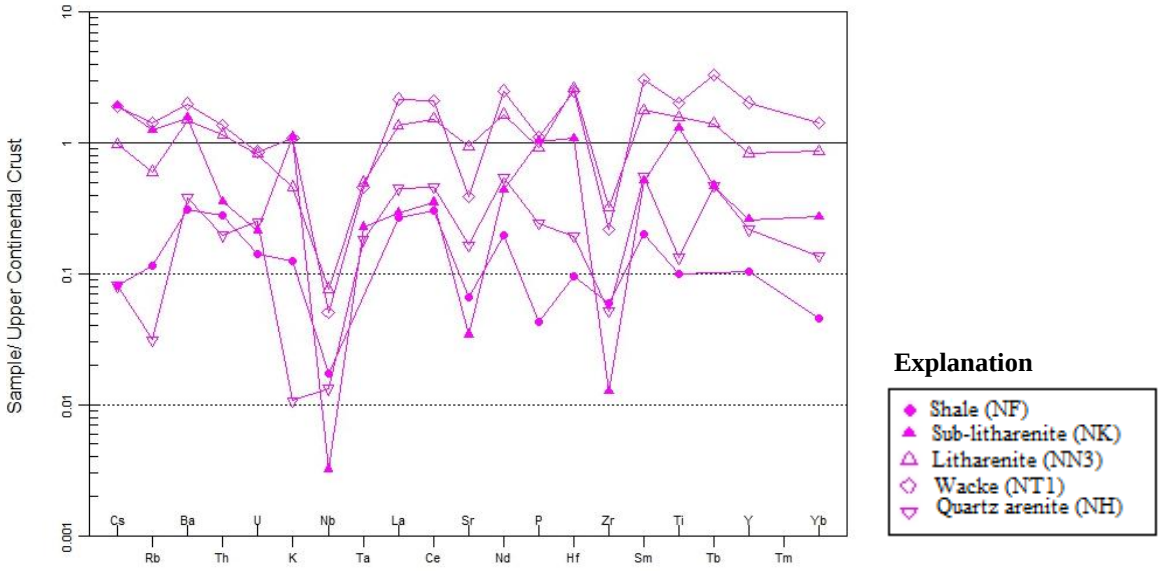


Figure 4.13: Multi-element spider diagram in shale and sandstones from the study area (chondrite normalizing values, Taylor and McLennan, 1995).

Hayashi *et al.* (1997) propsed that Al_2O_3/TiO_2 is useful in determining the provenance of sedimentary rocks. Hayashi *et al.* (1997) further assigned Al_2O_3/TiO_2 ratios of 3 – 8 for mafic igneous source rocks, 8 – 21 for intermediate igneous source rocks and

21 – 70 for felsic igneous rocks. The Al_2O_3/TiO_2 ratios for shale and sandstone in the study area range from 16 – 20 whereas, the sub-litharenite (NK) has a ratio of 43 (Table 4.4).

Roser and Korsch (1988) proposed a discriminant diagram using the functions F1 and F2 (Appendix IV) to determine the tectonic setting of terrigenous sedimentary rocks. The Lessel sandstones and shale plot within the P4 field which represents granite-gneiss provenance (Fig. 4.14). The average REE of sandstone was plotted along with REE of the granitic rocks in the study area. The plot shows that the REE pattern in sandstones is similar with that of medium-grained muscovite granite (NW2) and banded gneiss (Fig. 4.15).

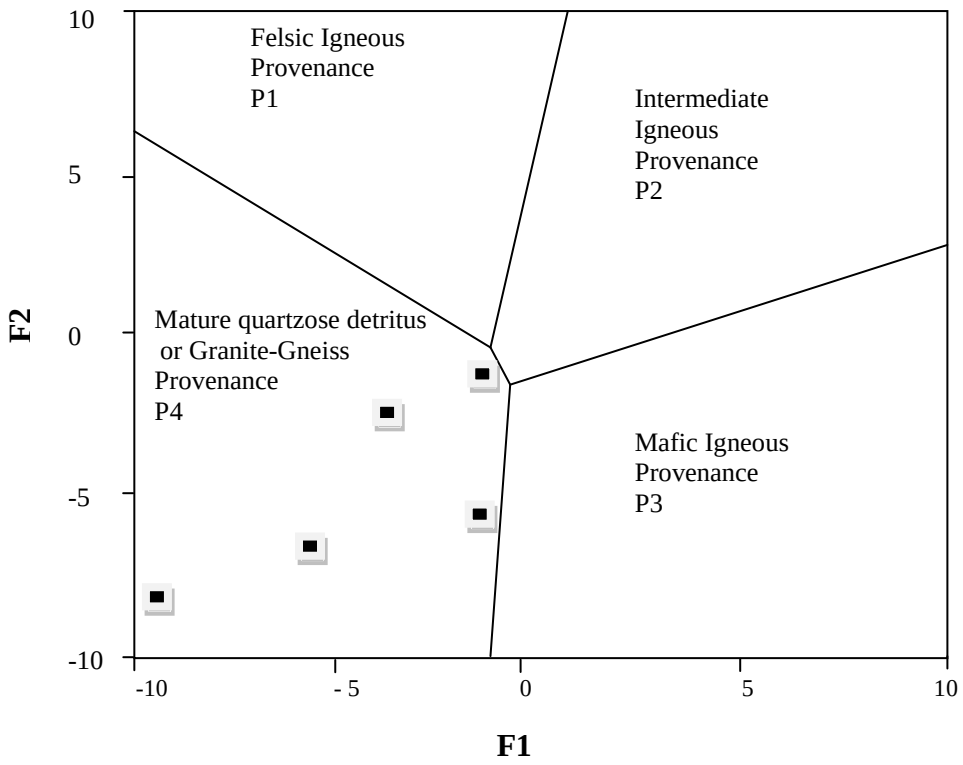


Figure 4.14: Provenance discriminant function plot of the Lessel Sandstones and Shale (after Roser and Korsch, 1988).

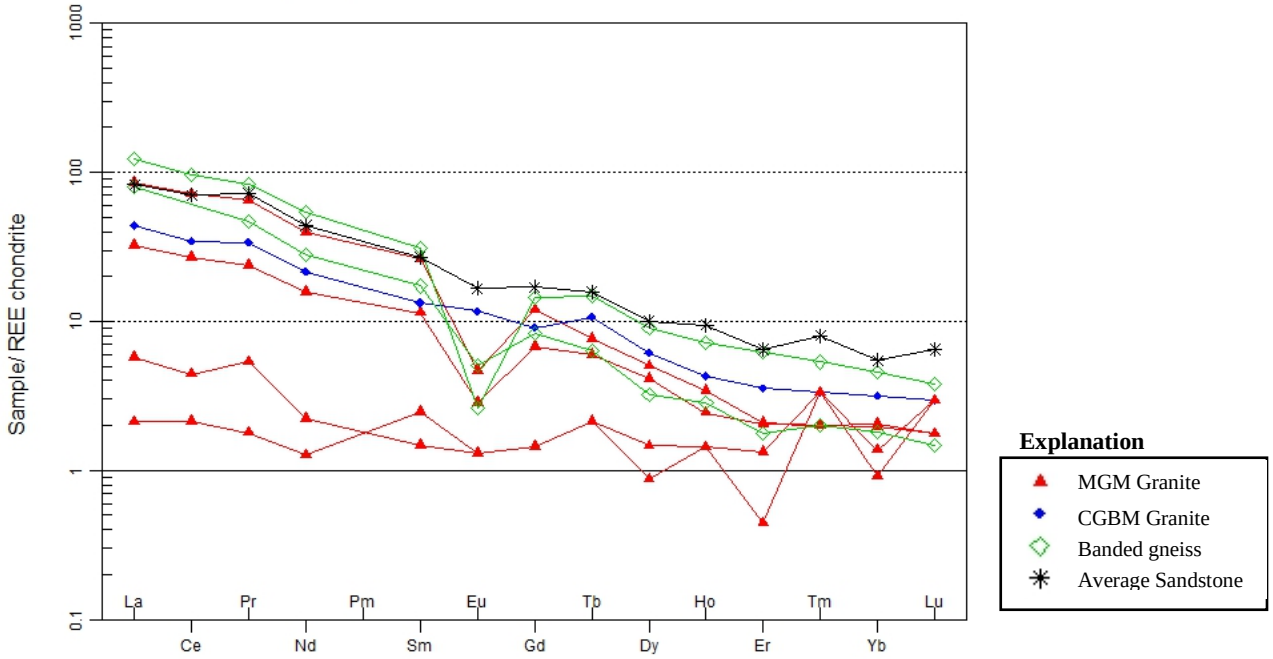


Figure 4.15: Rare earth elements distribution pattern of average sandstone and granitic rocks from the study area (chondrite normalizing values, Nakamura, 1974).

Total REE concentration in sandstones ranges from 36.5 - 335.6 ppm with ΣLREE/ΣHREE of 7.7 - 23. Rare earth element distribution of the sedimentary rocks normalized to chondrite values of Wakita *et al.* (1971) is presented in Figure 4.16. The REE distribution plot exhibits REE pattern (La_N/Yb_N = 9.8 - 54) with a gentle slope for the LREE relative to the flat HREE with negative Eu anomaly ranging from 0.4 - 0.9 in the sandstones and shale.

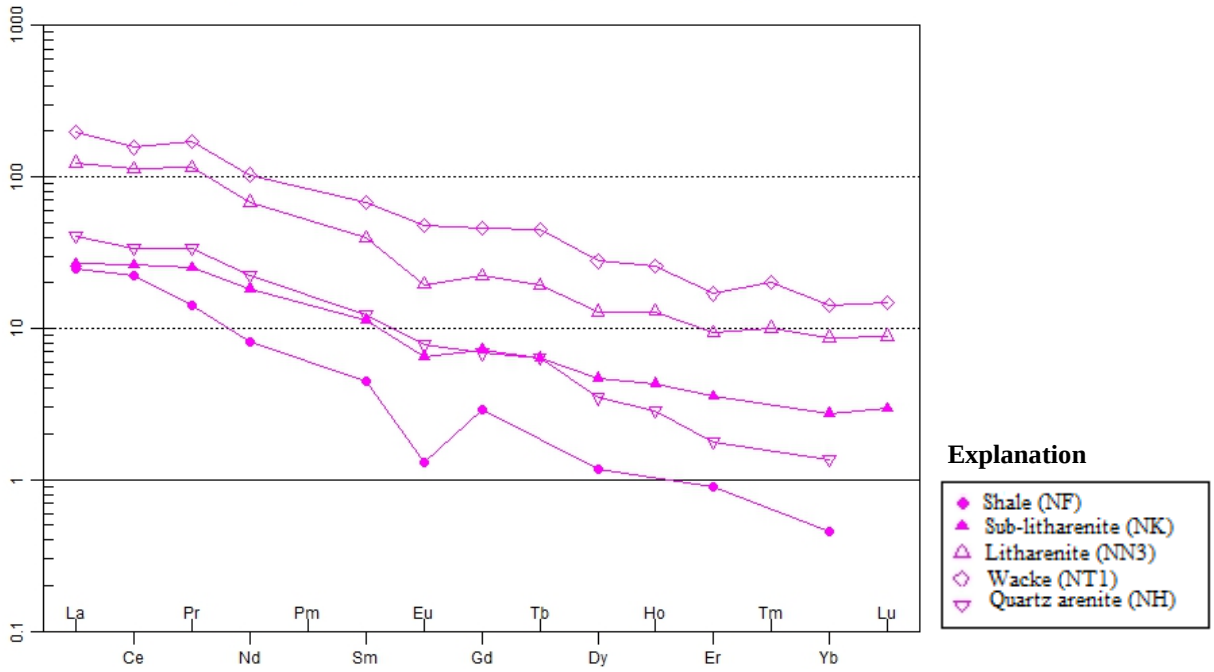


Figure 4.16: Rare earth elements plot of shale and sandstones in the study area (chondrite normalizing values, Wakita *et al.*, 1971).

4.13 GEOCHEMISTRY OF BARYTE

The concentration of BaO increases gradually from the barren rocks to the mineralized rock reaching maximum in baryte vein with BaO content in baryte vein varying from 79.2 – 83.7 wt. % (Table 6.8). SiO_2 content of mineralized gneiss and sandstones ranges from 24.9 – 62.6 wt. % and 77.1 – 75.7 wt. % respectively. In baryte veins, SiO_2 content is low varying from13.3 – 20.5 wt. % (Table 4.8).

The content of Fe_2O_3 increases from 7.2 – 8.8 wt. % in the barren sandstones (NN3, NT1) to 7.1 - 12.5 wt. % in the mineralized sandstones (NN1, NQ1) but very much depleted (0.1 – 1.9 wt. %) in the baryte veins (Tables 4.4 and 4.8). The other major oxides TiO_2, Al_2O_3, MnO, MgO, Na_2O, K_2O, and P_2O_5 are enriched in the barren and mineralized rocks but depleted in the baryte veins. Calcium oxide (CaO) content in mineralized gneiss (NO2) and lead-zinc sulphide vein (NO3) is high (18.2 wt. % and 4.9

wt. % respectively) in mineralized gneiss from Bunde area. Conversely, CaO content in all other mineralized rocks and baryte veins are low ranging from 0.03 – 0.1 wt. %. The major oxides concentration in baryte veins is generally depleted compared to the mineralized host rocks and barren sandstones/granitic rocks.

Table 4.8: Major oxides concentration in mineralized host rocks, baryte veins and lead-zinc sulphide veins from the area of study (all values are in wt. %)

Major Oxides	Mineralized Gneiss		Mineralized Sandstone		Baryte Veins			Lead-Zinc Sulphide Veins	
	NO2	NO4	NN1	NQ1	NM	NO5	NQ2	NN2	NO3
SiO_2	77.1	75.7	62.6	24.9	20.5	18.9	13.3	92.2	35.0
TiO_2	0.1	1.7	1	0.5	0.01	0.01	0.1	0.2	0.04
Al_2O_3	2.9	9.5	17.1	9.6	0.2	0.05	1.1	3.4	0.8
Fe_2O_3	0.1	1.4	7.2	12.5	0.1	0.04	1.9	2.3	0.1
MnO	0.01	0.01	0.01	0.9	0.01	0.01	0.2	0.9	0.01
MgO	0.1	0.5	1.4	0.6	0.01	0.01	0.1	0.2	0.01
CaO	18.2	0.1	0.04	0.1	0.04	0.03	0.1	0.1	4.9
Na_2O	0.2	0.01	0.05	0.01	0.01	0.01	0.01	0.01	0.01
K_2O	1.6	3.2	5.2	1.7	0.01	0.01	0.2	0.7	0.3
P_2O_5	0.1	0.1	0.2	0.1	0.01	0.01	0.01	0.01	0.01
BaO	0.3	3.5	0.2	48.9	79.2	80.9	83.7	0.05	51.4
SrO	0.1	0.04	0.003	0.4	0.5	0.3	0.6	0.07	0.4
TOTAL	100.4	96.4	94.95	100.4	100.7	100.7	101.2	100.0	100.0

There is a positive correlation of the base metals Pb, Zn and Cu with one another in the mineralized rocks and baryte veins (Table 4.9). The highest content of Pb, Zn, Cu recorded in baryte from the northern part and gradually decreases southwards in the study area (Table 4.9). Pb is strongly positively correlated with Zn and moderately positively correlated with Cu. Copper has a strong positive correlation with Ag, Cd, Fe_2O_3, and MnO.

Table 4.9: Trace elements concentration in mineralized host rocks, baryte veins and lead-zinc sulphide veins from the area of study (all values are in ppm except the element ratios)

Sample	Mineralized Gneiss		Mineralized Sandstone		Baryte Veins			Lead-Zinc Sulphide Veins	
					Bunde	Lessel-Mbagwa	Ihugh	Lessel-Mbagwa	Bunde
Trace Elements	**NO2**	**NO4**	**NN1**	**NQ1**	**NM**	**NO5**	**NQ2**	**NN2**	**NO3**
Ni	5.3	20	23	20	20	20	20	4.4	20
Sc	1.4	20	17	9	1	1	2	6	1
Be	1	1	3	5	1	2	1	1	2
Co	39.1	25.2	30.6	35.7	12.5	19.3	14.5	72.3	26.2
Cr	8.7	146.1	204.5	131.5	73.1	29.2	29.2	58.4	43.8
Cs	0.7	1.2	6.6	6.3	0.1	0.1	0.5	0.8	0.1
Ga	4.65	14.9	22.9	16.1	2.6	3.5	2.3	8.2	7.7
Hf	5.1	3.2	7.8	2.5	1.9	1.3	2	1.74	2.3
Nb	0.7	8.4	12.4	9.5	1.6	0.3	1	0.05	1.5
Rb	8.5	138.8	192.4	113.3	0.3	0.1	9.6	25.3	6.1
Sn	1.3	1	1	1	1	1	1	0.1	1
Ta	1.1	0.8	1	1.6	4.4	6.2	3.8	0.3	3
Th	4.1	0.6	8.9	9.5	0.2	0.2	1.1	2.6	0.8
U	0.9	0.2	2.1	2.9	0.1	0.1	0.2	0.4	0.1
V	2	252	87	71	27	8	13	31	15
W	200	162.9	113.5	13.1	77.4	96.9	43	200	144.1
Zr	14.6	105.8	280.8	86.5	1.4	1.2	10.6	1.5	8.7
Y	77.5	2.4	30.7	19	2	1.8	4.5	2.6	4.9
Mo	0.67	0.5	0.1	4.4	0.1	0.1	1	0.6	0.2
Cu	4.3	200.2	30.3	51	25.1	66.4	7	150.2	121.1
Pb	404.96	5132.1	488.2	713.7	414.2	1294.6	25.6	5446.6	>10000
Zn	569.7	366	234	146	93	3764	54	2925.9	>10000
As	1	10.6	0.5	8.5	0.5	0.5	1.9	0.2	0.5
Cd	0.04	0.5	0.3	0.1	0.3	9.8	0.1	12.6	23.4
Ag	96	0.7	0.1	0.1	0.3	0.3	0.1	499	1.9
Au	0.1	28.7	5.4	4.3	5.9	7.2	2.3	0.1	34.2
Hg	<0.01	0.04	<0.01	<0.01	0.03	0.03	<0.01	<0.01	0.09
Ratio									
Ba/Sr	41.1	96.9	54.4	13.8	147.4	268.3	131.1	0.7	11.9

Trace element data for the baryte normalized to the values of Taylor and McLennan (1995) exhibit an almost similar pattern in all three baryte samples (Fig. 4.17). The baryte samples are highly enriched in Ba, Sr but strongly depleted in Rb, K, Ce, Zr. The trace elements Th, Y, La and Ce are positively correlated in the baryte from the different locations. Cerium content in baryte from Ihugh is fairly depleted but strongly depleted in barytes from Lessel-Mbagwa and Bunde.

The trace element distribution pattern in baryte veins and the mineralized rocks slightly differs from what is observed in the barren rocks. The multi-element plot shows high enrichment in Ba, Sr and high depletion in Rb, Th, U, K, Ce, Nd, P, Hf, Zr, Ti (Fig. 4.18 a, b, c).

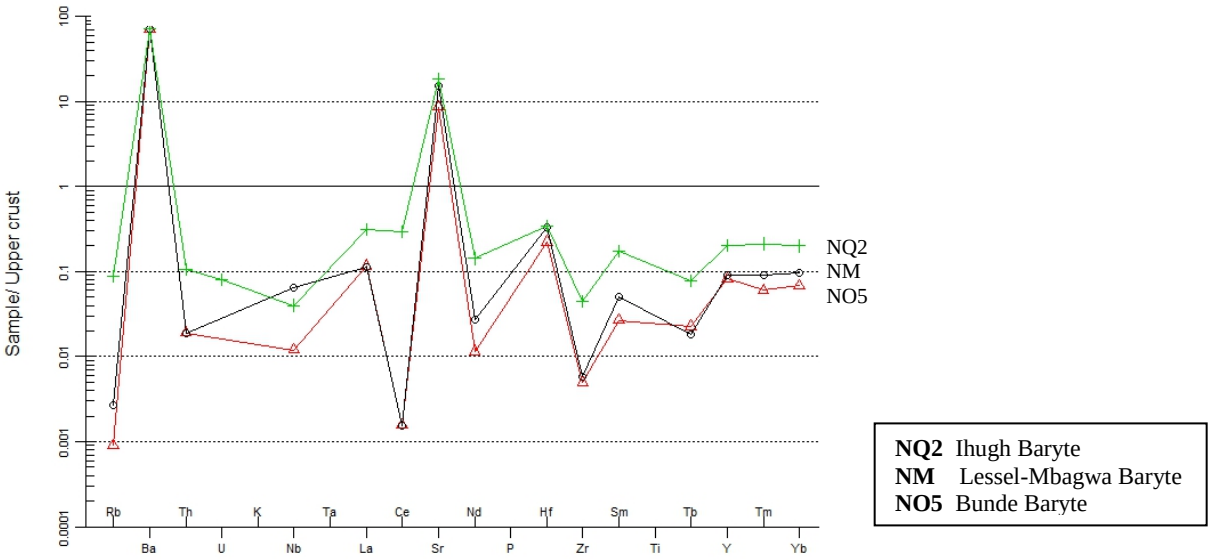
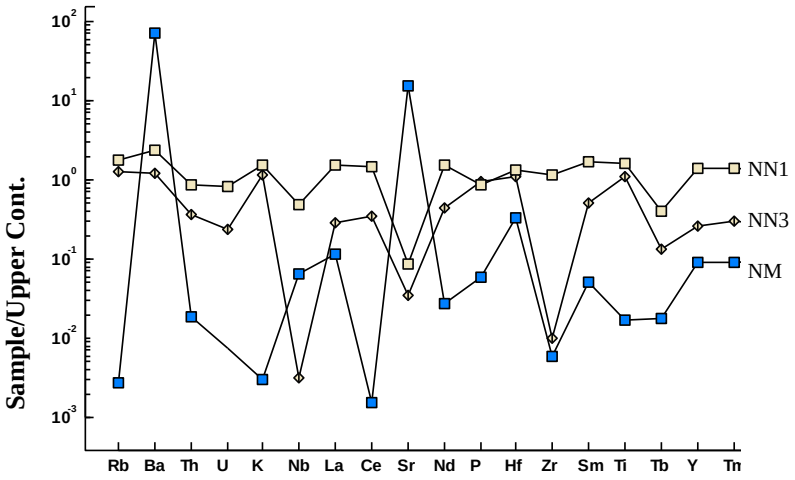
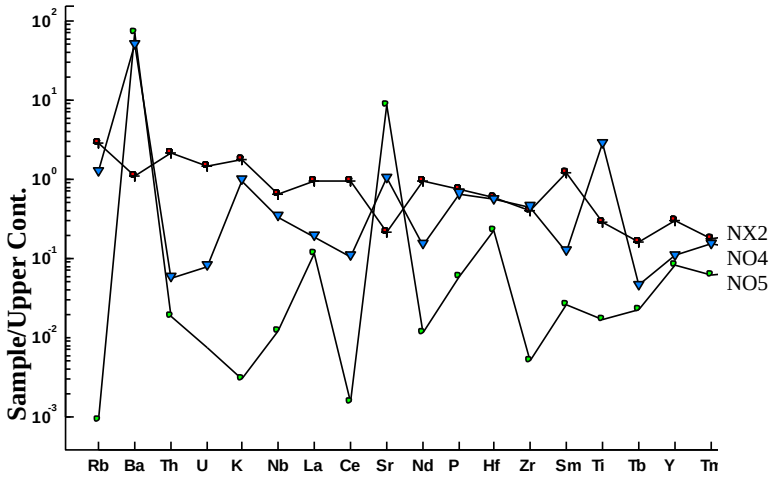


Figure 4.17: Multi-element spider diagram of baryte from Lessel-Mbagwa, Bunde and Ihugh (chondrite normalizing values, Taylor and McLennan, 1995)



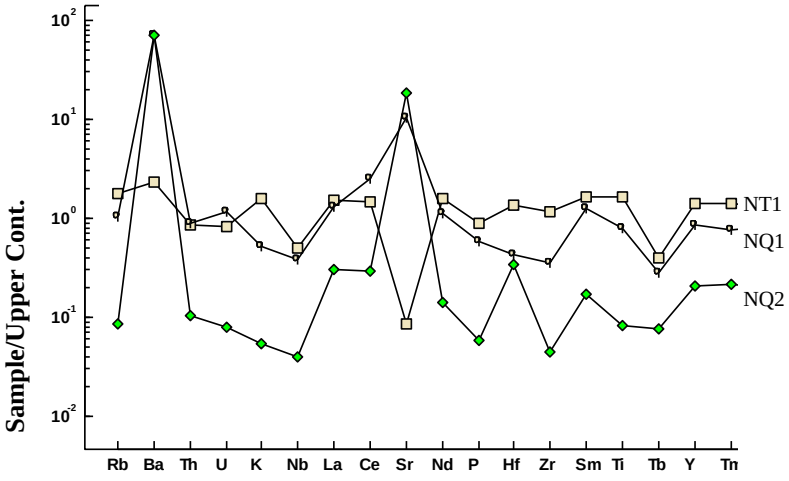
NN3 Barren Sandstone
NN1 Mineralized Sandstone
NM Lessel-Mbagwa Baryte Vein

a.



NX2 Barren Gneiss
NO4 Mineralized Gneiss
NO5 Bunde Baryte Vein

b.



NT1 Barren Sandstone
NQ1 Mineralized Sandstone
NQ2 Ihugh Baryte Vein

c.

Figure 4.18: Trace elements variations in baryte vein, mineralized host rock and barren rock from (a) Lessel-Mbagwa (b) Bunde (c) Ihugh (chondrite normalizing values, ` Taylor and McLennan, 1995).

However, Ce is slightly depleted in baryte from Ihugh (Fig. 6.16 c) and there is also a slight Ti enrichment baryte from Bunde (Fig. 6.16 b). Ba/Sr is low in barren sandstones (2.5 – 71) and gneiss (2.3 – 2.4), moderately high in mineralized sandstones (13.8 – 54.4) and gneiss (41.1 – 96.9) but very high in the baryte veins (131.1 – 268.3) (Tables 6.2, 6.5 and 6.8).

Rare earth elements plot of baryte normalized to chondrite values of Nakamura (1974) shows that baryte from Lessel-Mbagwa and Bunde have similar distribution pattern (Fig. 4.19). However the pattern for baryte from Ihugh differs slightly, displaying strong enrichment in LREE relative to HREE. Rare earth element abundances in the baryte veins are low in baryte from Bunde (7.2 ppm), Lessel-Mbagwa (7.3 ppm) and fairly high in baryte from Ihugh (39.4 ppm) (Table 4.10). The ΣREE in baryte is generally lower than ΣREE abundances in mineralized and barren rocks (Table 4.10). The La_N/Yb_N and ΣLREE/HREE ratio in baryte are 10.8 and 1.7 in Lessel-Mbagwa; 15.6 and 1.2 in Bunde; 14.1 and 5.0 in Ihugh. In addition, barytes from the three main localities exhibit strong negative Eu/Eu* of 0.04, 0.05 and 0.02 in addition to strong positive Gd/Gd* of 17.1, 18.6 and 21.4 in barytes from Ihugh, Lessel-Mbagwa and Bunde areas respectively. Strong negative Ce/Ce* of 0.06 is evident in barytes from Bunde and Lessel-Mbagwa while baryte from Ihugh shows positive Ce/Ce* of 1.3. The rare earth elements Dy, Ho, Er and Lu are not reflected in barytes profiles from Lessel-Mbagwa and Ihugh areas. Dysprosium (Dy) is also singularly not reflected in baryte profile from Bunde (Fig. 4.19). The reason for this is that the values of Dy, Ho, Er, and Lu in the barytes are low and therefore below the limit of detection of the analytical instrument (Inductively Coupled Plasma Mass Spectrometer) employed in the analysis of the sample. The detection limit of

Inductively Coulped Plasma Mass Spectrometer for the rare earth elements; Dy, Ho, Er and Lu are 0.05, 0.02, 0.03 and 0.01 ppm respectively.

Table 4.10: Rare earth elements concentration in mineralized host rocks, baryte veins and lead-zinc sulphide veins from the area of study (all values are in ppm except the element ratios)

Sample	Mineralized Gneiss		Mineralized Sandstone		Baryte Veins			Lead-Zinc Sulphide Veins	
Rare Earth Elements	**NO2**	**NO4**	**NN1**	**NQ1**	**NM**	**NO5**	**NQ2**	**NN2**	**NO3**
La	24	5.7	46.1	38.6	3.4	3.5	9.3	4.3	8.6
Ce	44.6	6.8	93.3	163.5	0.1	0.1	18.7	22.47	11.3
Pr	5.5	0.9	10.9	7.8	0.04	0.02	1.17	1.3	1.4
Nd	18.5	3.9	40.6	29.1	0.7	0.3	3.7	4.7	4.7
Sm	4.6	0.6	7.5	5.7	0.2	0.12	0.8	0.8	0.8
Eu	1	0.02	1.5	0.02	0.02	0.02	0.02	0.1	0.02
Gd	6	1	6.7	6.5	2.4	3.1	4.6	0.7	3.6
Tb	1.2	0.1	0.9	0.6	0.04	0.05	0.2	0.1	0.1
Dy	6.5	0.6	5.7	3.6	0.05	0.05	0.1	0.6	0.3
Ho	1.4	0.1	0.9	0.6	0.02	0.02	0.1	0.1	0.1
Er	3.3	0.3	2.9	1.9	0.03	0.03	0.3	0.3	0.2
Tm	0.4	0.1	0.5	0.3	0.03	0.02	0.1	0.1	0.1
Yb	2.3	0.3	2.9	1.8	0.21	0.2	0.4	0.3	0.4
Lu	0.3	0.04	0.4	0.2	0.01	0.01	0.1	0.1	0.02
ΣREE	119.6	20.3	220.9	260.4	7.2	7.3	39.4	35.7	31.2
LREE	97.2	7.9	198.5	244.8	4.5	3.9	33.7	33.6	26.8
HREE	22.4	2.4	22.4	15.6	2.7	3.3	6.7	2.1	4.4
Ratios									
ΣLREE/ΣHREE	4.3	7.4	8.9	15.7	1.7	1.2	5	15.9	6.1
Eu/Eu*	0.6	0.1	0.6	0.01	0.04	0.05	0.02	0.4	0.03
Ce/Ce*	-	-	-	-	0.06	0.06	1.3	-	-
Gd/Gd*	-	-	-	-	18.6	21.4	17.1	-	-
Ce_N/Sm_N	-	-	-	-	0.1	0.2	5.6	-	-
Ce_N/Yb_N	-	-	-	-	0.1	0.2	10.8	-	-

The REE profiles of barytes from the study area were compared with profiles of hydrothermal fluids, precipitates and baryte occurrences in other areas as proposed by Bozkaya and Gokce (2004) in order to estimate probable environment of formation (Table 4.11; Figs. 4.20 to 4.23). The plot of Ce_N/Sm_N against Ce_N/Yb_N shows the location of

barytes in relation to possible source materials and mineralizing hydrothermal fluid (Table 4.11; Fig. 4.24).

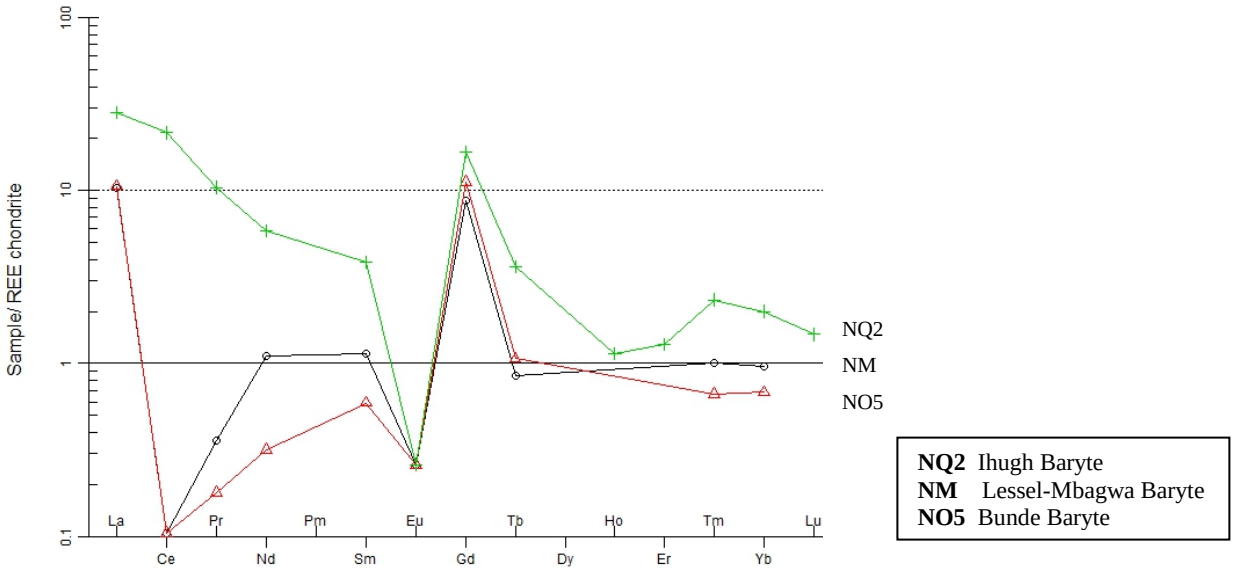


Figure 4.19: Rare earth element plot in baryte from Lessel-Mbagwa, Bunde and Ihugh (chondrite normalizing values of Nakamura, 1974).

Compared with the surrounding rocks, the average REE profile of baryte shows dissimilar patterns (Fig. 4.20). There is however, a moderately strong similarity between baryte from Ihugh (NQ2) and the lead-zinc sulphide veins from Lessel-Mbagwa and Bunde (Fig. 4.21). However, when compared individually, a slightly strong similarity in REE profiles and low REE abundance exist between the seawater dominated hydrothermal fluid and the baryte from Lessel-Mbagwa and Bunde (Figs. 4.22 and 4.23). The average baryte REE profile is fairly similar to that of the pelagic baryte (MB2) compared to the hydrothermal and diagenetic barytes (Fig. 4.24). The plot of Ce_N/Sm_N versus Ce_N/Yb_N shows that baryte from Lessel-Mbagwa and Bunde are in close proximity with seawater and MB2 (Fig. 4.25). Baryte from Ihugh however lies far from this field with the closest hydrothermal fluid being that of BA2 (Bulgarian hydrothermal fluid 2) (Fig. 4.25).

Table 4.11: REEs comparison of barytes from Lessel-Ihugh area against barytes and hydrothermal systems in some parts of the world (modified from Bozkaya and Gokce, 2004)

Element	Sea-water[a]	MB2[a]	MB9[a]	CB3[a]	TA[b]	BA1[b]	BA2[b]	EPR 21[b]	Salton Sea[c]	TS1[d]	TS2[d]	TSb	TSpz
La	3.1	13	143	75	–	–	–	–	–	12.23	27.2	5.40	6.45
Ce	1.2	3.5	309	103	62.5	21.4	46.3	331.5	706	21.53	60.76	6.30	16.88
Pr	0.64	–	12.5	–	–	–	–	–	–	2.98	8.06	0.41	1.35
Nd	2.5	–	–	–	21.5	8.9	16.8	102.5	226	10.22	27.7	1.56	4.70
Sm	0.43	0.38	7.4	0.98	4.65	1.75	3.2	19	22.6	2.21	5.48	0.38	0.81
Eu	0.12	0.1	1.7	0.45	0.3	0.55	0.4	32.5	305	0.43	1.58	0.02	0.06
Gd	0.65	–	–	–	3.5	3.75	2.4	25	25	1.62	4.68	3.37	2.03
Tb	0.14	–	–	–	–	–	–	–	–	0.36	0.9	0.09	0.11
Dy	0.82	0.54	14	1	3.2	5.95	2	19.2	17.3	1.09	3.42	0.05	0.43
Ho	0.22	0.18	5.7	–	–	–	–	–	–	0.23	0.8	0.04	0.01
Er	0.68	–	18	–	2.2	4.1	1.2	11.7	10.6	0.39	1.42	0.12	0.24
Tm	0.15	–	–	–	–	–	–	–	–	0.07	0.45	0.04	0.05
Yb	0.63	–	26	–	2.2	4.2	1.25	13.3	9.33	0.37	1.20	0.27	0.33
Lu	0.17	–	–	–	–	–	–	–	–	0.07	0.30	0.02	0.02
Y	–	–	–	–	–	–	–	–	–	–	–	2.77	3.45
Ce_N/Sm_N	0.67	2.22	10.08	25.36	3.24	2.95	3.49	4.09	7.33	2.68	15.05	1.98	4.91
Ce_N/Yb_N	0.49	0	3.07	0	7.35	1.32	9.58	6.34	19.25	13.1	2.35	3.70	13.53

References

(a) Guichard *et al.* (1979)

(b) Michard and Albarede (1986)

(c) Michard (1989)

(d) **TS1 & TS2** - This Study: Average REE concentration of granitic rocks and sandstones respectively

Baryte Samples

MB2: pelagic baryte (Central Pacific)

MB9: deeply buried (diagenetic) baryte (Northeast Pacific)

CB3: hydrothermal vein baryte (Sterling, Colorado, USA)

TSb -This Study: Average baryte (see Table 5.10 for Ce_N/Sm_N and Ce_N/Yb_N values in individual baryte)

TSpz - This Study: Average Pb-Zn sulphide veins

Hydrothermal Fluid Samples

TA - Average of the Tibet AH-9 & AH-35 values.

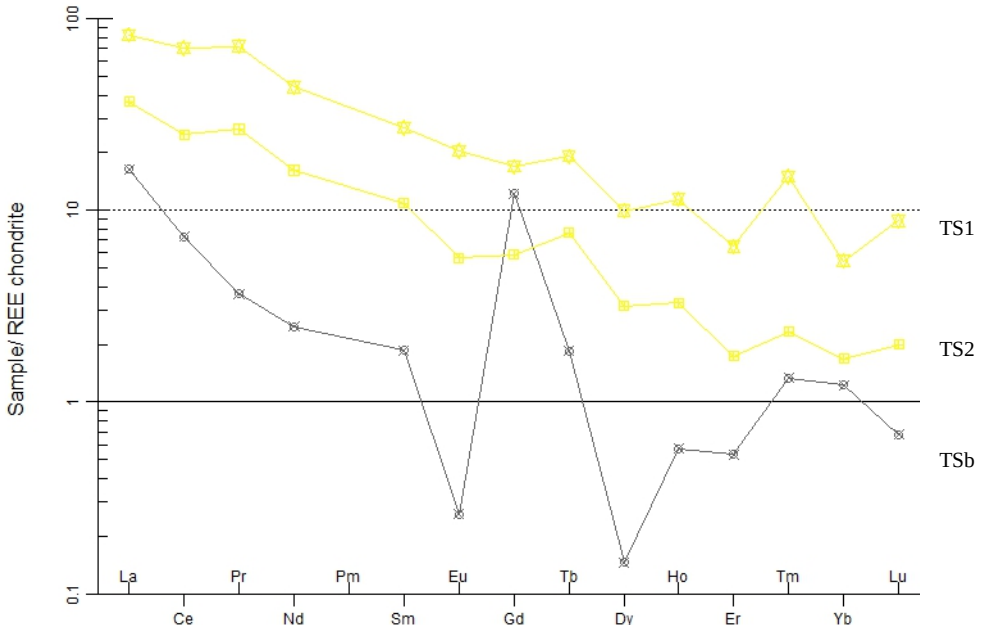
BA1 - Average of the Bulgaria–1 BU–14 & BU-13 values (pH<7.5)

BA2 - Average of Bulgaria–2 BU-26. BU-04 BU-21 values (pH>7.5)

EPR21 - Average of the East Pacific Rise; 21ºN–SW 1149–2.1157–2

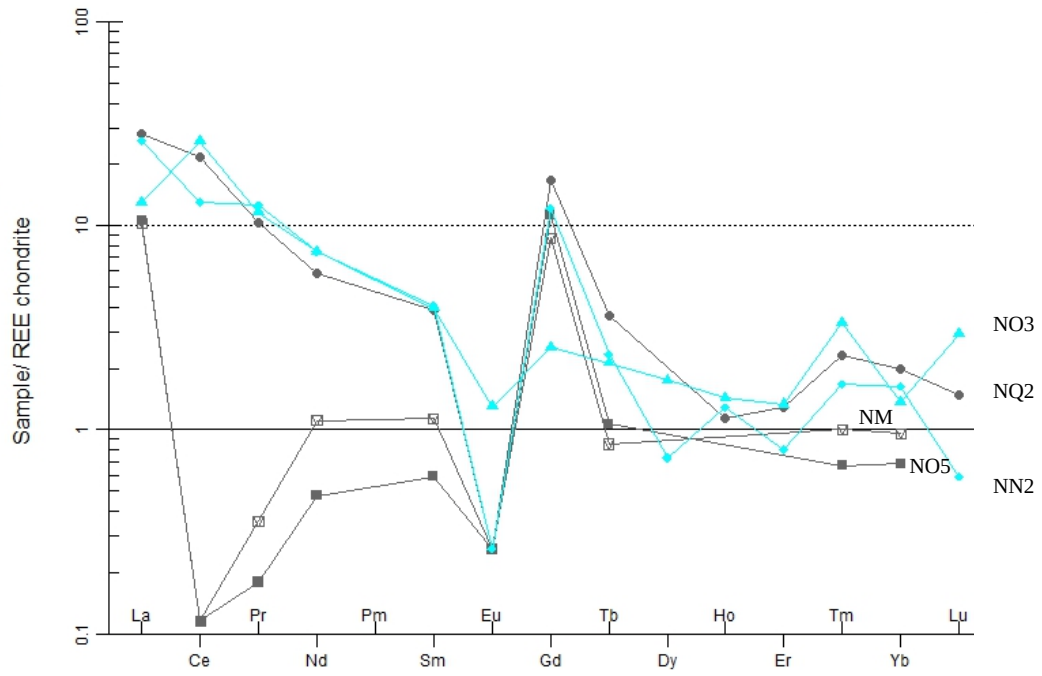
Salton Sea Hydrothermal fluid

Seawater - Seawater dominated hydrothermal fluid



TS1 Average REE of Granitic rocks (this study)
TS2 Average REE of Sandstone (this study)
TSb Average Baryte (this study)

Figure 4.20: Comparison of the rare earth elements profiles of average baryte in this study with the surrounding rocks from Lessel-Ihugh area.



NQ2 Ihugh Baryte
NN2 Pb-Zn vein in Sandstone
NM Lessel-Mbagwa Baryte
NO3 Pb-Zn sulphide vein in Gneiss
NO5 Bunde Baryte

Figure 4.21: Comparison of the rare earth elements profiles of average baryte with lead-zinc sulphide veins from Lessel-Ihugh area

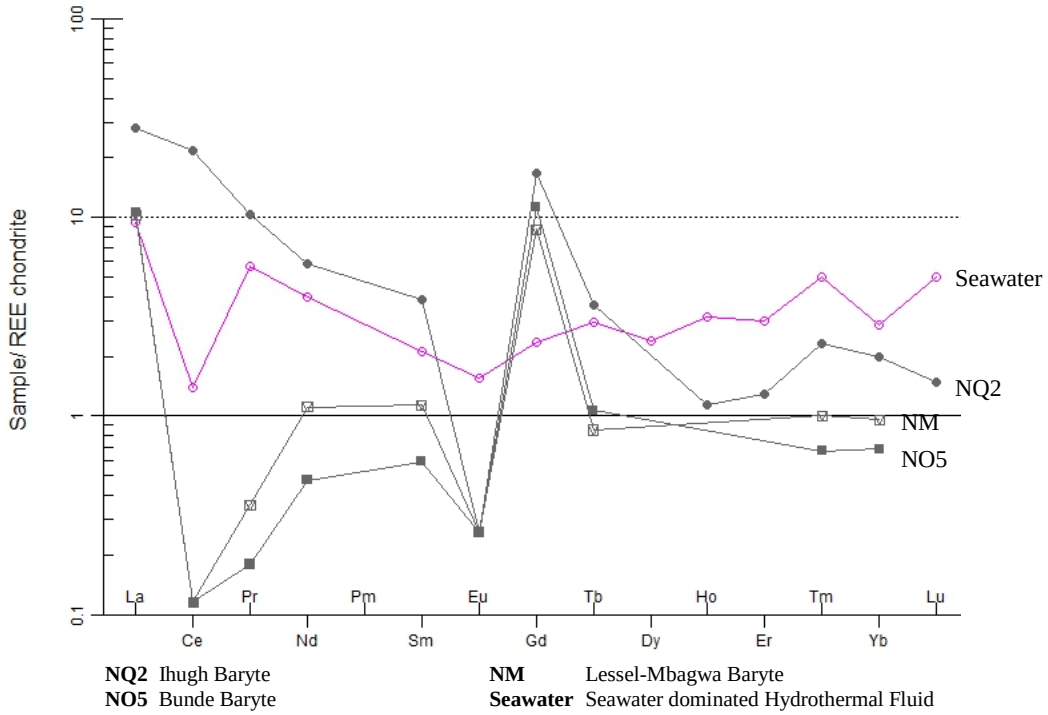


Figure 4.22: Comparison of the rare earth elements profiles of barytes from the study area with seawater dominated hydrothermal fluid.

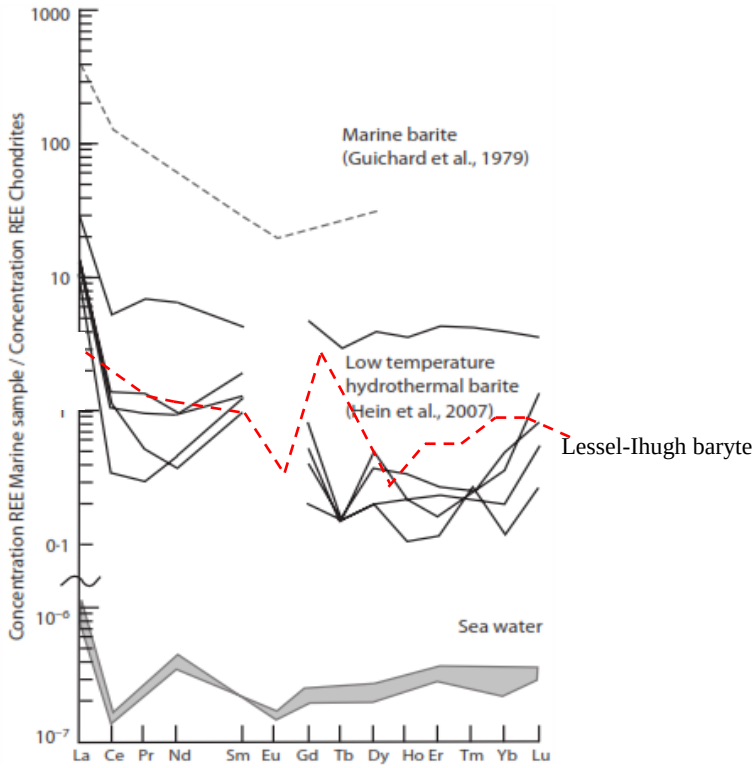
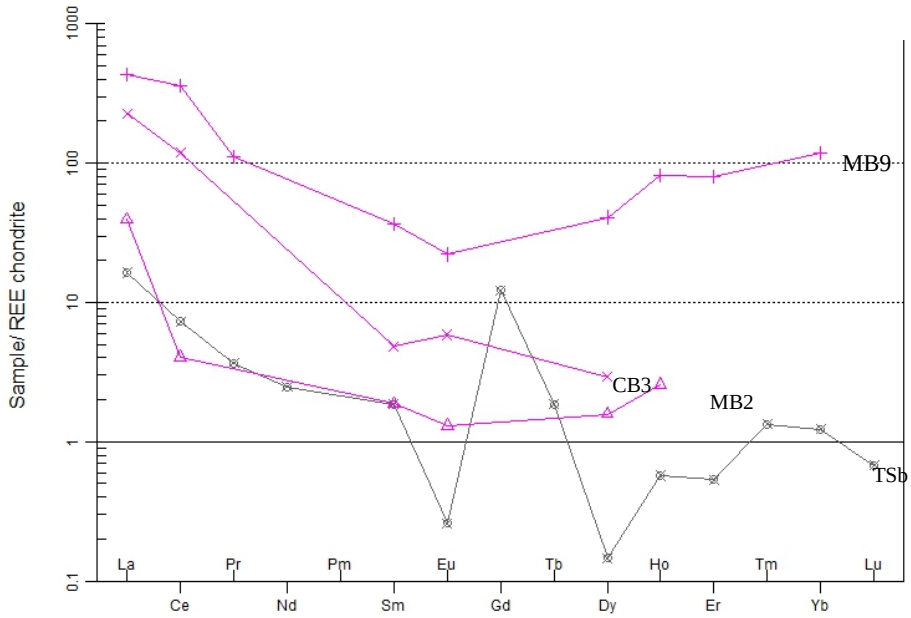


Figure 4.23: The distribution of rare earth elements in marine baryte, low temperature hydrothermal baryte compared with baryte from Lessel-Ihugh area (modified from Griffith and Paytan, 2012)



CB3 Hydrothermal Vein Baryte **MB2** Pelagic Baryte **MB9** Diagenetic Baryte **TSb** Average Baryte (this study)

Figure 4.24: Comparison of the rare earth elements profiles of average baryte in the study area with barytes from marine, diagenetic and hydrothermal environments.

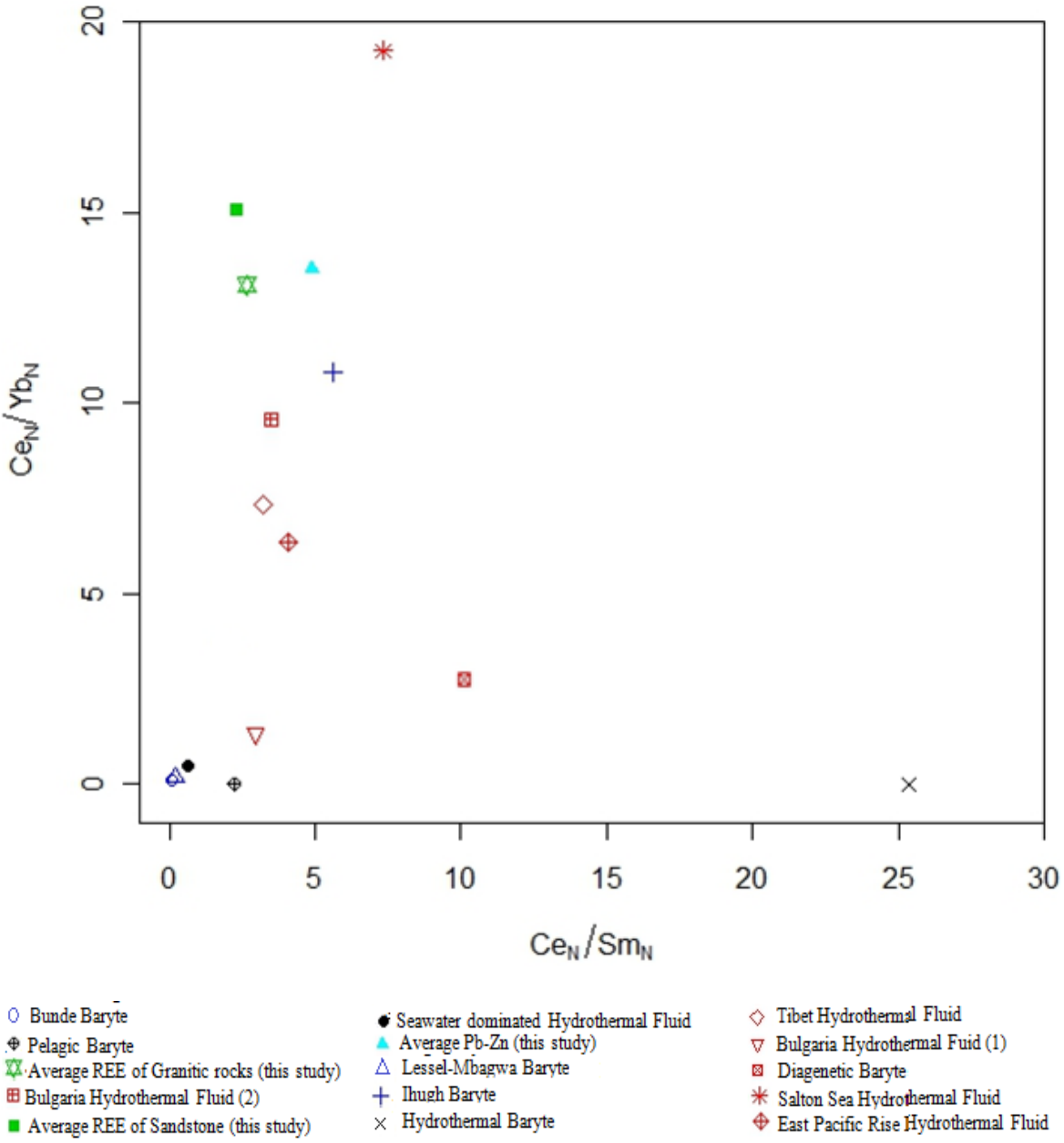


Figure 6.25: Binary plot of Ce_N/Sm_N against Ce_N/Yb_N showing distribution of baryte, Pb-Zn sulphide veins, granitic rocks and sandstones of Lessel-Ihugh area along with various hydrothermal fluids and baryte occurrences in the world.

4.14 GEOTECHNICAL CHARACTERISTICS

Three baryte samples (NM, NO5 and NQ2) were collected from each of the baryte bearing zones in the study area in order to test their mechanical properties. The result

obtained from the moisture content, uniaxial compressive strength, density tests (Table 4.12) in addition to the geochemistry (Tables 4.8, 4.9) of the barytes from Lessel-Ihugh area is compared with geotechnical and geochemical characteristics of barytes in other parts of Nigeria (Table 4.13). The moisture content, compressive strength and specific gravity of the baryte samples varies from 0.42 to 1.18%, 2.02 to 5.36 N/mm^2 and 3.65 to 4.01.

Silica content is high in barytes from Lessel-Ihugh area relative to other areas. Barium oxide (BaO) content of barytes in the study area is higher than that of barytes from Cross River State (Table 6.13). By contrast, BaO content of barytes in the study area is lesser than the BaO content reported for baryte from Lessel (Nwafor *et al.*,1997), Azara baryte (Omada, 1985; Omada and Ike, 1996) and Dareta baryte (Daspan and Imagbe, 2010). The high BaO content in barytes recorded by Nwafor *et al.* (1997) stemmed from the fact that the values of BaO and SiO_2 were documented collectively rather than individually (Table 4.13). Thus there is a weak comparison between barytes in this study with that of Nwafor *et al.* (1997) based on BaO and SiO_2 content. High SiO_2 and low Fe_2O_3 content is characteristic of barytes from Lessel-Ihugh area whereas barytes from Cross River State have low SiO_2 and high Fe_2O_3 content. Thus, baryte from Lessel Mbagwa exhibit high strength and SiO_2 in addition to low BaO, moisture content and moderate specific gravity. Baryte from Bunde area displays low strength and specific gravity, high SiO_2 with moderate BaO and moisture content. Baryte from Ihugh shows low strength, SiO_2, as well as high BaO, moisture contents and specific gravity (Table 4.12).

Table 4.12: Moisture content, uniaxial compressive strength and specific gravity of barytes from Lessel-Ihugh area

Sample Location	Moisture Content*							Uniaxial Compressive Strength (UCS)*							Specific Gravity*			
	IR (kg)	SR (kg)	TR (kg)	FOR (kg)	FIF (kg)	FR (kg)	MC* (%)	Mass (g)	Ave. Breadth (mm)	Ave. Length (mm)	Ave. Width (mm)	C/Area = LxB (mm^2)	Failure Load (kN)	UCS (N/mm^2)	Volume (cm^3)	Density (g/cm^3)	Density of water (g/cm^3)	Specific Gravity
Lessel-Mbagwa	4.84	4.84	4.82	4.82	4.82	4.82	0.42	340.3	27.37	61.38	51.22	1679.97	9.0	5.36	86.05	3.95	1	3.95
Bunde	3.93	3.93	3.91	3.91	3.90	3.90	0.77	293.8	29.97	67.43	39.88	2020.88	4.5	2.02	80.59	3.65	1	3.65
Ihugh	0.86	0.86	0.86	0.85	0.85	0.85	1.18	132.4	11.39	84.87	34.13	966.67	2.0	2.07	32.99	4.01	1	4.01

*mathematical formulae are stated in Chapter Three IR – Initial Reading SR – Second Reading TR – Third Reading FOR – Fourth Reading
FIF – Fifth Reading FR – Final Reading LxB – Length x Breadth C/Area – Cross-sectional area $1N/mm^2$ – 1Mpa

Table 4.13: Major oxides and some selected trace elements in barytes from Lessel-Ihugh area compared with those in other parts of Nigeria.

Sample Location	BaO (wt.%)	SiO_2 (wt.%)	SrO (wt.%)	Fe_2O_3 (wt.%)	CaO (wt.%)	Pb (ppm)	Zn (ppm)	Cu (ppm)	Cd (ppm)	Hg (ppm)	Specific gravity	UCS (N/mm^2)	Moisture Content (%)
L/Mbagwa[a]	79.20	20.50	0.50	0.10	0.04	414	93	25.10	0.30	0.03	4.01	5.36	0.42
Bunde[a]	80.90	18.90	0.30	0.04	0.03	1294	3764	66.40	9.80	0.03	3.65	2.02	0.77
Ihugh[a]	83.70	13.30	0.60	1.20	0.10	25.60	54	7.00	0.10	0.01	3.95	2.07	1.18
Okurike[b]*	71.28	0.05	0.06	21.40	0.25	6.70	-	14.40	0.90	1.50	4.40	29.40	1.50
Gabu[c]*	64.60	1.58	0.14	18.31	0.28	-	-	-	0.20	0.03	3.53	31.00	0.45
Alifokpa[c]*	55.53	1.39	0.64	22.32	0.03	-	-	-	0.24	0.01	3.65	24.75	0.40
Osina[c]*	58.77	1.47	0.63	25.65	0.29	-	-	-	0.02	0.29	3.70	25.00	0.31
Lessel[d]	91.85		-	0.51	1.96	-	-	-	-	-	4.35	-	1.15
Azara[e]	89.00	3.08	0.88	1.51	1.07	26.67	-	46.67	-	-	4.17	-	-
Dareta[f]	87.92	1.26	0.56	2.35	0.86	-	-	-	-	-	4.20	-	-

a. Values from this study
b. Average values from Akpan *et al.* (2014)*
c. Average values from Ene *et al.* (2012)*
d. Values from Nwafor *et al.* (1997)
e. Average values from Omada (1985); Omada and Ike (1996)
f. Average values from Daspan and Imagbe (2010)
*collectively referred to as barytes from *Cross River State*

Strontium oxide (SrO), CaO, Pb, Zn, Cu, Cd and Hg content in barytes from the study area show no significant difference with barytes from Azara, Dareta, Lessel (Nwafor *et al.,* 1997) and barytes from Cross River except for the high Pb, Zn and Cd content recorded in barytes from Bunde.The specific gravity of barytes in the Lessel-Ihugh area is lower than that from Okurike (Akpan *et al.,* 2014), Lessel (Nwafor *et al.,* 1997), Azara and Dareta. Uniaxial compressive strength values of barytes in the Lessel-Ihugh area is lower than that from Cross River State (Table 4.13).

On the basis of colour, crystal size, silica and iron oxide mineral contents, Omada (1985, 1987) and Omada and Ike (1996) have distinguished three distinct varieties of barytes namely pink, white and smoky varieties. Baryte crystals from Lessel-Ihugh area are of variable size (1 – 6 mm), generally vitreous in luster and subhedral to euhedral in shape. For the purpose of comparison, other physical characteristics of barytes from Azara and Lessel-Ihugh area are presented in Table 4.14.

Table 4.14: Mineralogical and physical characteristics of barytes from Lessel-Ihugh area compared with those from Azara area.

Location	Variety	Properties	Mineral Associations	Quality
Azara	Pink Baryte	Subhedral crystals 2 to 6 mm in size, Sub-vitreous luster	Baryte, quartz (10-15% by volume), iron oxide minerals	Grade II – requires beneficiation before it can be used in any industry.
	White Baryte	Euhedral crystals 2 to 4 cm in size, vitreous luster	Baryte (No quartz or iron oxide minerals)	Grade I – suitable for use in oil and gas industry as drilling mud, paint and chemical industry.
	Smoky Baryte	Euhedral crystals 3 to 5 cm in size, crystals are freely grown, voids are common, vitreous luster.	Baryte (No quartz or iron oxide minerals)	Grade I – suitable for use in oil and gas industry as drilling mud.
Lessel-Ihugh	Pink Baryte	Clear white to pinkish white colour, subhedral to suhedral crystals 1 to 6 mm in size, crystals are freely grown, vitreous luster.	Baryte, quartz, opaque minerals (iron oxide, galena)	Grade II - requires beneficiation

CHAPTER FIVE

DISCUSSION, CONCLUSION AND RECOMMENDATIONS

5.1 DISCUSSION

5.1.1 Granitic Rocks in Lessel-Ihugh Area

The medium-grained muscovite granite at Akaajime and Mbatoo as well as banded gneiss are potassium-rich K_2O/Na_2O (> 1) relative to the sodium-rich (K_2O/Na_2O < 1) medium-grained muscovite granite from Mbason and the coarse-grained biotite muscovite granite from Mbaakase.

The Total Alkali Silica (TAS) diagram (Fig. 4.4) shows that these rocks are granitic rocks and their chemical compositions are consistent with acidic igneous rock suite. The TAS diagram also reveals that the banded gneiss is derived from igneous protholith. The Harker diagram (Fig. 4.6) shows that SiO_2 is positively correlated with Na_2O and displayed strong negative correlation with Al_2O_3, K_2O, CaO, P_2O_5, Fe_2O_3, MgO, showed both positive and negative correlation with SiO_2 whereas TiO_2 did not show any clearly defined correlation. The relationship between these oxides and silica suggests that the granitic rocks resulted from fractional crystallization. The negative and positive trend in Fe_2O_3, MgO could reflect early and late crystallization of iron and magnesium oxides.

On the Y+Nb versus Rb discrimination diagram (Fig. 4.9) the granitic rocks plot in the syn-collisional and volcanic arc granite fields of Pearce *et al.* (1984). This is in agreement with the arc or syncollisional origin of the Older Granites of Nigeria as proposed by Fitches *et al*. (1985), Odewumi and Olarewaju (2013)**.** Similar granitic rocks with volcanic arc and syncollisional affinity emplaced during the Pan-African orogeny has also been reported in various parts of northern Nigeria by Olarewaju and Rahaman (1982),

northcentral Nigeria by Ezepue and Odigi (1993); Okonkwo and Winchester (2004), southeastern Nigeria by Ukwang and Ekwueme (2009); Obiora (2012) and southwestern Nigeria by Okonkwo and Folorunsho (2013). These granitic rocks termed the "Older Granites" in Nigeria have been dated at 750-500 Ma during the Pan-African orogenic event (Rahaman *et al*., 1983; Fitches *et al*., 1985; Ekwueme and Kroner, 1998).

It has been established that the large lithophile elements Rb, Ba, substitutes for K in potassium feldspar and micas while Sr replaces Ca and K in plagioclase and potassium feldspar respectively (Rollinson, 1993). These incompatible trace elements are normally enriched in residual melt fractions. In line with the proposition of Taylor (1965) low Ba, Sr content in the granitic rocks obviously points to late stage magmatic differentiation while the high Rb concentration suggests late stage crystallization of plagioclase feldspar. As advanced by Rollinson (1993), negative Nb anomalies observed in the multi-element plot (Fig. 6.6) is characteristic of the continental crust and may indicate crustal involvement during magma generation processes. The depletion in Ti content recorded in the granitic rocks suggests ilmenite fractionation. Yttrium (Y) is usually accommodated by calcic-amphibole, apatite and titanite (Wyborn, 1983; Ewart and Griffin, 1994). Thus, low Y content is probably due to the low concentration of these minerals. Nickel (Ni), Co are normally concentrated in olivine minerals and Cr in spinel, clinopyroxene. High concentrations of Ni, Co, Cr indicate a mantle source and limited fractionation. Low Ni, Co, Cr values in the granitic rocks suggests that the calc-alkaline rocks are well fractionated.

The Ba/Sr and Ba/Rb values ranges from 3.1 - 11 and 0.1 – 19.2 respectively. The trace elements Ba, Sr, Rb are usually concentrated in the later stages of magmatic

differentiation. Increasing Ba/Rb and Ba/Sr values are thus indicative of late stage magmatic differentiation. Obiora and Ukeagbu (2010) have reported that more evolved or fractionated, biotite-rich granitic intrusions have higher values of Ba/Sr ratios and lower Ba/Rb than the less fractionated more mafic intrusions. This trend as reported by Obiora and Ukeagbu (2010) is also consistent with the observation of Rahaman *et al.* (1988), Obiora, (2012) on granitic rocks of the southeastern basement complex of Nigeria.

The ΣREE of granitic rocks in the Lessel-Ihugh area (5.6 to 183.7 ppm) is comparable to similar granites documented by Ukaegbu and Ekwueme (2005) [7 – 180 ppm] and Obiora (2012) [7 – 206 ppm] in southeastern Nigeria. The ratio of light to heavy rare earth elements (ΣLREE/ΣHREE) 2.3 to 20 indicates that these rocks are generally LREE enriched relative to HREE. The values of La_N/Yb_N, Ce_N/Yb_N, La_N/Sm_N are normally higher in residual magma than the parent magma thus suggesting that the granitic rocks formed from a more fractionated magma (Ukaegbu and Ekwueme, 2005). Positive Eu anomaly is exhibited by pegmatite (1.3) and coarse-grained biotite muscovite granite (1.1) while the medium-grained muscovite granites and banded gneiss show negative Eu anomaly ranging from 0.1 to 0.9. Europium anomalies are chiefly controlled by feldspars; Eu^{2+} (negative anomaly) is compatible in plagioclase and K-feldspars in contrast to Eu^{3+} which are incompatible. According to Rollinson (1993) positive Eu anomaly is probably due to magma assimilation/contamination. Plagioclase fractionation, is therefore, responsible for the negative Eu anomaly exhibited by the medium-grained granite and banded gneiss. The role of plagioclase in fractional crystallization is also indicated by the positive correlation existing between La/Ce, La/Pr, Ce/Pr and Ce/Nd (Appendix V). According to O'nions and Pankhurst (1974), well developed fractionation pattern and

pronounced negative Eu anomaly are characteristic of the calc-alkaline rocks. The positive Eu anomaly displayed by the coarse-grained biotite muscovite granite and its position in the VAG field reflects plagioclase accumulation most likely inheirited from a meta-igneous protholith that was subducted into the mantle during magma genertion (Miller *et al.*, 2011). This also explains the moderately high Fe_2O_3, MgO, MnO relative to similar oxides in the other granitic rocks.

Rare earth elements distribution pattern and the level of enrichment in the granitic rocks show that they have undergone some degree of fractionation. This agrees with the findings of Onyeagocha (1986); Olarewaju (1987); Ukaegbu and Ekwueme (2005, 2006); Obiora and Ukaegbu (2010); Obiora (2012) on calc-alkaline rocks in the Nigerian Precambrian Basement Complex.

5.1.2 Sedimentary Rocks in Lessel-Ihugh Area

Silica (SiO_2) content in the sandstones from Lessel-Ihugh area is higher (73.7 – 97.2 wt. %) than the SiO_2 value (66%) recorded by Taylor and McLennan (1985) for sandstones. Silica enrichment is a measure of sandstone maturity and since the abundance of SiO_2 is controlled by quartz minerals, the sandstones from Lessel-Ihugh area are quartz-rich and can be said to be mineralogically mature. Dabard (1990) interpreted positive correlation between Al_2O_3 and K_2O, Na_2O, MgO, CaO, Fe_2O_3, TiO_2 in sandstones of the Armorican Massif (France) to suggest that these oxides are associated with clay minerals such as illite. Similar positive relationship in sandstones of the Lessel-Ihugh area is probably attributed to the presence of illite. High K_2O/Na_2O reflects the high proportion of K-bearing minerals such as K-feldspar, muscovite and illite to Na-feldspar which are more easily broken down. The high proportion of stable silica-rich minerals like quartz

compared to the proportion of unstable minerals such as Na-feldspar also suggests that these rocks are mineralogically mature (Sabaou *et al.,* 2009). Sandstones in the Lessel-Ihugh area are classified as wacke, litharenite, sub-litharenite and quartz-arenite. Based on their average composition however, these sandstones can be generally classified as sub-litharenite.

The Al_2O_3/TiO_2 ratio of sandstones and shale from the Lessel-Ihugh area range from 4.1 – 69.3. This suggests that the sandstones are derived largely from intermediate and partly from felsic igneous rocks. Also, the tectonic discrimination diagram of Roser and Korsch (1988) suggests that the sediments were derived from mature quartzose detritus source. According to Liard (1972) mature quartzose detritus are mainly derived from deeply weathered granitic-gneissic terrane. Sandstones derived from this terrane are quartz-rich, poor in feldspars and rock fragments (Fig. 4.13).

The calculated CIA values recorded in sandstones and shale vary from 73.2 – 88 with an average of 79. The CIA diagram further indicate that weathering was severe and primary source rock minerals (plagioclase, K-feldspars, biotite) have been removed by weathering. Thus, the high CIA values in sandstones, shale from the Lessel-Ihugh area suggest that these rocks have undergone significant chemical weathering and alteration. Th/U values in the sandstones and shale are generally greater than the standard value of 4.0 thus supporting intense weathering in the source area. According to Roddaz *et al.* (2006) Th/U values > 4.0 is characteristic of clastic sedimentary rocks. The high proportion of quartz at the expense of primary clay minerals elevates the SiO_2/Al_2O_3 and` consequently results in a decrease in the abundance of most trace elements (McLennan *et al.*, 1993). The positive correlation between Al_2O_3, Ba, ΣREE, Th, Rb, U with K_2O further suggests that

the concentration of these elements is controlled by clay minerals and micas (McLennan *et al.,* 1983; Rahaman and Suzuki, 2007 and Tawfik *et al.,* 2011). Strontium (Sr) content is affected by the presence of CaO, therefore Sr depletion in the sandstones implies removal of feldspars particularly plagioclase during weathering.

The degree of weathering undergone by sandstones and shale especially the feldspar content accounts for the depletion of some of the trace elements Zr, Nb, Y, Th, U which are enriched in felsic minerals (Feng and Kerrich, 1990). Cobalt (Co), Ni, V, Cr are generally low in the sandstones except for the slightly high values recorded in sub-litharenite and quartz-arenite (Table 4.5). Ferro-magnesian minerals control the concentration of Fe, Co, Sc, Ni, V, W and Cr (Rollinson, 1993) and these elements generally show similar behavior in magmatic processes but they may be fractionated during weathering (Feng and Kerrich, 1990). Mafic and felsic source rocks differ significantly in Eu/Eu*, La/Sc, Th/Sc, La/Co, Th/Co and Cr/Th ratio and hence provide useful information about the provenance of sedimentary rocks (Cullers *et al.,* 1988; Cullers, 1994, 2000; Cullers and Podkovyrov, 2000). La/Co ranges from 1.8 - 13.8 in felsic rocks and 0.14 - 0.30 in mafic rocks while Th/Co ratio varies from 0.04 - 3.25 in felsic rocks and 0.04 - 1.40 in mafic rocks (Cullers, 1994, 2000). The La/Co and Th/Co ratio in these sandstones lies within the range indicated for mafic rocks. Thus, the high Co concentration could be linked to a basic source rock.

REE content in clastic sedimentary rocks is determined by their concentrations in the rocks from which they are sourced (Taylor and McLennan, 1985; Hoatson *et al.,* 2011). According to Cullers (1994) high ΣLREE/ΣHREE ratio and negative Eu anomalies are generally characteristic of sandstones derived from felsic rocks, whereas sandstones

derived from mafic rocks exhibit low ΣLREE/ΣHREE ratio and weak negative Eu anomaly. The average REE pattern of the sandstones and shale compared with REE patterns of the granitic rocks matches that of medium-grained muscovite granite and banded gneiss (Fig. 4.15). The trace and REEs distribution therefore suggests that the sandstones, shale from the Lessel and Ihugh areas were probably derived from granite/gneiss in the study area and there could have also been a contribution from basic rocks in the surrounding area.

5.1.3 Field Occurrence and Mineralogical Features of Barytes from Lessel-Ihugh Area

The genetic model for the formation of PbS-ZnS-$BaSO_4$ in the Benue Trough was proposed by Olade and Morton (1985), Akande and Abimbola (1987), Akande *et al.* (1989), Ekwere and Ukpong (1994) and Ene *et al.* (2012). Oden (2012) also reported that the discordant vein type baryte mineralization is the most common type of baryte in the Benue Trough.

Field studies reveal that baryte veins are structurally controlled by major NE-SW and minor NW-SE trending fractures. Previous studies have shown that the distribution and structural characteristics of PbS-ZnS-Baryte-Flourite mineralization were affected by tectonic activities related to the opening of the Benue Trough (Maurin and Benkhelil, 1990; Ofoegbu and Odigi, 1990). The Benue Trough has suffered deformation along NE-SW trending axes producing multiple folds and fractures which are cut by steeply dipping N-S compressional faults and fracture systems (Nwachukwu, 1972). According to Ofoegbu and Odigi (1990), these structures have been observed to cut through both the sedimentary cover and basement rocks. Baryte veins in the Lessel-Ihugh area run through the basement

gneiss and the Turonian Lessel Sandstone via these NE-SW and NW-SE fractures. The porous/loose nature of sandstones as observed at Mbakase (southeast of Ihugh) also provides suitable environment for precipitation of baryte as lenses. The structurally controlled mineralization therefore confers an epigenetic vein and cavity type deposit on the barytes from Lessel-Ihugh area.

The injection of hydrothermal fluids into the fracture system initiated restricted wall-rock alteration process between the vein and adjacent wall-rock. The vein and host rock contact north of the study area shows peripheral wall-rock alteration. Paradis *et al.* (1998) stated that the minimal nature of wall-rock modification obviously points to low thermal conditions that prevailed during ore mobilization and precipitation from hydrothermal fluids. The vuggy nature of baryte veins also supports near surface precipitation.

Baryte crystals in baryte veins from Lessel-Ihugh area are subhedral to euhedral in form ranging from 1 to 6 mm in size and exhibit vitreous luster. The textural and mineralogical character of barytes from Lessel-Ihugh area is similar to the pinkish baryte variety proposed by Omada (1987) (Table 4.14). The sequence of mineralization process based on field data and petrographic studies indicate that the mineralization process commenced with the deposition of opaque minerals (galena, sphalerite, iron-oxides), quartz, followed by early baryte, late baryte and then again by the opaque minerals. Quartz and early formed baryte minerals were affected by external stress creating multiple micro-fractures. Based on sequence of deposition and the admixed nature of PbS-ZnS with baryte, the mineralization most likely occurred in pulses rather than at one stretch. The compact nature and well formed shape of the late baryte indicate that it was unaffected by

any form of stress thus adding to its dense attribute. The packed nature of the late baryte however set off pressure on the early formed quartz therefore contributing to its strained bladed shape. The crystal size and growth of baryte minerals therefore, depended upon (a) low temperature as observed in proximal wall-rock alteration, vuggy nature of baryte veins in addition to (b) fluctuating pressure conditions based on strained/bladed form of quartz minerals and micro-structures cutting through baryte crystals.

5.1.4 Geochemistry of Baryte in Lessel-Ihugh Area

An inverse relationship exists between BaO and SiO_2 implying that as BaO content in baryte increases, silica content will invariably reduce. Kurt *et al.* (1998) stated that low Fe_2O_3 concentration (0.1 - 0.5%) is an indication that baryte mineralization occurred at low temperatures; thus the low Fe_2O_3 content (0.04 - 1.9%) in baryte of Lessel-Ihugh area indicates that it was formed in low temperature regime. Wall-rock alteration (epidotization) is characterized by enrichment in Ca, Sr and sometimes Eu, Sc, Ti, Cr (Lesher *et al.*, 1986). High CaO content recorded in mineralized gneiss and lead-zinc sulphide vein probably suggests enrichment of Ca during epidotization.

High values of TiO_2 (0.1 – 1.6%), Cu (109 – 161 ppm) in baryte from Turkey has been attributed to mineralizing fluids of hydrothermal origin from volcanic and intrusive rocks (Kurt *et al.*, 1998). Marchig *et al.* (1985) and Kurt *et al.* (1998) also suggested that high Zn (2 – 793 ppm) content in baryte is related to volcanic activity. Ortigoza-Cruz *et al.* (1994) and Kurt *et al.* (1998) further attributed high Sr (9605 – 13,603 ppm) content in baryte to a source connected with volcanic activity. Jurkovic *et al.* (2011) also asserted that high content of Sr (9379 – 13767 ppm) content in the baryte could be derived from

hydrothermal fluids. Werner (1958), Starke (1964) and Kurt *et al.* (1998) reported that high Ba/Sr (60 to 100) is related to epithermal hydrothermal origin.

The chemical composition in baryte from the Lessel-Ihugh area (Tables 4.8 to 4.10) reveal that TiO_2 (0.01 - 0.1%) and Cu (7 - 66.4 ppm) contents are low, while Zn (54 - 3764%), Sr (3018.4 - 6382.8%) and Ba/Sr ratio (131.1 – 268.3) are high. Ba/Sr ratio is low in barren sandstones and gneiss (2.3 – 71), moderately high in mineralized sandstones and gneiss (13.8 – 96.9) but very high in the baryte veins (131.1 – 268.3). This suggests significant substitution of Ba over Sr in K-rich minerals. The trace elements Ba, Sr, Pb, Zn are more enriched in mineralized rocks and baryte veins compared to their normal background concentration in barren rocks.

In line with the observation of Kurt *et al.* (1998), low TiO_2 and Cu content in baryte from Lessel-Ihugh area rules out a volcanic origin. However, Ti enrichment is observed in mineralized gneiss from Bunde (Fig. 4.18b). Titanium (Ti) is compatible during the early stages of fractionation. Its enrichment in mineralized gneiss suggests it was remobilized from Ti-rich rock or introduced during epidotization. According to Najime (2014) the magmatic rocks of the Gboko area show Ti enrichment. Thus, it is likely that Ti derived from the volcanics of the Gboko area. The abundance of Zn and Sr however indicates that the origin of baryte could still be linked with an igneous environment. Carmicheal (1965) reported high Ba content in the range of 3370 to 6850 ppm from sanidine feldspars in trachytes. The high Ba content in sanidine is due to the similarity in ionic radii of Ba and K which enable more complete diadochy. Bas and Temur (1992) reported that monzonite, diorite and basalt/andesite in Ciftehan Complex, Canakci area of Central Turkey are Ba source rocks with Ba content of 2000 ppm, 2056

ppm and 2750 ppm respectively. Ortigoza-Cruz *et al.* (1994) also reported high Ba content in andesitic volcanics and Albian limestones of La Mintta district (Rio Grande Rift Basin), southwest Mexico. The magmatic rocks farther north of Lessel-Ihugh area as reported by Najime (2014) comprises of basalts, trachy-andesites and dacites that are enriched in Ba. The sandstones and granitic rocks of the Lessel-Ihugh area contain an average Ba content of 631.4 and 395.9 ppm respectively. Therefore, if Ba was leached from the surrounding rocks by hydrothermal fluids, then it could not have been leached from the Lessel-Ihugh rocks.

The multi-element plot of barytes from Lessel-Mbagwa, Bunde and Ihugh areas exhibit almost similar profiles and this probably suggests that barytes from all three (3) areas are genetically related (Fig. 4.17). Enrichment of Ba, Sr and depletion of K, Rb suggest residual fluids rich in Ba and Sr.

Barytes in the Lessel-Ihugh area are characterized by low REE content (7.2 – 39.4), slight enrichment of LREE/HREE (1.2 – 5), strong negative Eu anomaly (0.02 – 0.05), strong positive Gd anomaly (17.1 – 21.4). In addition, barytes from Lessel-Mbagwa and Bunde have negative Ce anomaly (0.06) while baryte from Ihugh have positive Ce anomaly (1.3). The barytes from Lessel-Ihugh area are similar to baryte deposits from Bijgan (Iran) (Ehya, 2012) marked by low Sr concentrations (1 – 2%), low total REE abundances (6.25 – 17.39), negative Eu anomaly, positive La and Gd anomalies in addition to enrichment of LREE relative to HREE.

Total REE content in baryte is generally low relative to the sandstones, shale and granitic rocks. Guichard (1979) reported that barytes derived from the deep-sea are distinct in that they are REE enriched relative to barytes of shallow marine and hydrothermal

origin which have lower total REE content (Fig. 4.23). Michard *et al.* (1995) proposed that the high REE concentration obtained for deep-sea baryte by Guichard (1979) were most likely representing samples which were contaminated with continental material such as anatase, rutile, zircon and sphene. According to Palinkas and Jurkovic (1994), Bozkaya and Gokce (2004), Jurkovic *et al.* (2011) low REE content in barytes points to late-stage mineralization.

The REE chondrite normalized plot shows that baryte from Lessel-Mbagwa and Bunde display similar LREE and HREE pattern indicating that they are genetically related (Fig. 4.19). Strong negative Eu anomalies are recorded in barytes from Lessel and Ihugh areas ranging from 0.02 to 0.05. The behavior of Eu in a system is sensitive to temperature conditions (Bau, 1991). Eu may be depleted in low temperature environment and enriched in high environment (Vaslsami and Cann, 1992). The Bad Grund baryte in Germany exhibits positive Eu anomalies. This is interpreted to have resulted from deep crustal vein mineralization by precipitation from a sulphate-rich evaporitic brine and hot Ba-rich fluids at a temperature >250°C (Zheng and Hoefs, 1993; Möller and Luders, 1993).

The REE pattern of baryte from Ihugh is slightly different from that of Lessel-Mbagwa and Bunde with regards to Ce anomaly. Positive Ce anomalies are general features of alkaline, carbonate-rich and aerobic lake waters (Möller and Bau, 1993). Negative Ce anomaly has been reported for low temperature fluids such as sea water (Piper, 1974; German and Elderfield, 1989, 1990), mud, carbonaceous ooz, chert in oceanic environment (Toyoda *et al.,* 1990) and in hydrothermal metalliferous precipitate (Minai *et al.,* 1992). The trace element chemistry of seawater is a balance between the flux

of REEs from the continental crust derived from erosion and the flux derived from hydrothermal alteration of the oceanic crust (Derry and Jacobsen, 1990).

Ce in seawater may be oxidized to relatively insoluble quadrivalent Ce^{4+} which can be rapidly removed from seawater by hydrothermal fluids, resulting in a negative anomaly of Ce (Shimuzu and Masuda, 1977; Elderfield and Greaves, 1982) and LREE depletion (Ding and Zhong, 1996). The negative Ce reflects the incorporation of REE directly from seawater under oxic conditions. According to Shimuzu and Masuda (1977) if volcanic activity was directly responsible for mineralization, the mineral formed would show positive Ce anomaly and such is the case with barytes vein deposits of Central Turkey (Kurt *et al.,* 1998). Thus, negative Ce anomaly is characteristic of modern seawater and is also reflected in fluids that are derived from recent seawater such as sulphate-rich evaporitic brines (Oostingh, 2011). Pelagic baryte which precipitates directly from the depleted seawater will therefore exhibit negative Ce anomaly (Piper, 1974). Thus the negative Ce anomaly in baryte from Lessel-Mbagwa and Bunde suggests that they precipitated under oxidizing conditions. The positive Ce anomaly in baryte from Ihugh is indicates that baryte mineralization took place under reducing conditions.

Fluid inclusion and isotope data from the Benue Trough have shown that the mineralizing fluids were sulphate-rich brines having evolved from evaporitic sequences with fluid temperatures ranging from 95 – 200^{o}C (Akande *et al.,* 1989). Akande *et al.* (1992) and Akande (2000) reiterated that strongly modified heated basinal brines (Na-Ca-Cl brines) in the Benue Trough are non-boiling sedimentary brine systems containing pyrobitumens at temperatures between 70^{o}C and 260^{o}C (averaging 152^{o}C). Hence, the negative Ce anomaly obtained in baryte from Lessel-Ihugh area is expected since

evaporites of the Benue Trough were derived from seawater. Negative Eu anomalies therefore imply that the baryte from Lessel-Ihugh area was precipitated under low temperature conditions. The fluid temperature range (95 – 200 ^{o}C) stated by Akande *et al.* (1989) attests to the low temperature environment of formation.

Baryte precipitates over a relatively large range of pressure (1 – 200 bars) and temperature (0 – 400 ^{o}C) in many different geological settings (Hanor, 2000). The extremely low solubility of baryte enhances the ability of natural solutions such as seawater to maintain Ba or SO_4^{2+} but not both. Baryte solubility increases with increasing pressure and temperature upto 100 ^{o}C, then it progressively decreases (this is the stage when precipitation occurs) with increasing temperature (Hanor, 2000).

Strong positive Gd anomalies are recorded in barytes from Lessel-Mbagwa, Bunde and Ihugh (Fig. 4.19). The concentration of Gd is controlled by fractionation of its host accessory minerals; monazite, xenotime (Hoatson *et al.,* 2011) and phosphate (Ding *et al.,* 2005). Gd anomaly is rare to come by. It was first reported by Bau and Dulski (1996) in river waters and was later recorded in river and seawater from Tokyo and Nagoya regions in Japan (Nozaki *et al.,* 2000; Zhu *et al.,* 2004). Ogata and Terakado (2006) also recorded Gd anomalies in seawaters and river waters from Osaka Bay in Japan. Ogata and Terakado (2006) concluded that Gd anomaly resulted from contamination of these waters by dilution of Sewage Treatment Plants (STP) effluents with dissolved phosphorus and nitrogen nutrient concentrations (P, NH_4, NO_2, NO_3). Oostingh (2011) explained that anomalous Gd concentrations in some Archean barytes using the ICP-MS technique were possibly caused by interfering PrO (Praseodymium oxide) with which the baryte solution was spiked. Phosphorus is a common element in accessory minerals and nutrient concentrations in

STP. The concentration of P_2O_5 in barytes from Lessel-Ihugh area is low and therefore, contribution of P to Gd anomaly is ruled out. According to Ehya (2012) positive Gd anomaly exhibited by baryte deposits from Bijgan (Iran) is characteristic of marine chemical sediments such as phosphate, nitrates, Fe-Mn formations, evaporites and carbonaceous chert. Bolhar *et al.* (2004) and Ledevine *et al.* (2015) stated that strong depletion in LREE and positive La, Gd (Gd/Gd* = 4.76) and Y anomalies are key characteristics of modern seawater. Modern seawater is richer in oxygen, SO_4^{2+} and poor in Ba whereas ancient seawater was characterized by little free oxygen, poor SO_4^{2+} and enriched in Ba millions of years ago (Hanor, 2000). Since very few articles have documented strong positive Gd anomaly especially with regard to the genesis of baryte, the opinion of Bolhar *et al.* (2004), Oostingh (2011) and Ledevine *et al.* (2015) is upheld in this work.

A comparison of REE profiles of sandstones, shale, granitic rocks to average baryte in Lessel-Ihugh area show that they are unrelated (Fig. 4.20). Thus, baryte could not have been sourced from the granites, banded gneiss, shale and sandstones in the study area. The similarity in REE profiles of Pb-Zn sulphide vein and baryte from Ihugh suggests that they are related and could have deposited about the same time, from similar mineralizing fluid but under different environmental conditions based on their Ce anomalies (Fig. 4.21). Thus, it can be deduced that Pb-Zn sulphide veins are not entirely absent in Ihugh area but are probably concealed by sandstone overburden.

Seawater is characterized by low REE contents (Appendix VI), negative Ce and Eu anomalies (Rollinson, 1993). Therefore the similarity in REE distribution pattern of seawater with average baryte in the study area implies that the mineralizing fluid from

which barytes from Lessel-Ihugh area were derived had an input from seawater fluid (Figs. 4.22 and 4.23). LREE pattern displayed by pelagic baryte (MB2) and average baryte in this study are somewhat similar. Pelagic baryte is also derived from seawater (Griffith and Paytan, 2012) and their close similarity to baryte in the study area suggests that barytes from Lessel-Ihugh area was derived from a hydrothermal fluid that interacted with seawater.

On the Ce_N/Sm_N versus Ce_N/Yb_N diagram barytes from Lessel-Ihugh area plot away from the granites, banded gneiss, sandstones and shale fields (Fig. 4.25). This further suggests that Ba was not derived from the granitic rocks and the sandstones/shale in the Lessel-Ihugh area but elsewhere. Baryte from Lessel-Mbagwa and Bunde plot not far from seawater hydrothermal fluid thus suggesting that they were deposited by seawater derived hydrothermal fluid. Ce_N/Sm_N and Ce_N/Yb_N values of the average Pb-Zn sulphide veins plot adjacent to that of the granitic rocks (TS1) and this could mean that the components of the Pb-Zn sulphide veins were sourced from the granitic rocks in the Lessel-Ihugh area which is in line with the observation of Maurin and Lancelot (1987) and Akande *et al.* (1989). Lead (Pb) in galena from the Benue Trough was interpreted by Maurin and Lancelot (1987), Akande *et al.* (1989) to have been derived from detrital feldspars which were eroded from the Lower Paleozoic basement gneisses and migmatites as well as pre-Albian sediments.

The major factors responsible for the formation of mineral deposits include; source of water, source of ore/mineral component, fluid circulation/movement, depositional environment (Misra, 2000). The genetic processes leading to baryte mineralization in Lessel-Ihugh area is constrained by:

i. Source of water which is probably connate water (trapped seawater) or magmatic water (derived from the magmatic intrusions).

ii. This study has shown that the banded gneiss and granites to be the source of Pb and Zn. The anomalously high Ba contents in the magmatic rocks (basalts, trachyandesites, dacites) makes them suitable source rocks for Ba.

iii. The heat necessary for fluid circulation/movement was produced by igneous intrusions in the area during magmatism. Fluid temperatures were moderately low as indicated by proximal wall-rock alteration (epidotization), low concentrations of high temperature elements/minerals such as Cu, Ti, Fe.

iv. Barium (Ba) leached from the basalts, trachy-andesites, dacites flowed into fractures or cavities and mixed with infiltrating sulphate-rich connate water resulting in the precipitation of baryte.

5.1.5 Geotechnical Attributes of Baryte in Lessel-Ihugh Area

Geotechnical testing of barytes from northcentral Nigeria (Ribi, Azara, Jobe, Sauni, Gidan-Soja, Wuse, Akiri, Dogondaji, Kumar and Aloshi areas) by Ikejiaku (2007) and southeastern Nigeria (Gabu, Alifokpa and Osina areas) by Ene *et al.* (2012) reveals that the quality of baryte is controlled by depth of occurrence and presence or absence of associated minerals. Barytes from Gabu-Alifokpa-Osina areas are characterized by low strength at greater depths and are poor in gangue minerals. Ene *et al.*, (2012) attributed the high strength recorded in barytes from Gabu-Alifokpa-Osina areas to be as a result of its shallow occurrence and also to the presence of gangue minerals (such as quartz) due to co-recrystallization of baryte with relatively harder minerals (Table 4.13). Ene *et al.* (2012)

further noted that low porosity and moisture content of barytes from Gabu-Alifokpa-Osina area have contributed to its high specific gravity.

Barytes from Lessel-Ihugh area have specific gravity of 3.65 to 4.01, moisture content of 0.42 to 1.18% and uniaxial compressive strength of 2.02 to 5.36 N/mm^2 (Table 4.12). Baryte from Lessel Mbagwa is characterized by high strength and SiO_2 content, moderate BaO content and specific gravity in addition to low moisture content. The high strength value recorded in baryte from Lessel-Mbagwa is due to its high quartz content which recrystallised with the baryte. The high quartz content consequently resulted to a decline in BaO content. Baryte from Bunde area is characterized by high SiO_2, moderate BaO and moisture content in addition to low strength and specific gravity. The strength of baryte is affected by the amount of moisture held within the structures. These structures such as fractures and vugs could have created zones of weakness in the baryte mineral thereby lowering its density and consequently reduce its specific gravity.

Baryte from Ihugh is characterized by high BaO, moisture content and specific gravity as well as low strength and SiO_2 content. Low strength is probably due to low SiO_2 content. The co-recrystallisation process between baryte and low quartz will therefore yield low strength barytes. Its high specific gravity is attributed to the BaO content. The high moisture content could be connected to shallow water logged pit from which baryte samples were collected.

5.1.6 Economic Geology

The geological material of interest is essentially baryte and to a lesser extent gneiss, granite and sandstone. The gneiss, granite, sandstone fragments are quarried and used as building/construction materials. The percentage composition of BaO and specific gravity

of baryte is critical in determining its end use (Tables 4.13, 4.14 and 5.1). The geochemical and geotechnical data generated from this research have shown that the barytes from Lessel-Ihugh fall below the specification standards for use in petroleum, chemical/pharmaceutical industries in addition to paper, paints, lithopone, glass and heavy concrete industries as outlined by Lorenz and Gwosdz (2003). However, barytes from Lessel-Mbagwa and Ihugh fall within the range required for the manufacture of filler and extender (Table 5.1).

Presently, mining of baryte in the Lessel-Ihugh area is carried out exclusively by artisanal miners. According to Chaanda *et al.* (2010) the total national demand of baryte in Nigeria is estimated at 10,000,000 ton per annum. The few processing plants in the country produce a little above 4,000 metric tons per annum creating a wide supply gap (Chukwunenye, 2006). Mining baryte requires a lot of labour both mechanized and human labour. The crate as seen in Plate XXVIIa is used as weighing scale. This crate takes about 900 – 1000 kg (approximately 1 metric ton) of baryte which costs ten thousand naira (₦10,000.00) as at the year 2013. The price may vary depending on the amount of pure baryte mixed with rock overburden (*Tama*) (Plate XXVII b, c). Baryte may therefore have to undergo beneficiation to improve the quality. Mining activities have produced gullies in some parts of the area which are gradually turning into small ponds that may consequently result to large scale degradation of the environment (Plate XXVII d).

Table 5.1: Specifications and end uses of barytes

PROPERTIES	SPECIFICATIONS			END USES			
	API[1]	OCMA[2]	IS[3]	Paper		Paint	
				Barytes	Blanc fixe	Barytes	Blanc fixe
Chemical Composition (M.-%)							
$BaSO_4$	>92	>92	>94	>94	>97	>94	>97
$SrSO_4$							
Al_2O_3	LCP*	LCP*	LCP*	0.05	0.02	0.05	0.02
Fe_2O_3				<2.6 (6)		<2 (6)	
SiO2							
CaO							
CaF_2							
Volatile components				<0.8	<0.8	<0.5[9]	<0.5[9]
Carbonate			<1.5			0.7-1.1	
Mn (ppm)							
Fe (ppm)							
As (ppm)						<500	
Pb (ppm)							
Cd, Hg (ppm)	<3 bzw.1[8]						
Water soluble alkaline earth metals (ppm)	<200						
Water soluble substances (ppm)		<0.1	<0.02	<0.2	<0.2	<0.2 (0.5)	<0.2
Physical Properties							
Moisture content (M.-%)							
pH				6-8	8-10	6-8	8-10
Density (g/cm^3)[14]	>4.2	>4.2	>4.15	4.48	4.35	4.3-4.4	4.3-4.4
Viscosity (cP)[4]		<125					
Oil absorption (g/100g)[5]				10-12			
Remission (%)							
- MgO Standard				95	98	95	98
- $BaSO_4$ Standard Merck				92	92	94-95	
- Elrephro				95			
-Green Filter				95.5			
Grain size (um)							
- Range							
	<3M.-% >80		<2 M.-%	0.1-30	0.1-50	<0.5 M.-% >40	
- Mean	<5-15 M.-%>40		>53				
				2.0-5.0	0.5-2.0	1.1	0.5-1.4
Grain size distribution (M.-%)							
<20 um				100			
<15 um				99			
<12 um						100	
<10 um				95		99	
<8 um						98	
<6 um				80		92	
<4 um						78	
<2 um				35		45	

*Low contents are not a problem 1. American Petroleum Industry 2. Oil Company Material Association 3. Indian Standard4. Suspension with density = 2.5g/cm^3 in Centipoise 5. DIN 53199 6. Sulphides <0,1 ppm; colour white, odourless 7. No heavy metals 8. For future applications in oil and gas drilling in deep oil-gas boreholes; Alaska-specification

Table 5.1 (continued)

PROPERTIES	END USES								
	Filler/Extender			Lithopone	Chemical Industry	Glass	Pharma-ceutical Products	X-ray Contrast Medium	Heavy Concrete
	Rubber	Plastics	Brake pads						
Chemical Comptn. (M.-%)									
$BaSO_4$	88-97 (>80->90)		>95(>90)	>95 (-98)	>94 (-97)	>96-98	>97.5		>90
$SrSO_4$			<2	<1.0(2)	<1-2				<2
Al_2O_3				<1.0[10]		<0.15			
Fe_2O_3	<0.02		<1		<1-2	<0.2-0.4			<1
SiO2	<2.0	<3.0		2.0-5.0	<2 (4)	1.5-2.5			
CaO				<1.0	<2				
CaF_2					<0.5				
Volatile components	<0.5	<0.5							0
Carbonate					<1.5				
Mn (ppm)	<5,000								
Fe (ppm)								<10	
As (ppm)							<4 (<1)	<10	
Pb (ppm)	-7	-7			<5,000		<10[6]	<10[12]	
Cd, Hg (ppm)									
Water soluble alkaline earth metals (ppm)									
Water soluble substances (ppm)	<0.3	<0.3						<0.37	
Physical Properties									
Moisture content (M.-%)	<0.5	<0.5			<0.5	<3			
pH	6-9	6-9				9			
Density (g/cm^3)[14]	4.1-4.48	4.1-4.3	>4.3			4.1-4.3			>4.2[13]
Viscosity (cP)[4]									
Oil absorption (g/100g)[5]	10-12	10-12							
Remission (%)									
- MgO Standard									
- $BaSO_4$ Standard Merck	86-91	86-91							
- Elrephro									
-Green Filter									
Grain size (um)									
- Range									
	<0.4M.-% >75;		<85-99 M.-%	800-4,000		100-630[11]			
- Mean	0-50		<50						
								<10	
Grain size distribution									
(M.-%)									
<20 um	98-100						90		
<15 um	98								
<12 um									
<10 um	65-82								
<8 um									
<6 um	45-60								
<4 um									
<2 um	15-20								

9. incl. humidity 10. $Al_2O_3 + Fe_2O_3$ 11. <5 M.-% - %>160um 12. Heavy metals in general
13. Bulk density of gravel fraction 4.20-4.28g/cm^3, sand fraction 4.24-4.31g/cm^3 14. Usually means bulk density

a.  b. 

c.  d. 

Plate XXVII: Baryte heap at (a) Lessel-Mbagwa (b) Bunde (c) Tarzoho-Mbakase, Ihugh areas (d) Gullies produced during mining activities (arrows indicate pits)

5.2 CONCLUSION

The area of study is covered by Cretaceous sedimentary rocks consisting largely of arenaceous Lessel Sandstone and underlain by basement gneiss and Older Granites rocks comprising of medium-grained muscovite granite and coarse-grained biotite muscovite granite. Structural features in the area comprise of fractures with predominant NE-SW and marginal NW-SE trends.

The granitic rocks have high silica content of (74.5 to 85.5%). They are largely peraluminous and are relatively potassium-rich. The granites show strong affinity to volcanic arc and syn-collisional tectonic setting associated with the Pan-African orogeny.

The granitic rocks in Lessel-Ihugh area have low to moderate REE content with negative Eu in medium-grained muscovite granite, banded gneiss but with positive Eu anomaly in coarse-grained biotite muscovite granite.

The sandstones in this area are classified as wacke, litharenite, sub-litharenite and quartz arenite based on major oxides geochemistry. The sandstones are quartz-rich and therefore are mineralogically matured sandstones. The sandstones/shale were derived from the medium-grained muscovite granite and banded gneiss in the study area with respect to their Al_2O_3/TiO_2 ratio (16 – 43) and REE patterns. In addition, the source area from which sandstones/shale is derived were highly weathered as indicated by high CIA (73 - 88) and Th/U values (3 – 7.5). The quartz-rich nature and mineralogical maturity of the sandstones from Lessel-Ihugh area are typical of clastic sedimentary rocks derived from rocks of the earth's upper crust.

Baryte vein system is structurally controlled by fractures and joint patterns in the Lessel Sandstone and gneiss. Mineralization occurs in form of veins in sandstones at Lessel-Mbagwa and banded gneiss at Bunde/Mbatoo areas while at Mbakase (Ihugh) they occur as lenses. Baryte veins vary in widths from veinlets (<1 to 3 cm) to minor veins (4 to 20 cm) and large veins (0.8 to 4 m) whereas baryte lenses vary in thickness from 0.5 – 1 cm

The BaO concentration in baryte is a measure of its percentage purity whereas the high content of SiO_2, SrO, Pb and Zn accounts for the gangue minerals. Barium (Ba), Sr concentration and Ba/Sr ratio could be used as indicator elements in exploration of baryte mineralization. Trace element studies and REE distribution pattern has shown that Ba was not derived from the Lessel sandstones and granitic rocks but from an external source

probably the basalts, trachy-andesites, dacites, nepheline, syenites, gabbros and quartz diorite further north of the study area.

Barytes in the Lessel-Ihugh area are characterized by low REE content (7.2 – 39.4), slight enrichment of LREE/HREE (1.2 – 5), negative Eu anomaly (0.02 – 0.05), positive Gd anomaly (17.1 – 21.4). In addition, barytes from Lessel-Mbagwa and Bunde have negative Ce anomaly (0.06) while baryte from Ihugh have positive Ce anomaly (1.3). REE patterns confirm that barytes from Lessel-Mbagwa, Bunde and Ihugh areas are genetically related, although precipitated under different environmental conditions (that is redox and temperature/pressure conditions) at the time. Negative Ce anomalies recorded in baryte from the study area further indicates that seawater had an input in the mineralizing fluid. The very strong positive Gd anomaly (17.1 – 21.4) recorded in this work is attributed to (a) analytical errors in the preparation and analytical technique employed during laboratory analysis of baryte samples (b) character of modern seawater. The REE profile of Pb-Zn sulphide veins is also similar to baryte from Ihugh area. The probability of discovering Pb-Zn sulphide veins which still remain buried is high at Ihugh area.

In summary, the activities that led to the mineralization of baryte in Lessel-Ihugh area are as follows:

i. The tectonic event which occurred during the Santonian to Early Campanian re-established NE-SW trending structural pathways and was accompanied by mafic to intermediate volcanic activities. The heat from these volcanic activities was the driving force for the hydrothermal fluid. During this time, Ba was leached from Ba-rich source rocks such as volcanic (basalts, trachy-andesites and dacites).

ii. Mixing of Ba-bearing hydrothermal fluid and SO_4^{2-} rich fluid took place under fluctuating reducing-oxygenating conditions in low temperature or near-surface environment that allowed for precipitation of baryte within fracture systems.

iii. Baryte mineralization probably took place during the Santonian to Campanian and is of the epithermal epigenetic vein and cavity type.

iv. Barytes from Lessel-Ihugh area are less dense at shallow depth and are off-white mostly with a pinkish tint. At greater depths however, it is dense, crystalline, appears clear white to pinkish white in colour. The colour deviation from clear white is due to contamination by iron minerals.

In conclusion, baryte from Lessel-Ihugh areas are of the pink variety and therefore, impurities which will invariably lower the quality are not unexpected. The geochemical and geotechnical attributes have shown that barytes from Lessel-Ihugh area fall below American Petroleum Institute (API), Oil Company Material Association (OCMA), Indian Standard (IS) specification standards and are therefore of grade II but can be beneficiated to improve its quality.

5.3 RECOMMENDATIONS

i. Additional studies especially on sulphur isotopes of barytes should be carried out so as to add to the value of major oxides and trace elements data already accumulated.

ii. A combination of suitable analytical technique such as Instrumental Neutron Activation Analysis and Column Chromatography or ICP-MS and Column Chromatography, should be employed in the analysis of barytes and host rocks. The sample preparation as outlined by Oostingh (2011) should be adhered to in order to eliminate or reduce analytical errors to the barest minimum.

iii. Detailed geotechnical tests for samples at deeper levels should be carried out in the various baryte fields to further ascertain the degree of variation on quality with depth.

iv. Gravity and magnetic survey of the area should undertaken to delineate concealed baryte and Pb-Zn veins since most parts of the area are covered by vegetation and sediments.

CONTRIBUTIONS TO KNOWLEDGE

The following are the major contributions of this study to knowledge:

1. Production of geological map of the area on a scale of 1:40,000
2. Determination of the geochemical characteristics of barytes from Lessel-Ihugh area
3. Establishment of the geotechnical attributes, varieties and quality of barytes from Lessel-Ihugh area

REFERENCES

Adeigbe, O.C. and Jimoh, Y.A. (2013). Geochemical finger prints: implications for provenance, tectonic and depositional settings of the Lower Benue Trough sequence, southeastern Nigeria. *Journal of Environment and Earth Science*, 3(10): 1-31.

Agagu, O.K., Fayose, E.A. and Petters, S.W. (1985). Stratigraphy and sedimentation in the Senonian Anambra Basin of eastern Nigeria. *Journal Mining and Geology* 22, 377-385.

Agumanu, A.E. (1989). The Abakaliki and Ebonyi Formations: subdivisions of the Albian Asu River Group in the southern Benue Trough, Nigeria. *Journal African Earth Sciences* 9, 195-207.

Ajayi, C.O. (1987). Origin of salts and barytes in the Middle Benue Trough: A suggested model from gravity data. In: Matheis G., and Schamelimier H. (Eds.) *Current Research in African Sciences*, Rotterdam, Balkema Press. 455-456.

Akande S.O. and Abimbola A.F. (1987). Aspect of the genesis of lead-zinc-fluorite-baryte mineralization In the Nigeria Benue Trough. In: Matheis G., Schamelimier H. (Eds.) *Current research in African Earth Sciences*. Balkema Press, 365-369.

Akande, O., Zentelli, M., and Reynolds, P.H. (1989). Fluid inclusion and stable isotope studies of Pb-Zn-flourite-baryte mineralization in the Lower and Middle Benue Trough, Nigeria, *Mineral Deposita*, 24, 183 – 191.

Akande, O., Hoffknecht, A. and Erdtmann, B.D. (1992). Environment of ore formation and achizonal metamorphism in Pb-Zn-flourite-baryte deposits of the Benue Trough, Nigeria. *Geologie en Mijnbouw*, 71, 131-144.

Akande S.O. (2000). Hydrocarbon Source rock potential and Thermicity in the Cretaceous Rift Basins of Nigeria. *Proceeding volume Association of Afro-Asian Petroleum Geochemists* (AAPG 5th International Conf.) Garg. A.K. Banergee, V. (editors). B.R. Publishers, New Delhi, 103-107.

Akpan, A.E., Ebong, E.D., Ekwok S.E., and Joseph S. (2014). Geophysical and geological studies of the spread and industrial quality of Okurike baryte deposit. *American Journal of Environmental Sciences*, 10(6):569-577.

Akpeke, G. B; Ekwueme, B. N. and Ephraim, B. E. (2006). The nature and origin of the Baryte Mineralization in Akpet area, Oban Massif, Southeastern. *Nigeria. Journal of Geological Sciences*, 4(2): 139-146

ASTM D7012 (2007). Standard test method for compressive strength and elastic moduli of intact rock core specimens under varying states of stress and temperatures. In:

Annual Book of ASTM Standards (Vol. 04.08). West Conshohocken American Society for Testing and Materials.

Banerjee, I. (1980). A subtidal bar model for the Eze-Aku sandstone, Nigeria. *Sedimentary Geology*, 25, 291-304.

Bas, H. and Temur, S. (1992). S.U. Müh.-Mim. Fak. Derg., 1-2.

Bau, M. (1991). Rare-earth element mobility during hydrothermal and metamorphic fluid-rock interaction and the significance of the oxidation state of europium. *Chemical Geology*, 93, 219-230.

Bau, M. and Dulski, P. (1996). Anthropogenic origin of positive gadolinium anomalies in river waters. *Earth Planetary Science Lett*ers, 143, 245–255.

Benkhelil, J. (1982). The Benue Trough and the Benue Chain. *Geology Magazine*, 119(2): 155-168.

Benkhelil, J. (1989). The origin and evolution of the Cretaceous Benue Trough, Nigeria. *Journal of African Earth Science*, 8, 251-282.

Benkhelil, J. and Robineau, B. (1983). La Benoue (Nigeria). Une chainean intracontinentale de style atlasique. *Comptes Rendus de l'Academie des Sciences,* Paris (D) 290, 1517-1520.

Benkhelil, J., Guiraud, M. P., Ponsard, J.F. and Saugy, L. (1989). The Bornu-Benue Trough, the Niger Delta and its onshore: tectono-sedimentary reconstruction during the Cretaceous and Tertiary from geophysical data and geology. In: Kogbe, C.A. (ed), *Geology of Nigeria (2nd revised edition)* Rock View (Nigeria) Ltd., Jos, Nigeria. 277-309.

Binks, R. M. and Fairhead, J.D. (1992). A plate tectonic setting for Mesozoic rifts of West and Central Africa. *Tectonophysics*, 213, 141-151.

Bock, B., Mclennan, S.M. and Hanson, G.N. (1998). Geochemistry and provenance of the Middle Ordovician Austin Glen Member (Normanskill Formation) and the Taconian Orogeny in New England. *Sedimentology*, 45, 635-655.

Bogue, R. G. (1951). Baryte prospect near Gabu, Ogoja Province. *Geological Survey of Nigeria Report* No. 1014 (unpublished).

Bolhar, R., Kamber, B. S., Moorbath, S., Fedo, C. M., and Whitehouse, M. J. (2004). Characterization of early Archaean chemical sediments by trace element signatures, Earth *Planetary Science Letters*, 222, 43–60.

Bonel, K.A. (2005). Barytes. *British Geological Survey* publication. 1-28.

Bouch, J.E., Naden, J., Shepherd, T.J., Young, B., Benham, A.J., McKervey, J.A. and Sloane, H.J. (2008). Stratabound Pb-Zn-Ba-F mineralization in the Alston Block of the North Pennine Orefield (England) – origins and emplacement. *British Geological Survey Research Report, RR/08/06,* 1-35.

Bozkaya, G. and Gokce, A. (2004). Trace and Rare Earth Element Geochemistry of the Karalar (Gazipasa-Antalya) baryte-galena deposits, Southern Turkey. *Turkish Journal of Earth Sciences*, 13, 63-76.

Brown, E. T. (1981). Rock characterization Testing and Monitoring: *ISRM Suggestion Methods*. New York: International Society for Rock Mechanics, Pergamon Press.

Bunnett, R.B. and Okunrotifa, P.O. (1984). General geography in diagrams for West Africa: *Tropical Climates*. Longman Ltd., UK. 185-193.

Burke K.C. and Whiteman, A.J. (1970). Geological History of the Benue Valley and adjacent areas. In: *African Geology*, University of Ibadan Press. 187-206.

Burke K.C., Dessauvagie, T.F.J. and Whiteman, A.J. (1971). Opening of the Gulf of Guinea and geological history of the Benue depression and Niger Delta. *Nature*, 233, 51-57.

Burke, K.C., Dessauvagie, T.F.J. and Whiteman, A.J. (1972). Geological History of the Benue valley and adjacent areas. In: Dessauvagie, T.F.J. and Whiteman, A.J. (eds), *African Geology*. Ibadan University Press, Ibadan, Nigeria, 187-205

Burke, K. and Whiteman, A.J. (1973). Uplift, rifting and the break-up of Africa. In: *Implications of continental drift to the earth sciences* (Edited by Tarling, D.H. and Runcorn, S.K.). Academic Press, London, UK, 735-755.

Burke, K. and Dewey, J. (1973). Plume generated triple junction: Key indicators in applying Plate tectonics to old rocks. *Journal Geology*, 81, 406 – 433.

Burke, K. and Dewey, J.F. (1974). Two plates in Africa during the Cretaceous. *Nature*, 249, 313-316.

Carmicheal, J.S.E. (1965). Trachytes and their feldspar phenocrysts. *Mineralogy Magazine*, 34, 107-125.

Chaanda, M.S., Obaje, N.G., Moumouni, A., Goki, N.G. and Lar, U.A. (2010). Environmental Impact of Artisanal Mining of Barytes in Azara Area, Middle Benue Trough, Nigeria. *Journal of Earth Science*, 4, 38 - 42.

Chukwunenye, M.E. (2006). Design and cost estimates of a prototype small-scale barite processing plant. Barites Consulting Nigeria, *Unpublished Memoirs*, 26.

Clark S.H.B., Gallagher M.J. and Poole F.G. (1990). World baryte resources; a review of recent production patterns and a genetic classification. Transactions of the Institute of Mining and Metallurgy, Section B, *Applied Earth Sciences* 99, 125–132.

Crook, K. A. W. (1974) Lithogenesis and geotectonics: the significance of compositional variation in flysch arenites (greywackes). *Society of Economic Paleontologist and Mineralogist* Special Publication 19, 304–310.

Cullers, R. L. (1994). The controls on the major and trace element variation of shales, siltstones, and sandstones of Pennsylvanian–Permian age from uplifted continental blocks in Colorado to platform sediment in Kansas, USA. *Geochimica et Cosmochimica Acta,* 58, 955–4972.

Cullers, R. L. (2000). The geochemistry of shales, siltstones and sandstones of Pennsylvanian–Permian age, Colorado, USA: Implications for provenance and metamorphic studies. *Lithos*, 51, 181–203.

Cullers, R. L. and Podkovyrov, V. N. (2000). Geochemistry of the Mesoproterozoic Lakhanda shales in southeastern Yakutia, Russia: Implications for mineralogical and provenance control, and recycling. *Precambrian Research*, 104, 77–93.

Cullers, R. L., Basu, A. and Suttner, L. J. (1988). Geochemical signature of provenance in sand-size material in soils and stream sediments near the Tobacco Root batholith, Montana, USA. *Chemical Geology*, 70, 335–348.

Cratchley, J.D. and Jones, G.P. (1965). An interpretation of the geology and gravity anomalies of the Benue Valley, Nigeria. *Overseas Geol. Surv. Geophysical*, 1, 26.

Dabard, M. P. (1990). Lower Brioverian formations (Upper Proterozoic) of the Armorican Massif (France): Geodynamic evolution of source areas revealed by sandstone petrography and geochemistry. *Sedimentary Geology*, 69, 45–58.

Dandume, S.G. (1978). *The Stratigraphy of the Konshisha River Basin in the Lower Benue Trough, Nigeria.* Unpublished B.Sc. Thesis, Ahmadu Bello University, Zaria, Nigeria.

Daspan, R. I. and Imagbe, L.O. (2010). Preliminary investigation of the origin and quality of barytes in the Tsareta Tungan Kudaku area, Northwestern Nigeria Basement Complex, Nigeria. *Continental Journal of Earth Sciences,* 5, 8 - 13.

Derry, L.A. and Jacobsen, S.B. (1990). The chemical evolution of Precambrian seawater: evidence of rare earth elements in banded iron formations. *Geochimica et Cosmochimica Acta*, 54, 2965-2977.

Ding, L and Zhong, D. (1996). Characteristics of rare earth elements and cerium anomalies in cherts from the Paleo-Tethys in Changning- Menglian Belt in western Yunnan, China. *Science in China* (Series D), 39(1): 35-45.

Ding, S., Liang, T., Zhang, C., Yan, J. and Zhang, Z. (2005). Accumulation and fractionation of rare earth elements in wheat: controlled by phosphate precipitation, cell wall absorption and solution complexation. *Journal of Experimental Botany*, 56(420): 2765-2775.

Edu, E. E. (2006). *Interim report on assessment of baryte resources in Taraba State, Nigeria*. Nigerian Geological Survey Agency Report (unpublished).

Ehya, F. (2012). Rare earth element and stable isotope (O, S) geochemistry of barite from Bijgan deposit, Markazi Province, Iran. *Mineralogy and Petrology,* 104(1):81-93.

Ekwere S. J. and Ukpong E.E. (1994). Geochemistry of saline groundwater in Ogoja, Cross-River State, Nigeria. *Journal of Mining and Geology*, 29, 23-30.

Ekwueme, B. N. and Kroner, A. (1998). Single zircon evaporation ages from the Oban Massif, Southeastern Nigeria. *Journal of African Earth Sciences, 26,* 195-205.

Ekwueme, B.N. and Akpeke, G.B. (2012). Occurrence and Distribution of Baryte Mineralisation in Cross River State, Southeastern Nigeria. *Global Journal Geological Sciences*, 10(1): 85-98.

Elderfield, H. and Greaves, M.J. (1982). The rare earth elements in seawater. *Nature,* 296, 214-219.

Ene, E.G., Okogbue, C.O. and Dim, C.I.P. (2012). Structural styles and economic potential of some baryte deposits in the Southern Benue Trough, Nigeria. *Romanian Journal of Earth Sciences*, 86(1): 27-40.

Ewart, A. and Griffin, T.J. (1994). Application of proton-microprobe data to trace element partitioning in volcanic rocks. *Chemical Geology*, 117, 251-284.

Ezepue M.C. (1984). The geologic setting of lead-zinc deposits at Ishiagu, Southeastern Nigeria. *Journal of African Earth Sciences*, 2, 97-101.

Ezepue, M.C. and Odigi, M.I. (1993). Petrology and geochemistry of monzodiorites, granodiorites and granites from the Pre-Cambrian Terrain between Kabba and Lokoja, SW Nigeria. *Journal of Mining and Geology*, 29, 27-39.

Farrington, J.L. (1952). A preliminary description of the Nigerian Lead-Zinc field. *Economic Geology*, 47(6): 583-608.

Fairhead, J.D. (1988a). Mesozoic plate tectonics reconstructions of the Central South Atlantic Ocean: the role of the West and Central African rift system. *Tectonophysics, 181,* 155-192.

Fairhead, J.D. (1988b). Late Mesozoic rifting in Africa. In: *Triassic-Jurassic rifting, continental breakup and the origin of the Atlantic Ocean and passive margins. Part B* (Edited by Manspeizer, W.). Elsevier, Amsterdam, Netherlands, 821-831.

Fairhead, J.D. and Green, C.M. (1989). Controls on rifting in African and the regional tectonic model for the Nigeria and Niger Delta rift basins. *Journal African Earth Sciences,* 8, 231-249.

Fairhead, J.D. and Binks, R.M. (1991). Differential opening of the Central and South Atlantic Oceans and the opening of the West African rift system. *Tectonophysics,* 187, 191-203.

Feng, R. and Kerrich, R. (1990). Geochemistry of fine-grained clastic sediments in the Archean Abitibi greenstones belt, Canada: implications for provenance and tectonic setting. *Geochimica et Cosmochimica Acta,* 54, 1061-1081.

Fitches, E. C., Ajibade, A. C., Egbuniwe, I. G., Holt, R. W., and Wright, J. B. (1985). Late Proterozoic schist belts and plutonism in Northwestern Nigeria. *Journal of Geological Society of London,* 142, 312-337.

Freeth, S.J. (1978a). Tectonic activity in West Africa and the Gulf of Guinea since Jurassic times - an explanation based on membrane tectonics. *Earth Planetary Science Letters,* 38, 298-300.

Freeth, S.J. (1978b). A model for tectonic activity in West Africa and the Gulf of Guinea during the last 90 m.y. based on membrane tectonics. *Geologische Rundschau,* 67, 675-687.

Freeth, S.J. (1979a). Tectonic activity in West Africa and the Gulf of Guinea – reply to comments by R.S. Thrope and J.B. Wright. *Earth Planetary Science Letters,* 42, 329-331.

Freeth, S.J. (1979b). Deformation of the African plate as a consequence of membrane stress domains generated by post-Jurassic drift. *Earth Planetary Science Letters,* 45, 93-104.

Freeth, S.J. (1990). The origin of the Benue Trough. In: Edited by Ofoegbu, C.O., *The Benue Trough, Structure and Evolution*. Vieweg and Sohn, Braunschweig, Germany, 217-227.

Genik, G.J. (1993). Petroleum geology of Cretaceous-Tertiary rift basins in Niger, Chad and the Central African Republic. *Bulletin American Association Petroleum Geologists*, 77, 1405-1423.

German, C. R. and Elderfield, H. (1989). Rare earth elements in Saanich Inlet, British Columbia, a seasonally anoxic basin. *Geochimica et Cosmochimica Acta*, 53, 2561-2571.

German, C. R. and Elderfield, H. (1990). Rare earth elements in the NW Indian Ocean. *Geochimica et Cosmochimica Acta*, 54, 1929-1940.

Grandia, F., Cardellach, E., Canlas, A. and Banks, D. (2003). Geochemistry of the fluids related to epigenetic carbonate hosted Zn-Pb deposits in the Maestrad Basin, Eastern Spain: Fluid inclusions and isotope (Cl, C, O, S, Sr) evidences. *Economic Geology*, 98, 933-954.

Grant, N.K. (1971). South Atlantic, Benue Trough and Gulf of Guinea Cretaceous triple junction. *Bulletin Geological Society of America*, 82, 2295-2298.

Griffith, E.M. and Paytan, A. (2012). Baryte in the ocean – occurrence, geochemistry and palaeoceanographic applications. *Sedimentology,* 1-19.

Guichard, F., Church, T., Treuil, M. & Jaffrezic, H. (1979). Rare earths in barytes: distribution and effects on aqueous partitioning. *Geochimica et Cosmochimica Acta,* 43, 983-997.

Guiraud, R. and Maurin, J.C. (1991). Le rifting en Afrique au Cretace inferieur: synthese structural, mise en evidence de deux etapes dans la genese des basins, relations avec les ouvertures oceaniques peri-africaines. *Bulletin Societe Geologique France,* 162, 811-823.

Guiraud, R. and Maurin, J.C. (1992). Early Cretaceous rifts of Western and Central Africa: An overview. *Tectonophysics,* 213, 153-168.

Hanor, J.S. (2000). Baryte-celestine geochemistry and environments of formation. In: *Reviews in Mineralogy and Geochemistry* – Sulphate Minerals (Eds. C.N. Alpers, J.L. Jambor and D.K. Nordstrom). Mineralogical Society of America, Washington, D.C., 193-275.

Harben P.W. (1999). The industrial minerals handbook, 3rd edition. Industrial Minerals Information Ltd, London.

Harben P.W. and Kužvart M. (1996). Industrial minerals: a global geology. Industrial Minerals Information Ltd, London.

Haskin, L.A., Wilderman, T.R., Frey, F.A., Collins, K.A., Keedy, C.R. and Haskin, M.A. (1966). Rare earths in sediments. *Journal of Geophysical Research B: Solid Earth* 71(24), 6091-6105

Hayashi, K., Fujisawa, H., Holland, H. D. and Ohmoto, H. (1997). Geochemistry of 1.9 Ga sedimentary rocks from northeastern Labrador, Canada. *Geochimica et Cosmochimica Acta,* 61, 4115–4137.

Hien, J.R., Zierenberg, R.A. , Maynard, J.B. and Hannington, M.D. (2007). Multifarious baryte-forming environments along a rifted continental margin, Southern California Borderland. *Deep-sea Research,* II(54): 1327-1349.

Herron, M.M. (1988) Geochemical classification of terrigenous sands and shales from core or log data. *Journal of Sedimentary Petrology*, 58, 820-829.

Hoatson, D.M., Jaireth, S. and Miezitis, Y. (2011). The major rare earth elements deposits of Australia: geological setting, exploration and resources. *Geoscience Australia*, 204.

Hoque, M. (1981). Pyroclastics, volcanism and tectonics of southern Benue Trough, Nigeria. 1981 IAVCE, Symposium on Arc Volcanism, Tokyo and Hakone. Abstracts Volume, 134-136.

Hoque, M. (1984). Pyroclastics from the Lower Benue Trough of Nigeria and their tectonic implications. *Journal of African Earth Sciences*, 2, 351-358.

Hoque, M. and Nwajide, C. S. (1984). Tectono-sedimentological evolution of an elongate intracratonic basin (aulacogen). The case of the Benue Trough of Nigeria. *Journal of Mining Geology,* 21, 19-25.

Ikejiaku, E.O. (2007). *Interim report on the assessment of baryte resources in Nassarawa State, Nigeria*. Nigerian Geological Survey Agency Report, 1-59.

Illies, J.H. (1970). Graben tectonics as related to crust-mantle-intereaction. In: J.H. Illies and S. Muller (eds) Graben problin schweizerbartsche verlaqsbuchhandlung. Stuttgard, 4- 27.

Irvine, T. M. and Baragar, W. R. (1971). A guide to the chemical classification of common volcanic rocks. *Canadian Journal of Earth Sciences,* 8, 523-548.

Jurkovic, I.B., Garasic, V. and Jurkovic, I.M. (2011). Geochemical characteristics of mercurian tetrahedrite, baryte and fluorite from the Dukobi Vagan, Glumac and Dubrave-Dugi Dol baryte deposits, south of Kresevo, Mid-Bosnian Schist Mountains. *Geologia Croatica,* 64(1): 49-59.

King, B.C. (1950). Speculations on the outline and the mode of disruption of Gondwana land. *Geological Magazine*, 87, 353-359.

Kogbe, C.A. (1989). The Cretaceous and Paleogene sediments of southern Nigeria. *Geology of Nigeria* second edition .Rock View Nigeria Limited, Jos, 325-334.

Kominz, M.A. (1984). Oceanic ridge volumes and seal level change – An error analysis. In: Schlee, J.S. (ed) interregional unconformities and hydrocarbon accumulation. *American Association Petroleum Geology*, 36, 109-127.

Kurt, H., Arslan, M., Bas, H. and Hekimbasi, E.B. (1998). Mineralogy and genesis of the Canakci (Ulukisla-Nigde) baryte vein deposits Central Turkey. *Mineralogical Magazine*, 62A, 832-833.

Lees, G.M. (1952). Foreland folding. Quarterly *Journal Geological Society of London*, 108, 1- 34.

Lesher, C.M., Gibson, H.L. and Campbell I.H. (1986). Composition-volume changes during hydrothermal alteration of andesite at Buttercup Hill, Noranda District, Quebec. *Geochimica et Cosmochimica Acta*, 50, 2693-2705.

Ledevine, M., Arndt, N., Davaille, A., Ledevine, R., and Simionovici, A. (2015). The rheological behaviour of fracture-filling cherts: example of barite Valley dikes, Barberton Greenstone Belt, South Africa. *Solid Earth*, 6, 253 – 269.

Laird, M. G. (1972). Sedimentology of the Greenland Group in the Paparoa Range, West Coast, South Island. N.Z.J. *Geology and Geophysics*, 15, 372-393.

Lieben, F., Moritz, R. and Fontbte, L. (2000). Mineralogy, geochemistry and age constraints on the Zn-Pb skarn deposits of Maria Christina, Quebrada Galena, Northern Chile. *Economic Geology*, 95, 1185-1196.

Lorenz, W and Gwosdz, W. (2003). Manual on the geological-technical assessment of mineral construction materials. *Geologishches Jahrbuch*, Sonderhefte Reihe H, SH 15, 330-337.

Maniar, P.D. and Piccoli, P.M. (1989). Tectonic discriminations of granitoids. *Geological Society of American Bulletin*, 101, 635-643.

Marchig, V.P., Moller, H. and Dulski, P. (1985). Foraminiferal ooze from the Galapogis rift area – hydrothermal impact and diagenetic mobilization of elements. *Marine Geology*, 62(1-2): 85-104.

Maurin, J.C., Benkhelil, J. and Robineau, B. (1986). Fault rocks of the Kaltungo lineament, NE Nigeria, and their relationship with Benue Trough tectonics. *Journal Geological Society of London*, 143, 587-599.

Maurin, J.C. and Lancelot, J.R. (1987). Origin des mineralization s de Pb-Zn de la Vottee de Benoue (Nigeria) dapres la composition en Pb des galenes et. de l'encaissaut. *Mineral Deposita*, 22, 99-108.

Maurin, J.C. and Guiraud, R. (1993). Basement control in the development of the Early Cretaceous West and Central African Rift System. *Tectonophysics*, 228, 81-95.

McConnell, R. B. (1949). Notes on the Lead-Zinc deposits of Nigeria and the Cretaceous Stratigraphy of Benue and Cross River Valleys. *Geological Survey of Nigeria Report,* 752 (unpublished).

McLennan, S.M., Hemming, S., McDaniel, D.K. and Hanson, G.N. (1993). Geochemical approaches to sedimentation, provenance, and tectonics. In: M.J. Johnson and A. Basu (Eds.), Processes Controlling the Composition of Clastic Sediments. *Geological Society of America Special Paper*, 284, 21-40.

Mclennan, S.M., Taylor, S.R. and Eriksson, K.A. (1983). Geochemistry of Archaean shales from the Pilbara Supergroup, Western Australia. *Geochimica et Cosmochimica Acta,* 7(7): 1211-1222.

Michard, A. (1989). Rare earth element systematics in hydrothermal fluids. *Geochimica et Cosmochimica Acta,* 53, 745-750.

Michard, A. and Albarade, F. (1 986). The REE content of some hydrothermal fluids. *Chemical Geology,* 55, 51-60.

Middlemost, E.A.K. (1997). Magmas, rocks and planetary development. Longman, Harlow. 324.

Miller, C., Thoni, M., Goessler, W. and Tessadri, R. (2011). Origin and age of the Eisenkappel gabbro to granite suite (Carinthia, SE Austrian Alps). *Science Direct,* 125(1): 434-448.

Minai, Y., Matsumto, R., Watanabe, Y. and Tominga, T. (1992). Geochemistry of rare earths and other trace elements in sediments from sites 798 and 799, Japan Sea. *Proceedings of the Ocean Drilling Program,* Scientific results vol. 127/128, 719-737.

Ministry of Mines and Steel Development (2008). *Barytes: Exploration Opportunities in Nigeria*. Abuja, 1-7.

Misra, K.C. (2000). Understanding mineral deposits. Springer Netherlands, XV, 845.

Möller, P. and Bau, M. (1993). Rare-earth patterns with positive cerium anomaly in alkaline waters from Lake Van, Turkey. *Earth Planetary Science Letters,* 117(3):671-676.

Möller, P. and Luders, V. (1993). Synopsis, in Monograph series on Mineral Deposits – Formation of Hydrothermal vein deposits: a case study of the Pb-Zn, baryte and fluorite deposits of the Harz Mountains (Eds. Moller, P. and Luders, V.), 30, 285-291.

Monnin, C. and Cividini, D. (2006). The saturation state of the world's ocean with respect to (Ba, Sr)SO_4 solid solutions. *Geochimica et Cosmochimica Acta*, 70, 3290–3298.

Morgan, J.W. (1983). Hotspots tracks and the early rifting of the Atlantic. *Tectonophysics,* 94, 123-139.

Murat, R.C. (1972). Stratigraphy and paleogeogrphy of the Cretaceous and Lower Tertiary in Southern Nigeria. In: T.F.J. Dessauvagie and A.J. Whiteman, (Ed), *African Geology*. Ibadan University Press, Ibadan, 251-266

Najime, T. (2010). Cretaceous Stratigraphy, Sequence Stratigraphy and Tectono-sedimentary evolution of Gboko Area, Lower Benue Trough, Nigeria. Unpublished Ph.D thesis, Department of Geology, Ahmadu Bello University, Zaria, Nigeria.

Najime, T. (2014). Geochemical Classification, Petrogenetic Association of Magmatic Rocks in the Gboko Area and the Tectono-Magmatic Influence on the Evolution of the (Gboko Area) Lower Benue Trough of Nigeria. *Journal of Environment and Earth Science,* 4(6): 34-47.

Nakamura, N. (1974). Determination of REE, Ba, Fe, Mg, Na and K in carbonaceous and ordinary chondrites. *Geochim Cosmochim Acta,* 38, 757-775.

Nesbitt, H.W. and Young, Y.M. (1982) Early Proterozoic climates and plate motions inferred from major element chemistry of lutites. *Nature,* 299, 715-717.

Nozaki, Y., Lerche, D., Alibo, D. S. and Tsutsumi, M. (2000). Dissolved indium and rare earth elements in three Japanese rivers and Tokyo Bay: evidence for anthropogenic Gd and In. *Geochimica et Cosmochimica Acta,* 64, 3975–3982.

Nwachukwu, S.O. (1972). The tectonic evolution of the southern portion of the Benue Trough. *Geological Magazine,* 109, 411-419.

Nwafor, G.I., Uduji, E.R. and Kwache, J.B. (1997). *Four giant mineral deposits in Benue State: Kaolin, Baryte, Gypsum and Limestone.* Nigerian Geological Survey Agency Report, 1-43.

Nwajide, C.S. (2012). Understanding the origin and structuration of the Benue Trough: A prerequisite for appreciating its earth materials resources potentials. In: Ashano, E.C., Ogezi, A.E (Eds.), *Proceedings of University of Jos PTDF chair endowment fund seminar*, 93-144.

Obiora, S.C. and Ukaegbu, V.U. (2010). Preliminary investigation of the petrogenesis and geotectonic setting of the Precambrian Basement Complex rocks around Northcentral Nigeria using trace and rare-earth elements geochemistry. *Journal Mining Geology*, 46, 127-137.

Obiora, S.C. (2012). Chemical characterization and tectonic evolution of hornblende-biotite granitoids from the Precambrian Basement Complex around Ityowanye and Katsina-Ala, southeastern Nigeria. *Journal of Mining and Geology*, 48(1):13-29.

O'Connor, J.M. and Duncan, R. A. (1990). Evolution of the Walvis Ridge-Rio Grande Rise hotspot system: implications for African and South American plate motions over plumes. *Journal Geophysical Research* 95, 17475-17502.

Oden, M.I. (2012). Baryte veins in the Benue Trough: Field Characteristics, the quality issue and some tectonic implications. *Environment and Natural Resources Research,* 2(2): 21 – 31.

Odewumi, S.C. and Olarewaju, V.O. (2013). Petrogenesis and geotectonic settings of the granitic rocks of Idofin-Osi-Eruku area, Southwestern Nigeria using trace element and rare earth element geochemistry. *Journal of Geology and Geoscience,* 2(1): 1-8.

Offodile, M.E. (1976a). A hydrogeological interpretation of the Middle Benue and Abakaliki Brinefields. *Journal of Mining and Geology*, 13(2):79.

Offodile, M.E. (1976b). A review of the geology of the Cretaceous of the Benue Valley. In: Kogbe, C.A. (Ed) *Geology of Nigeria*. Elizabeth Publications and Co., Lagos, 319-330.

Ofoegbu, C. O. (1984a). Interpretation of magnetic anomalies over the Lower and Middle Benue Trough of Nigeria. *Geophysical Journal Royal Astronomical,* 79, 813-823.

Ofoegbu, C. O. (1984b). An aeromagnetic study of the Lower Benue Trough, Nigeria. *Revista Brasilliera Geociencias,* 14, 54-59.

Ofoegbu, C. O. (1984c). A model for the tectonic evolution of the Benue Trough of Nigeria. *Geologische Rundschau,* 73, 1007-1018.

Ofoegbu, C. O. (1985). A review of the Geology of the Benue Trough of Nigeria. *Journal of African Earth Science,* 3, 283 – 291.

Ofoegbu, C. O. (1988). An aeromagnetic study of part of the Upper Benue Trough, Nigeria. *Journal African Earth Sciences*, 7, 77-90.

Ofoegbu, C.O. and Odigi, M.I. (1989). Basement structure and ore mineralization in the Benue Trough. In: Ofoegbu, C.O., (Ed) *the Benue Trough structure and evolution*. Vieweg, 239-248.

Ogata, T. and Terakado, Y. (2006). Rare element abundances in some seawaters and related rivers from Osaka Bay area, Japan: Significance of anthropogenic Gd. *Geochemical Journal*, 40, 463-474.

Ojoh, K.A. (1990). Cretaceous geodynamic evolution of the southern part of the Benue Trough (Nigeria) in the Equatorial domain of the South Atlantic. Stratigraphy, basin analysis and paleo-oceanography. *Bulletin Centres Recherches Exploration-Production Elf-Aquitaine*, 14, 419-442.

Okonkwo, C.T. and Winchester, J.A. (2004). Geochemistry of granitic rocks in Jebba area, Southwestern Nigeria. *Journal of Mining and Geology*, 40, 95-100.

Okonkwo, C.T. and Folorunsho, I.O. (2013). Petrochemistry and geotectonic setting of granitic rocks in Aderan area, Southwestern Nigeria. *Journal of Geography and Geology*, 5(1):30-44.

Olade, M.A. (1975). Evolution of Nigeria's Benue Trough (aulacogen). A tectonic model. *Geological Magazine*, 112, 575-583.

Olade, M.A. (1976). On the genesis of lead-zinc deposits in Nigeria's Benue rift (aulacogen). A re-interpretation. *Journal of Mining and Geology*, 17, 119-127.

Olade, M.A. (1979). The Abakaliki pyroclastics of southern Benue Trough, Nigeria: their petrology and tectonic significance. *Journal of Mining and Geology*, 16, 17-25.

Olade, M.A. and Morton, R.D. (1985). Origin of lead-zinc mineralization in the southern Benue Trough, Nigeria. Fluid inclusion and trace element studies. *Mineral Deposita*, 20, 76-80.

Oladapo, M.I. and Adeoye-Oladapo, O.O. (2011). Geophysical investigation of baryte deposit in Tunga, northeastern Nigeria. *International Journal of Physical Science*, 6, 4760-4774.

Olarewaju, V.O. (1987). Charnockite-granite association in SW Nigeria: Rapakivi granite type and charnockitic plutonism in Nigeria. *Journal of African Earth Sciences*, 6(1):67-77.

Olarewaju, V.O. and Rahaman, M.A. (1982). Petrology and geochemistry of Older Granites from some parts of northern Nigeria. *Journal of Mining and Geology,* 40, 95-100.

Omada, J. I (1985). The geology and geochemistry of baryte mineralization in the Azara area, Middle Benue Trough, Nigeria. Unpublished MS.c thesis, Department of Geology, Ahmadu Bello University, Zaria, Nigeria.

Omada, J. I (1987). Petrographic details of baryte mineralization in the Middle Benue Trough: A guide in exploration. *Paper presented at the 23rd Annual Conference of Nigerian Mining and Geosciences Society Abstract volume,* 23.

Omada, J. I. and Ike, E. C. (1996). On the economic appraisal of the baryte mineralization and saline springs in the Middle Benue Trough, Nigeria. *Journal of Mining Petrology and Economic Geology,* 91, 109-115.

O'nions, R.K. and Pankhurst, R.I. (1974). Rare earth element distribution in Archean gneisses and anorthosites, Godthab area, West Greenland. *Journal of Earth Planetary Science Letters*, 22, 328-338.

Onyeagocha, A.C. (1986). Geochemistry of basement granitic rocks from northcentral Nigeria. *Journal of African Earth Sciences,* 5(6):651-657.

Oostingh, K. (2011). Analysis of rare earth element concentrations in baryte: Determination of the environment of formation of Archean barytes by rare earth element fractionation measurements. Published M.Sc thesis, Department of Earth Sciences, Utrecht University.

Orajiaka S. (1964). Geology of the southern Obudu Plateau, Ogoja Province, Eastern Nigeria. *Le Naturaliste Canadian*, 3, 72-85.

Ortigoza-Cruz, F., Changkakoti, A., Morton R.D. and Gray, J. (1994). Strontium isotope geochemistry of baryte mineralization at La Minita, S.W. Mexico: *Sociedad Geologica Mexicana Boletin*, 52, 1-10.

Palinkaš, L.A. and Jurkovic, I. (1994). Lanthanide Geochemistry and Fluid Inclusion Peculiarities of the Fluorite from the Baryte Deposits South of Kreševo (Bosnia and Herzegovina). *Geologia Croatica*, 47(1):103-115.

Paradis S., Simandi G., Maclntyre D. and Orris G.J. (1998). Sedimentary-hosted, stratiform baryte, In: *Geologic fieldwork*, 1997, British Columbia Ministry of Employment and Investment Paper 1998-1, 24F-1-24F-2.

Pearce, J.A., Harris, N. W. and Tindle, A.G. (1984). Trace element discrimination diagrams for the tectonic interpretation of granitic rocks. *Journal of Petrology,* 25, 956-983.

Petters, S.W. and Ekweozor, C.M. (1982). Origin of Cretaceous black shales in the Benue Trough Nigeria. *Palaeogeography Palaeoclimatology Palaeoecology* 40, 311-319.

Piper, D. (1974). Rare earth elements in the sedimentary cycle: a summary. *Chemical Geology*, 19, 285-304.

Rahaman, A.A., Ukpong, E.E. and Azmatullah, M. (1981). Geology of parts of the Oban Massif, Southeastern Nigeria. *Journal of Mining Geology*, 18(1):52-59.

Rahaman, M. A., Emofurieta, W.O., and Caen-Vachette, M. (1983). The potassic granites of Igbeti area: Further evidence of of the polycyclic evolution of the Pan-African belt in Southwestern Nigeria. *Precambrian Research, 22,* 75-92.

Rahaman, M.A. Ekwere, M.S., Azmatullah, M. and Ukpong, E.E. (1988). Petrology and geochemistry of granitic intrusive rocks from the western part of Oban Massif, Southeastern Nigeria. *Journal of African Earth Sciences,* 7(1):149-157.

Rahaman, M.J.J. and Suzuki, S. (2007). Geochemistry of Sandstones from the Miocene Surma Southern Nigeria. In: T.F.J. Dessauvagie and A.J. Whiteman, (ed.), *African Geology*. Ibadan University Press, Ibadan, 251-266

Rajesh, H.M. (2007). The Petrogenetic characterization of intermediate and silicic charnockites in high grade-grade terrains: a case study from southern India. Contributions to *Mineralogy and Petrology*, 154, 591-606.

Ramos V.A. and de Brodtkorb M.K. (1989). Celestite, baryte, magnesite and fluorspar: stratabound through time and space. In: de Brodtkorb M.K. (ed.) *Non-metalliferous stratabound ore fields*. Van Nostrand Reinhold, New York, 297–321

Reyment, R. A. (1965). Aspects of Geology of Nigeria. Ibadan University Press, 148.

Roddaz, M., Viers, J., Brusset, S., Baby, P., Boucayrand, C. and Hérail, G. (2006). Controls on weathering and provenance in the Amazonian foreland basin: Insights from major and trace element geochemistry of Neogene Amazonian sediments. *Chemical Geology*, 226, 31- 65.

Rollinson, H.R. (1993). Using Geochemical Data: Evaluation, Presentation and Interpretation. Pub. John Wiley and Sons Inc. New York.

Roser, B.P. and Korsch, R.J. (1986). Determination of tectonic setting of sandstone-mudstone suites using SiO_2 content and K_2O/Na_2O ratio. *Journal of Geology*, 94(5):635-650.

Russell, M.J. (1978). Downward excavating hydrothermal cells and Irish type ore deposits 2, 67-110.

Sabaou, N., Ait-Salem, H. and Zazoun, R. S. (2009). Chemostratigraphy, tectonic setting and provenance of the Cambro-Ordovician clastic deposits of the subsurface Algerian Sahara. *Journal of African Earth Sciences*, 55, 158-174.

Shimizu, H., and Masuda, A. (1977). Cerium in chert as an indicator of marine environment of its formation. *Nature*, 266, 346-348.

Simpson, A. (1954). The Nigerian coalfield. The geology of parts of Onitsha, Owerri and Benue Provinces. *Bulletin Geological Survey Nigeria*, 24, 85.

Starke, R. (1964). Die strontiumgehalte der baryte. *Freiberger Forschungsh*, 150, 1-86.

Stoneley, R. (1966). The Niger Delata region in the light of the theory of continental drift. *Geological Magazine*, 103, 385-397.

Tawfik, H.A., Ghandour, I.M., Maejima, W. and Abdel-Hameed, A.T. (2011). Petrography and geochemistry of the Lower Paleozoic Araba Formation, Northern Eastern Desert, Egypt: Implications for provenance, tectonic setting and weathering signature. *Journal of Geosciences*, 54(1): 1-16.

Taylor, S.R. (1965). Application of trace elements in petrology. In: Ahrens, L.N., Press, F., and Runcorn, S.K., (Eds). *Physics and Chemistry of the Earth-Progress Series*, vol. 5.

Taylor, S.R. and McLennan, S.M. (1985). The continental crust: its composition and evolution. Blackwell, Oxford, 1-312.

Taylor, S.R. and McLennan, S.M. (1995). The geochemical evolution of the continental crust. *Reviews in Geophysics*, 33, 241-625.

Thompson, R.N. (1982). British Tertiary Province. *Scottish Journal of Geology*, 18, 49-107.

Thrush, P.W. (1968). A dictionary of mining, mineral and related terms: U.S. Bureau of Mines, (ed) 1049.

Tijani M.N., Leohnert E.P. and Uma K.O. (1996). Origin of Saline groundwaters in the Ogoja area, Lower Benue Trough, Nigeria. *Journal of African Earth Sciences*, 23, 237-256.

Toyoda, K., Nakamura, Y., Masuda, A. (1990). Rare earth elements of pelagic sediments. *Geochimica et Cosmochimica Acta*, 57, 579-595.

Ukaegbu, V.U. and Ekwueme, B.N. (2005). Petrographic significance of rare-earth element behavior in the basement rocks of southern Obudu Plateau, Bamenda Massif, Southeastern Nigeria. *Chinese Journal of Geochemistry* 24(2): 129-134.

Ukaegbu, V.U. and Ekwueme, B.N. (2006). Petrogenesis and geotectonic setting of the Pan-African Basement rocks in Bamends Massif, Obudu, Southeastern Nigeria: Evidence from trace element geochemistry. *Chinese Journal of Geochemistry*, 25(2):122-131.

Ukwang. E. and Ekwueme, B.N. (2009). Geochemistry and geotectonic study of granitic rocks of Southwest Obudu Plateau, Southeastern Nigeria. *Journal of Mining and Geology*, 45, 73-82.

Uma K.O. and Leohnert E.P. (1992). The brine fields of the Benue Trough, Nigeria: a comparative study of geomorphic, tectonic and hydrochemical properties. *Journal of African Earth Sciences*, 26, 23-29.

Umeji, A.C. (1981). The Precambrian of part of Southeast Nigeria: a magmatic and tectonic study. In: *Proceedings of the first symposium on the Precambrian geology of Nigeria*, 69-76.

Umeji, A.C. and Cean-Vachette, M. (1983). Rb-Sr isochron from Gboko and Ikyuen rhyolites and its implication for the age and evolution of the Benue Trough. *Geological Magazine*, 120, 529-533.

Uzuakpunwa, A.A. (1980). A Pre-Albian succession in parts of southwestern Nigeria. *Cahiers Geologiques*, 96, 761-779.

Vaslsami, E. and Cann, J.R. (1992). Mobility of rare earth elements in the zones of intense hydrothermal alteration in the Pindos ophiolite, Greece. In: Parson, L.M., Murton, B.J. and Browning, P., eds., *Ophiolites and their modern oceanic analogues*, Geological SocietySpecial Publication, 60, 219-232.

Wakita, H., Rey, P. and Schmitt, R.A., (1971). Abundances of the 14 rare-earth elements and 12 other trace elements in Apollo 12 samples: five igneous and one breccias rocks, and four soils: *Proceedings of the Second Lunar Science Conference*, The M.I.T. Press, 2, 1319- 1329.

Werner, C.D. (1958). Geochemie und paragenese der saxonischen schwerspat-flubspat-gange im schmalkaldener revier. *Freiberger Forschungshefte*, Reibe C, 47:117S, 24 Abb.; (Akademic-Verlag) Berlin–zgl. Diss. Univ. Halle-Wittenberg 1957.

Whiteman, A.J. (1982). Nigeria: *its petroleum geology, resources and potential.* Graham and Trotman, London, UK, 1:176 and 2:238.

Wright, J. B. (1968). South Atlantic continental drift and the Benue Trough. *Tectonophysics,* 6, 301-310.

Wright, J. B. (1981). Review of the origin and evolution of the Benue Trough in Nigeria. *Earth Evolution Sciences*, 2, 98-103.

Wright, J.B. (1989). Volcanic rocks in Nigeria. In: *Geology of Nigeria (second revised edition)* (Edited by Kogbe, C.A.). Rock View (Nigeria) Ltd., Jos, Nigeria, 125-173.

Wyborn, D. (1983). Fractionation processes in the Boggy Plain Zoned Pluton. Unpublished PhD Thesis, Australian National University, Canberra.

Yang, S.Q., Jing, H.W. and Wang, S.W. (2012). Experimental investigation on the strength, deformability, failure behavior and acoustic emission locations of red sandstone under triaxial compression. *Rock Mechanics and Rock Engineering*, 45, 801-818.

Zaborski, P.M. (1998). A review of the Cretaceous system in Nigeria. *Africa Geoscience Review,* 5, 385-483.

Zaborski, P.M. (2000). The Cretaceous and Paleocene transgressions in Nigeria and Niger. *Journal of Mining and Geology,* 26, 153-173.

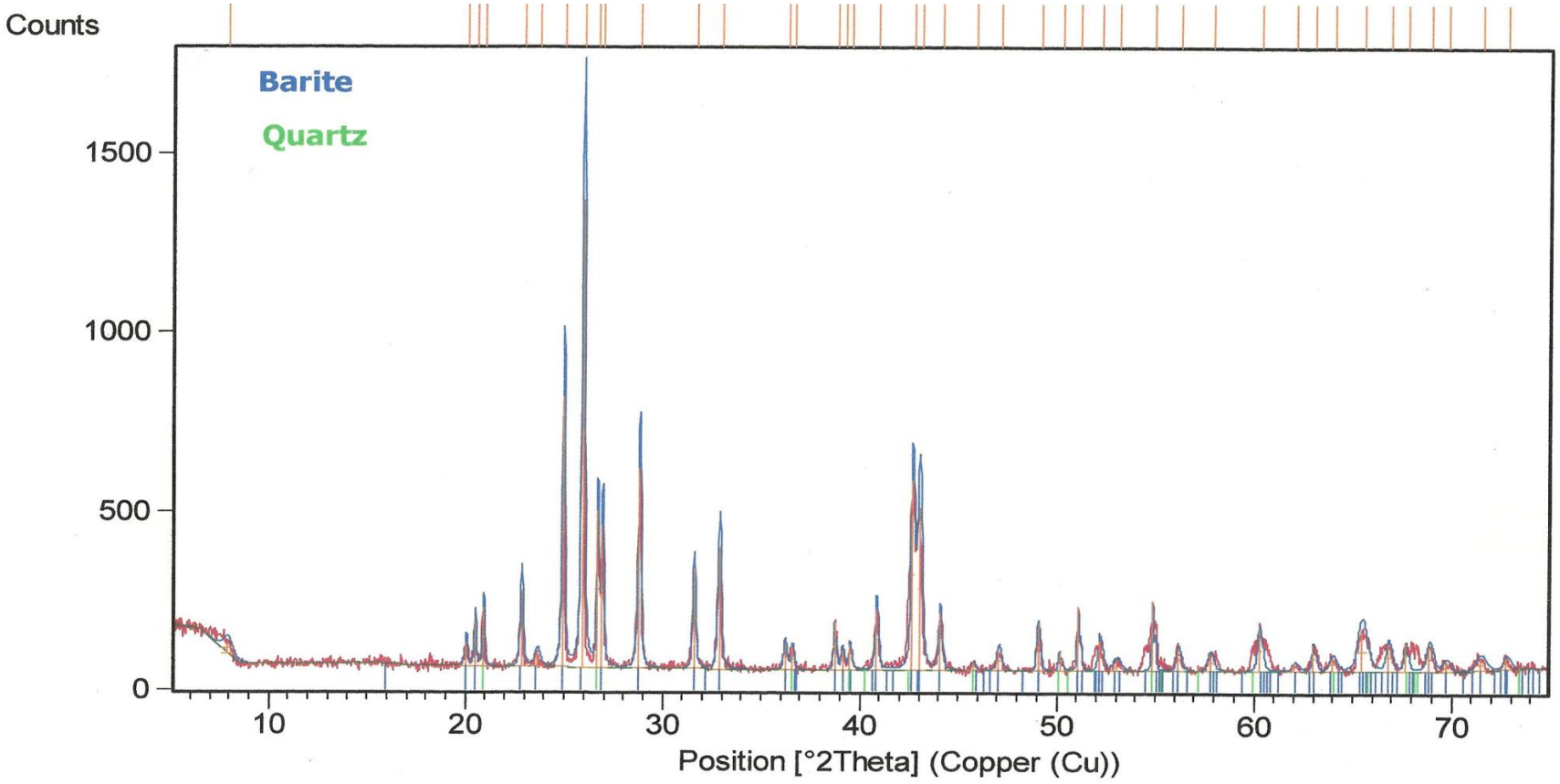
Zheng, Y.F. and Hoefs, J. (1993). Stable isotope geochemistry of hydrothermal mineralizations in the Harz mountains; II. Sulfur and oxygen isotopes of sulfides and sulfate and constraints on metallogenetic models. In: Moller, P and Luders, V. (Eds.), *formation of hydrothermal vein deposits*; a case study of the Pb-Zn, baryte and fluorite deposits of the Harz Mountains, 30, 211-230.

Zhu, C. (2004). Co-precipitation in the baryte isostructural family: Binary mixing properties. *Geochimica et Cosmochimica Acta,* 68, 3327–3337.

Zhu, Y., Hoshino, M., Yamada, H., Itoh, A. and Haraguchi, H. (2004). Gadolinium anomaly in the distribution of rare earth elements observed for coastal seawater and river waters around Nagoya City. *Bulletin of Chemical Society of Japan,* 77, 1835–1842.

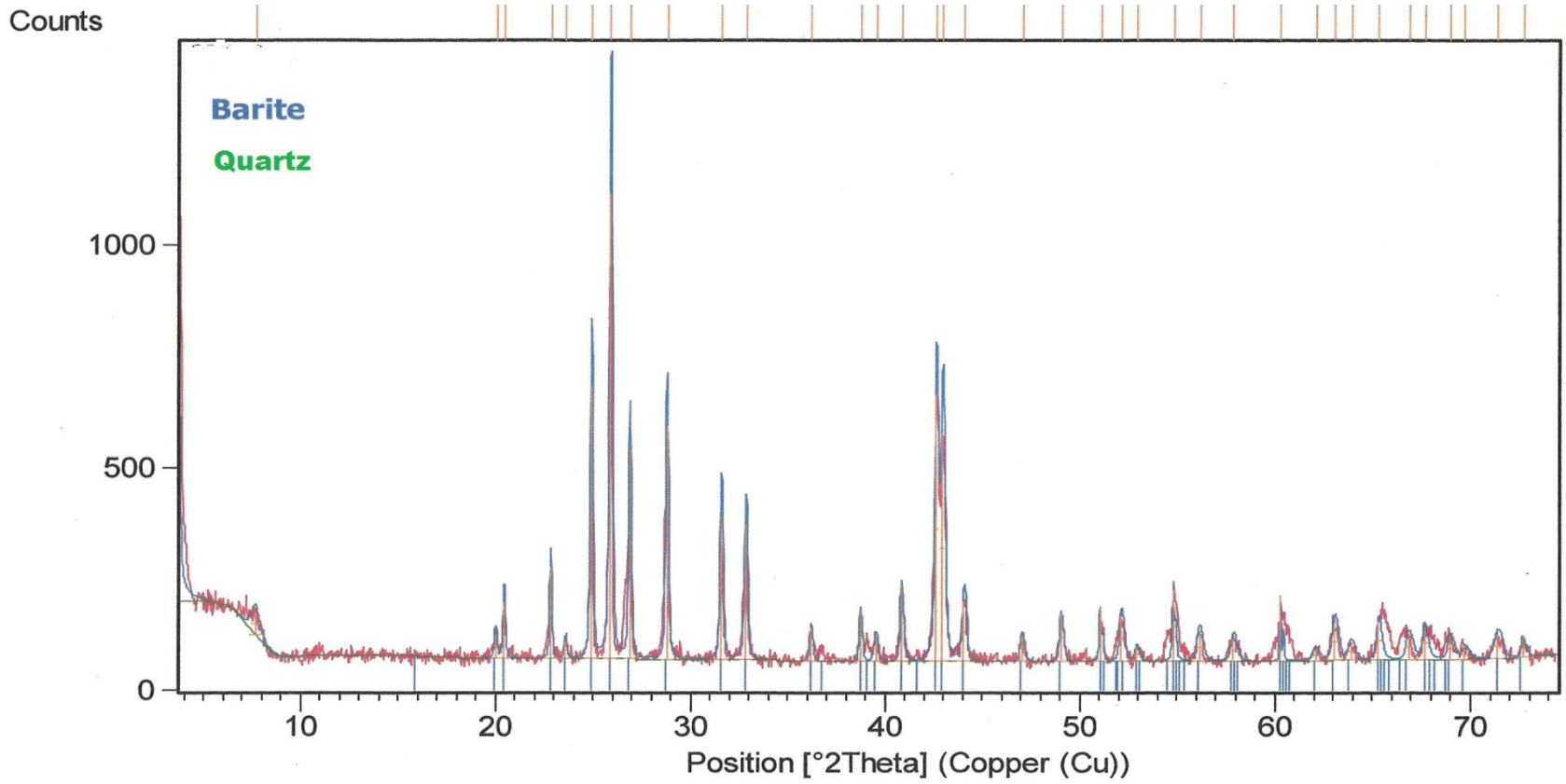
APPENDIX I

X-ray diffraction (XRD) sample identification: NM (baryte from Lessel-Mbagwa area)



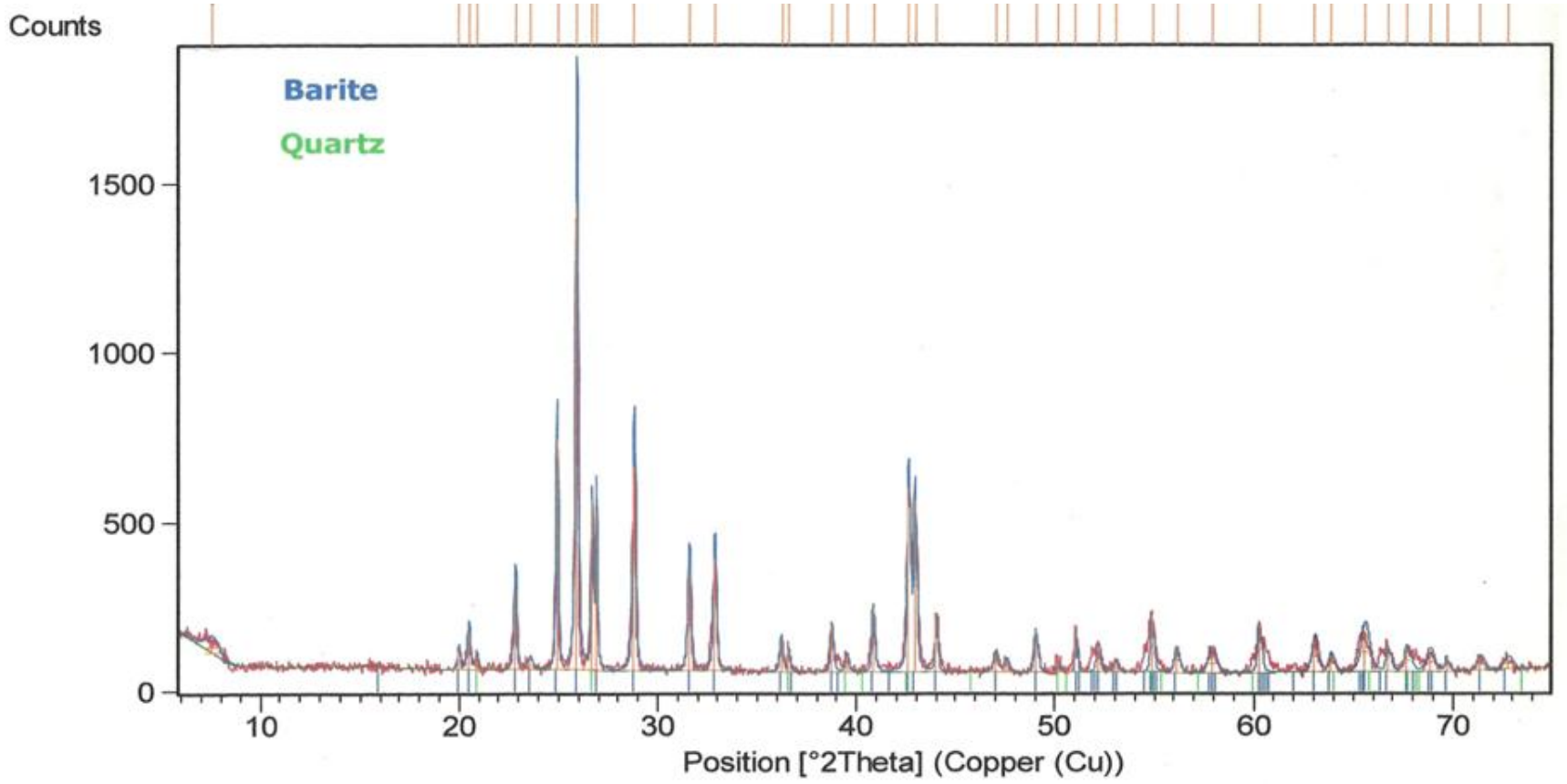
APPENDIX II

XRD sample identification: NQ2 (baryte from Ihugh area)



APPENDIX III

XRD sample identification: NO5 (baryte from Bunde area)



APPENDIX IV

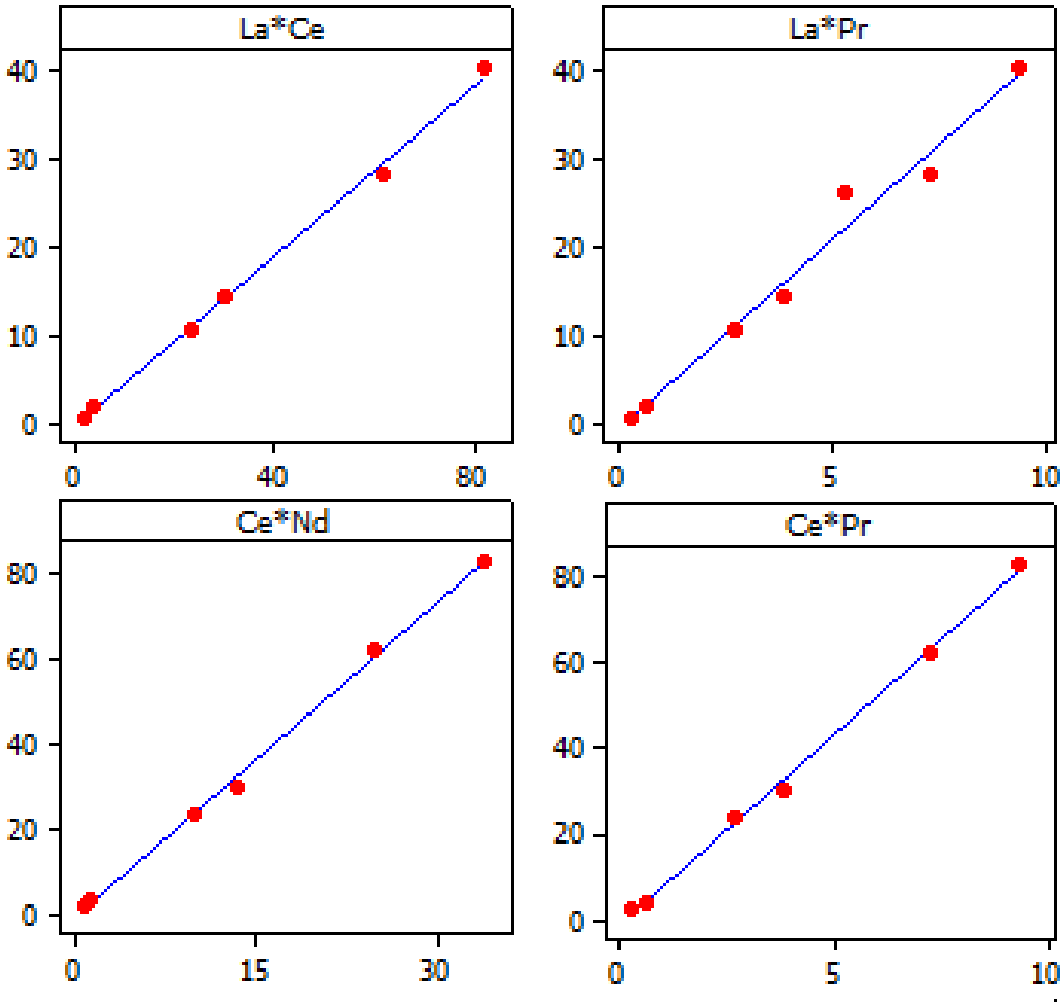
Provenance Discriminant Function Values

F1 = $-1.773TiO_2 + 0.607Al_2O_3 + 0.76Fe_2O_3 – 1.5MgO + 0.616CaO + 0.509Na_2O – 1.224K_2O – 9.09$

F2 = $0.445TiO_2 + 0.07Al_2O_3 – 0.25Fe_2O_3 – 1.142MgO + 0.438CaO + 1.475Na_2O – 1.426K_2O – 6.861$

APPENDIX V

Scatterplot of La/Ce, La/Pr, Ce/Nd and Ce/Pr ratios



APPENDIX VI

Standard sedimentary composition used for normalizing the REE concentrations (ppm) in sedimentary rocks.

(Ref.)	NASC (1)	NASC (2)	NASC (3)	NASC (4)	NASC (5)	ES (6)	PAAS (7)	Upper crust (8)	Typical seawater (9) (10^{-12} mol kg^{-1})	River water (10)
La	39.000	32.000	32.000	31.100	31.100	41.100	38.200	30.000	20.800	425.0
Ce	76.000	70.000	73.000	66.700	67.033	81.300	79.600	64.000	9.640	601.0
Pr	10.300	7.900	7.900			10.400	8.830	7.100		
Nd	37.000	31.000	33.000	27.400	30.400	40.100	33.900	26.000	21.100	365.0
Sm	7.000	5.700	5.700	5.590	5.980	7.300	5.550	4.500	4.320	80.4
Eu	2.000	1.240	1.240	1.180	1.253	1.520	1.080	0.880	0.823	20.7
Gd	6.100	5.210	5.200		5.500	6.030	4.660	3.800	5.200	83.5
Tb	1.300	0.850	0.850	0.850	0.850	1.050	0.774	0.640		
Dy					5.540		4.680	3.500	5.610	97.9
Ho	1.400	1.040	1.040			1.200	0.991	0.800		
Er	4.000	3.400	3.400		3.275	3.550	2.850	2.300	4.940	64.6
Tm	0.580	0.500	0.500			0.560	0.405	0.330		
Yb	3.400	3.100	3.100	3.060	3.113	3.290	2.820	2.200	4.660	51.7
Lu	0.600	0.480	0.480	0.456	0.456	0.580	0.433	0.320		
Y		27.000				31.800	27.000	22.000		

(Source: Rollinson, 1993)

(1) North American shale composite (Haskin and Frey, 1966).
(2) North American shale composite (Haskin and Haskin, 1966).
(3) North American shale composite (Haskin *et al.*, 1968).
(4) North American shale composite (Gromet *et al.*, 1984) — INAA.
(5) North American shale composite (Gromet *et al.*, 1984) — recommended.
(6) Average European shale (Haskin and Haskin, 1966).
(7) Post-Archaean average Australian sedimentary rock (McLennan, 1989).
(8) Average upper continental crust (Taylor and McLennan, 1981).
(9) Elderfield and Greaves (1982), Table 1, 900 m sample.
(10) Hoyle *et al.* (1984): River Luce, Scotland; 0.7 µm filter.

APPENDIX VII

a. Lineament trends in granitic rocks from the Lessel-Ihugh area

Lineament Trend	**Interval**	**Frequency**
140SW, 050NE, 040NE, 070NE, 140SE, 030NE, 035NE, 060NE, 110SE, 190SW, 210SW, 220SW, 050NE, 170SE, 190SW, 140SE, 255SW, 320NW, 060NE	$0 – 90^o$	8
	$91 – 180^o$	5
	$181 – 270^o$	4
	$271 - 360^o$	1

b. Lineament trends in sandstones from the Lessel-Ihugh area

Lineament Trend	**Interval**	**Frequency**
045NE, 284NW, 017NE, 010NE, 273NW, 068NE, 012NE, 151SE, 193SW, 352NW, 142SE, 300NW, 235SW, 200SW, 025NE, 044NE, 335NW, 187SW, 219SW, 050NE, 065NE, 086NE	$0 – 90^o$	10
	$91 – 180^o$	2
	$181 – 270^o$	5
	$271 - 360^o$	5